UNIVERSIDADE DE LISBOA
FACULDADE DE CIÊNCIAS
DEPARTAMENTO DE FÍSICA

Gait biomechanics in Cerebral Palsy children: comparison of Markerless and Marker-based motion capture systems

Raquel José da Costa

Mestrado em Engenharia Biomédica e Biofísica

Dissertação orientada por:
Prof. Dra. Filipa João
Prof. Dr. Nuno Garcia

2024

"As for the future, your task is not to foresee it, but to enable it"

Antoine de Saint Exupery

Trabalho realizado no âmbito do projeto

Referência do Projeto: PTDC/EMD-EMD/5804/2020
Título: Desenvolvimento de uma plataforma de simulação biomecânica baseada em modelos músculo-esqueléticos preditivos do efeito de intervenção ortopédica na melhoria da marcha em crianças com paralisia cerebral
Concurso * Programa * Área: PTDC 2020 * 3599-PPCDTI * Engenharia Médica
DOI: https://doi.org/10.54499/PTDC/EMD-EMD/5804/2020

Acknowledgments

If I made it here, it means that all the hard work and dedication during this 5-year journey paid off. It is certain that none of this would be possible without the support of so many people, who I really appreciate.

I was very well welcomed in the Biomechanics and Functional Morphology Laboratory of Faculty of Human Kinetics (FMH), so I would really like to say a sincere thank you to my supervisor, Professor Filipa João, for her continued availability and disposition to always provide such valuable guidance, knowledge and for supporting me during this year. Thank you so much for your patience to review this thesis. I would also like to thank the research group for taking me and for offering me the opportunity to continue working and contributing for the research of the biomechanics field and cerebral palsy. I am very thankful for all the lab members, who could always find time to focus on work but also to laugh and make sure everyone had a good time.

I would like to express my gratitude to Professor Nuno Garcia, my internal supervisor, for his availability to support me and answer all my questions. Thank you very much for the online meetings, your help was fundamental.

A special mention to my family is a must since they are the ones who have continuously shown up to support me throughout the years and are the ones that I know I can count on at any time of the day and for any reason. I am so appreciative of every single person that fits into this category, because family is not just defined by blood but by the love we share.

I am extremely grateful for my parents, who love and support me unconditionally, and for this reason, this dissertation is dedicated to them, Madalena and Leandro Costa. They thought me to be resilient, to never forget my values, and showed me that in the end, if I put effort and dedication to do my best, everything would always turn out fine. A huge thank you to my lovely grandma, my biggest supporter. Obviously, I want to thank the Santolas, for being the best family anyone could wish for, and for doing everything they can to provide us the best opportunities possible.

Thank you to my other half for always believing in me, for all the love, and for always pushing me to do better. Thank you to my friends of many years, Sofia, Luis and Bernardo, for being so ambitious and such a great example to follow. Finally, I want to thank Carol, Pinto and Lima, the first friends I made in the first days of university and the ones that stuck with me until the end.

Thank you to FCUL and to all the teachers who were involved and cared for their students during these 5 years.

Well, after all this time, I am soon to be a Biomedical engineer!

My sincere thanks to everyone.

Agradecimentos

Se cheguei até aqui, significa que todo o trabalho árduo e dedicação durante esta jornada de 5 anos valeu a pena. Certamente, nada disto seria possível sem o apoio de muitas pessoas, que eu aprecio bastante.

Fui muito bem recebida no Laboratório de Biomecânica e Morfologia Funcional da Faculdade de Motricidade Humana (FMH), por isso, gostaria imenso de dizer um sincero obrigado à minha orientadora, professora Filipa João, pela sua disponibilidade e disposição para fornecer sempre orientações e conhecimentos valiosos, e por me apoiar durante este ano. Muito obrigada pela paciência para rever esta tese. Gostaria de agradecer também ao grupo de investigação por me acolherem e por me oferecerem a oportunidade de continuar a trabalhar e contribuir para a investigação na área da biomecânica e paralisia cerebral. Estou muito grata por todos os membros do laboratório, que conseguiam ter sempre tempo para se focar no seu trabalho, mas também para nos rirmos e garantir que todos tinham um bom dia.

Quero expressar a minha gratidão ao professor Nuno Garcia, o meu orientador interno, pela sua disponibilidade para me apoiar e responder a todas as minhas dúvidas. Muito obrigada pelas reuniões online, a sua ajuda foi fundamental.

Uma menção especial à minha família é imprescindível, porque são os que continuamente me têm apoiado durante os anos e os que eu sei que posso sempre contar a qualquer momento do dia e por qualquer razão. Sou muito grata por cada pessoa que encaixo nesta categoria, porque família não é só definida por laços de sangue, mas pelo amor que partilhamos.

Sou extremamente grata pelos meus pais, que me amam e apoiam incondicionalmente, e por isso, esta dissertação é dedicada a eles, Leandro e Madalena Costa. Eles ensinaram-me a ser resiliente, a nunca esquecer os meus valores, e mostraram-me que no fim, se eu puser esforço e dedicação para fazer o meu melhor, tudo acaba sempre por correr bem. Um grande obrigado à minha avó, a minha maior apoiante. Obviamente, quero agradecer aos Santolas, por serem a melhor família que qualquer um poderia desejar, e por fazerem tudo o que está ao seu alcance para nos fornecer as melhores oportunidades possíveis.

Obrigada à minha outra metade por acreditar sempre em mim, por todo o amor, e por incentivar-me a fazer o meu melhor. Agradeço aos meus amigos, Sofia, Luís e Bernardo, por serem tão ambiciosos e por serem um ótimo exemplo a seguir. Finalmente, quero agradecer à Carol, Pinto e à Lima, as primeiras amigas que fiz nos primeiros dias de faculdade e as que ficaram comigo até ao fim.

Agradeço à FCUL e a todos os professores que estiveram envolvidos e que se importaram com os alunos durante estes 5 anos.

Bem, depois deste tempo todo, brevemente serei Engenheira Biomédica!

Um sincero obrigado a todos!

Abstract

Cerebral Palsy (CP) is intensively studied in clinical gait analysis (GA) using marker-based (MB) systems, which have many limitations. Markerless (ML) systems are a potential alternative that offer practical and technical benefits to perform GA.

This dissertation compares the joint kinematics and kinetics of CP children computed with the MB and the ML systems. Data were collected on fourteen children diagnosed with CP during the walking movement. The estimations of the joint kinematics and kinetics were compared using the root mean square difference and a Statistical Parametric Mapping package for statistical analysis.

The joint angles in the sagittal plane showed consistent waveform and good agreement between the systems at the ankle and knee joints, and consistent waveform but worse agreement at the hip and pelvic joints, which showed systematic offsets. The knee joint angles obtained the best agreement in the static and dynamic trials. The joint kinematics in the transverse plane obtained more inconsistent measurements between the systems. These differences between the systems seem to arise from joint center estimation errors.

Most significant differences in the joint kinetics estimations occurred during the swing phase. Overall, the joint moments and powers showed more inconsistencies and significant differences, which appear to be due to deviations in the segment center of mass and segment joint centers.

The results of this study emphasize the potential and concerns of Theia3D when assessing CP children. The joint kinematics are highly comparable in the sagittal plane, however, more work is necessary to improve estimations in other anatomical planes and the joint kinetics, especially for the use of this technology in clinical settings involving patients with abnormal gait patterns, such as CP patients.

Keywords: cerebral palsy, markerless motion capture system, clinical gait analysis, kinematics, kinetics

Resumo

A locomoção é uma tarefa importante e essencial para uma vida funcional e independente, que parece automática e bastante simples, no entanto, envolve processos complexos: requere músculos para mover os membros, controlo nervoso para a ativação dos músculos, equilíbrio, coordenação motora e muito mais. A capacidade de locomoção pode ser limitada em indivíduos com distúrbios motores, o que lhes acarreta desafios no seu dia a dia.

A Paralisia Cerebral (PC) é a causa mais comum de deficiência motora na infância, e é uma condição bastante complexa, que engloba um grupo de distúrbios permanentes que afetam o movimento, a postura e os músculos. Isto deve-se a lesões cerebrais que ocorrem nas fases mais essenciais para o desenvolvimento do cérebro, isto é, desde a fase perinatal até ao recém-nascimento.

Apesar da lesão cerebral não ser progressiva, sujeitos com PC têm bastantes complicações, como fraqueza muscular, perda do controlo motor seletivo, anomalias no sistema nervoso central, e não existe uma cura. Esta condição afeta os pacientes de formas e níveis diferentes, e por isso, a PC é uma condição bastante heterogénea que apresenta diferentes padrões de marcha.

De forma a melhorar a funcionalidade e a capacidade de realizar tarefas que envolvam o movimento com independência, os pacientes com PC são intensivamente estudados em analise de marcha clínica. Para monitorizar o seu progresso, uma ferramenta muito útil e vastamente utilizada em investigação e em ambientes clínicos é a análise de marcha tridimensional, que permite medir parâmetros da marcha como a cinética e cinemática. De forma a garantir uma análise precisa e detalhada, os sistemas de medição devem ser livres de erros, e a tecnologia utilizada deve ser fidedigna e com elevada precisão.

Sistemas de captura de movimento *marker-based* (MB), ou seja, que utilizam marcadores, têm sido a tecnologia de referência para a analise de marcha desde há muitas décadas, no entanto, a sua imprecisão inerente e limitações praticas associadas dificultam a sua utilização. Algumas limitações advêm da exigência associada à colocação dos marcadores nos sujeitos.

O avanço da tecnologia permitiu o desenvolvimento de sistemas de captura de movimento *markerless* (ML) que utilizam câmaras de vídeo e não necessitam de marcadores, e que são uma potencial alternativa à análise de marcha com sistemas MB. Através de algoritmos de *Machine Learning*, a necessidade de colocação de marcadores para adquirir dados relativos à marcha é eliminada, o que oferece bastantes benefícios práticos e técnicos tanto para os pacientes, como para os profissionais envolvidos na análise de marcha. Existem sistemas ML com aplicações na área da biomecânica. No entanto, os algoritmos utilizados *não* detetam os pontos anatómicos de interesse de forma precisa e adequada para uso em ambientes clínicos. Por outro lado, o Theia3D consiste numa tecnologia ML que utiliza a sua própria base de dados, cujas articulações dos indivíduos presentes nas imagens são identificadas por especialistas com conhecimento na área da anatomia. Além disso, constitui também um processo de duas verificações das imagens e da correspondente identificação das articulações, de forma a evitar erros, para que a base de dados seja o mais precisa possível para o uso na biomecânica. Os sistemas ML também constituem limitações e fatores que afetam a qualidade das suas medições.

A presente dissertação tem como objetivo comparar dados da cinemática e da cinética da pélvis e das articulações do membro inferior em crianças com PC durante a marcha, estimados

com os sistemas MB e ML. Para isso, catorze crianças com diagnóstico de PC, recrutadas através de dois centros de PC, participaram neste estudo. Inicialmente foi realizada uma recolha de dados com ambos os sistemas numa posição estática. Seguidamente, os participantes caminharam num ritmo confortável durante vários ensaios, enquanto os dados foram capturados simultaneamente com 8 câmaras de vídeo e 10 câmaras de infra-vermelhos, todas sincronizadas.

Os modelos utilizados consistiram no modelo CAST no caso da análise MB, que tem 6 graus de liberdade em cada segmento, e o modelo padrão do Theia3D, que constitui 6 graus de liberdade na pélvis e 3 graus de liberdade em cada coxa, perna e pé. Ambos os sistemas estimam as variáveis cinemáticas durante a marcha, e as variáveis cinéticas, normalizadas pela massa, são obtidas por dinâmica inversa.

A normalidade dos dados dos ensaios dinâmicos foi testada através de um teste Shapiro-Wilk no software SPSS *Statistics*, sendo as variáveis cinemáticas consideradas normais e as cinéticas não normais. A análise de dados foi realizada em MATLAB, e para a análise estatística, um teste t bilateral foi executado com um nível de significância de 5%, sendo este não paramétrico no caso das variáveis cinéticas. A raiz quadrada da diferença média (RMSD) de cada variável estimada pelos sistemas MB e ML nos ensaios dinâmicos foram calculadas para cada articulação.

Relativamente ao ensaio estático, a diferença entre os ângulos MB e ML no joelho foi mínima (<2.80º), aceitável no tornozelo (<5.26º) e consideravelmente grande na anca e na pélvis (>9.80º) no plano sagital. Os restantes planos anatómicos obtiveram diferenças aceitáveis no joelho e anca, e bastante reduzidas nas outras articulações.

No plano sagital, os ângulos das articulações do tornozelo e do joelho apresentaram boa concordância e consistência na forma das curvas médias entre os sistemas (RMSD<5.9º). Relativamente à pélvis e à anca, a forma das curvas também foi consistente, no entanto, não houve concordância entre as curvas dos ângulos durante o ciclo da marcha (RMSD>10.0º), com diferenças consideravelmente constantes. Os ângulos da articulação do joelho obtiveram a melhor concordância, com um desvio inferior a 2.8º nos ensaios estáticos, e diferenças reduzidas (RMSD<5.1º) nos ensaios dinâmicos. No plano transversal, foram observadas mais inconsistências entre os sistemas. As diferenças cinemáticas entre os sistemas MB e o ML parecem surgir de erros de estimação dos centros articulares.

A maioria das diferenças significativas nas variáveis cinéticas ocorreram durante a fase de balanço. O momento da articulação da anca obteve a melhor concordância entre os sistemas no plano sagital, mas a pior no plano frontal. A média dos RMSDs dos momentos e das potências das articulações demonstraram baixa concordância entre os sistemas, principalmente no plano frontal (momentos), em que os valores estimados são bastante menores. Em geral, as variáveis cinéticas demostraram mais inconsistências e diferenças significativas, que parecem advir de erros de estimação do centro de massa e dos centros articulares dos segmentos.

O desvio padrão dos RMSDs, tanto nos dados da cinemática como na cinética, demostra uma grande variabilidade entre as diferenças dos sujeitos. Relativamente aos momentos das articulações, existiram grandes diferenças entre os sistemas num participante em particular, o que influenciou bastante os resultados. Além disso, a amostra dos participantes é heterógena pois engloba sujeitos com diferentes tipos de padrões de marcha, o que também pode explicar a elevada variabilidade dos resultados.

Os resultados deste estudo enfatizam o potencial e algumas preocupações do sistema de captura de movimento ML ao analisar as articulações da pélvis, anca, joelho e tornozelo durante

a marcha de crianças com PC. A cinemática demonstrou ser um parâmetro bastante comparável entre os sistemas no plano sagital, no entanto, é necessário continuar a investigar e trabalhar para melhorar a cinemática das articulações nos outros planos anatómicos e a cinética das articulações do membro inferior, especialmente para o uso da tecnologia Theia3D em ambientes clínicos que envolvam pacientes com padrões anormais de marcha, como pacientes com PC.

Palavras-chave: paralisia cerebral, análise de marcha clínica, sistemas de captura de movimento markerless, cinemática, cinética

Table of Contents

List of Figures

List of Tables

List of Acronyms

2D	Two-Dimensional
3D	Three-Dimensional
CAST	Calibrated Anatomical Systems Technique
CGM	Conventional gait model
CNNs	Convolutional Neural Networks
COM	Center of mass
CP	Cerebral Palsy
DOF	Degrees of freedom
GA	Gait Analysis
GMFCS	Gross Motor Function Classification System
ID	Inverse Dynamics
IOR	Istituti Ortopedici Rizzoli
IK	Inverse Kinematics
MB	Marker-based
ML	Markerless
MOCAP	Motion Capture System
PAF	Project Automation Framework
QTM	Qualisys Track Manager
RMSD	Root Mean Square Difference
SCPE	Surveillance of Cerebral Palsy in Europe
SPM	Statistical Parametric Mapping

1 Introduction

1.1 Context and Motivation

It is true that each human is a unique individual, however, it is also true that there are daily tasks that all of us include in our routine, such as getting out of bed or getting dressed. Every day, people walk, sit down, stand up and climb stairs mostly without thinking. Daily living activities, which most people take for granted, may be impossible or very challenging to perform for people with impairment disorders.

Cerebral Palsy (CP) is a movement disorder that affects the muscles, posture and the subject's mobility. For them, gait can be a very complex task since it requires movement coordination and muscle activity. It is incurable, however with rehabilitation, treatment and research, it is possible to improve their quality of life and maximize, within the possible, their mobility.

Biomechanical gait analysis (GA) is a procedure that allows professionals to determine a diagnosis, an adequate treatment, monitoring of the condition, and if necessary, a surgery plan. The marker-based (MB) motion capture system has been the system of reference for instrumented GA for many years, however it still needs many improvements to provide better and more accurate results for patients, clinicians and healthcare professionals.

Nowadays, innovation is largely driven by technology. Information and knowledge have never been so available for access, so it is important to use these advantages to innovate in healthcare, which is crucial for improving health outcomes. Both patients and professionals would benefit by the development of devices that could make GA more time-efficient and convenient, and at the same time, improve patients' lives.

Markerless (ML) motion capture systems are innovative technologies that use algorithms to detect human body segments and their movement during GA. It provides many advantages and removes the inconveniences of the MB system. Its automation reduces human errors and enhances efficiency of the procedure. Recently, researchers have shown increasing interest in this technique, which has been assessed in healthy subjects and obtained similar kinematics results to the MB system. Nevertheless, there is the need to assess the feasibility of ML systems for subjects with gait impairments before using it in clinical settings.

The motivation of this dissertation is to study whether ML systems estimate the biomechanics parameters of the pelvic and lower limb joints of CP children similarly to MB systems. This research intends to contribute to the validation of Theia3D, used in the Biomechanics and Functional Morphology Laboratory (FMH). This is fundamental so that in the future, these children can have access to faster and more comfortable sessions of GA, whilst researchers and healthcare professionals, can substitute the time-consuming tasks by other important tasks to focus on the improvement of these children's quality of life.

1.2 Goals and Research Questions

The main goal of this dissertation is to determine whether the markerless motion capture system is as accurate as the marker-based motion capture system when assessing the pelvic and lower body kinematics and kinetics of subjects with CP during gait. In that case, this would be a step towards the validation of markerless motion capture to substitute the current reference method to analyze walking movements of patients with mobility impairments, which would provide many advantages for clinical patients, clinicians and researchers. To achieve this goal, the two research questions are listed below:

Table 1.1. Research questions of the dissertation.

Research Questions
1. How accurate does the markerless system measure the joint kinematics of children with Cerebral Palsy compared to the marker-based motion capture system during the static and the dynamic trials?
2. How accurate does the markerless system measure the joint kinetics of children with Cerebral Palsy compared to the marker-based motion capture system during the dynamic trial?

Table 1.2. Main goals of the dissertation

Goals
1. To compare the joint kinematics, such as the angles of the ankle, knee, hip and pelvic joints obtained with marker-based and markerless motion capture systems during the static and dynamic trials.
2. To compare the joint kinetics (moments of force and power) of the ankle, knee, hip joints for both motion capture systems during the dynamic trials.

1.3 Structure of the dissertation

The structure of this dissertation is arranged into six chapters, which are briefly listed below:

Chapter 1 consists of the introduction, that presents the context and motivation of this dissertation, the goals, research questions and the structure of the document.

Chapter 2 contains a literature review on Cerebral Palsy, its associated gait deviations, and a relevant background about instrumented gait analysis. A research review on the marker-based motion capture system and its current limitations, and the markerless motion capture systems, more specifically Theia3D, is introduced.

In Chapter 3, the experimental procedures to collect and process the data are explained. The characteristics of the participants, the inclusion criteria, as well as the ethical approval are also included. The chapter also describes the data analysis and statistical analysis of the study.

Chapter 4 shows the comparison results of the gait analysis between the marker-based and markerless motion capture data. This chapter presents the kinematic measurements during the static trials, and the kinematics and kinetics during the dynamic trials.

Chapter 5 discusses the outcomes of the experimental study and compares them with findings from the current literature. A discussion about the results and the concerns associated are also displayed.

Finally, Chapter 6 summarizes the most relevant findings of the thesis and provides comments and future directions for this research topic.

2 Literature Review

2.1 Cerebral Palsy

CP is the most common cause of motor disability in childhood affecting approximately 700000 European citizens and 17 million individuals worldwide, with a prevalence between 1.5 and 3.0 cases per 1000 live births [1][2][3]. CP is not considered a disease, it is a description of a group of permanent disorders that affect movement, posture and muscle tone, due to a brain injury that occurs through the stages of perinatal to neonatal, which are crucial phases for brain development [4][5][6]. In 1964, Bax defined CP as "A disorder of posture and movement due to a defect or lesion in the immature brain", which has been the most frequently cited definition of CP [7]. It is a simple definition with the goal of being universally accepted, easily translated and understood by other languages.

The complexity of the motor impairments can be related to primary and secondary abnormalities. The primary impairments include muscle spasticity, weakness and loss of selective motor control, and secondary deficits are muscle contractures and bony deformities [4][8]. The injury is non-progressive, however, there are several secondary conditions that can negatively affect the functional capability of the child [6][9]. CP is also frequently associated with other complications related to sensation, perception, cognition, communication, behavior, and by epilepsy and secondary musculoskeletal problems [5].

This chronic neurodevelopmental disorder is characterized by heterogeneity in various aspects, such as etiology, risk factors, severity, type of disability, and other relevant considerations [10]. Patients with CP can be very different. Approximately 75% of children with CP are ambulatory [8]. Some individuals play professional sports, achieve a high level of education and live healthy lives, whereas others may never roll or speak, and require assistance from others to perform daily life activities throughout their lifetime [11]. Due to this extreme diversity, there has been a proposal to consider CP as a spectrum disorder instead of a unitary clinical condition [11].

There are several factors that can increase the risk for CP, such as congenital brain malformations and genetic predisposition [9]. Low birthweight and prematurity are the most important neonatal risk factors [4][9][12]. There are multiple causes for CP, but even though there is no cure, there have been advances in research and technology to provide treatment, rehabilitation strategies and assistive devices for these patients. CP is a lifelong disorder but most of the research focuses on the needs of the children [4].

2.2 Classification of Cerebral Palsy

There are many classification methods for individuals with CP. The Surveillance of Cerebral Palsy in Europe (SCPE) classification system is considered the benchmark and has been widely used internationally for research and clinical purposes. This simple and reliable system is illustrated in Figure 2.1. It categorizes CP into clinical types based on motor impairments that affect movement and posture, which can be of three different types: Spastic, Ataxic and Athetoid (or Dyskinetic) [5].

Spastic CP is the most prevalent type, as it occurs in 70-80% of the CP children. It affects the limbs causing muscular hypertonicity, stiffness, tightness, weakness, tremors and increased deep tendon reflexes [3][12][13]. Spasticity leads to gross movements oppositely to fine and individual movements, also, voluntary movements become slower and challenging [14]. Spastic CP can be bilateral or unilateral. If the limbs on both sides of the body are affected, it is bilateral, whereas unilateral only involves limbs on one side of the individuals' body [3]. Scissors gait with toe-walking is a characteristic gait pattern of this type of CP [13].

The Athetoid type is characterized by involuntary movements, which cause fine motor skills of the hands, feet and arms to be abnormally slow [15]. In addition, the execution of daily activities by this type of patients can be compromised by tremors. Within this category, children can have a Dystonic CP, if there is hypokinesia (muscle stiffness) and hypertonia (increased muscle tone). This subtype is characterized by the contraction of both agonist and antagonist muscles at the same time [14]. On the contrary, hyperkinesia and hypotonia characterize what is called Choreo-athetotic CP [3]. In this case, muscles including the proximal extremities and digits have fast disorganized and unpredicted contractions [14].

Finally, Ataxic CP is marked by an impaired balance and lack of muscle coordination that leads to a performance of movements with abnormal force, rhythm, and accuracy [3][15][16]. Additionally, the execution of daily activities that require fine motor skills, such as writing, can be compromised by tremors [13][15]. It arises from disturbances in the cerebellum and can lead to a wide-based gait [12][15]. Also, ataxia is rare and generally improves with time [14].

Some patients have a combination of the three types [15].

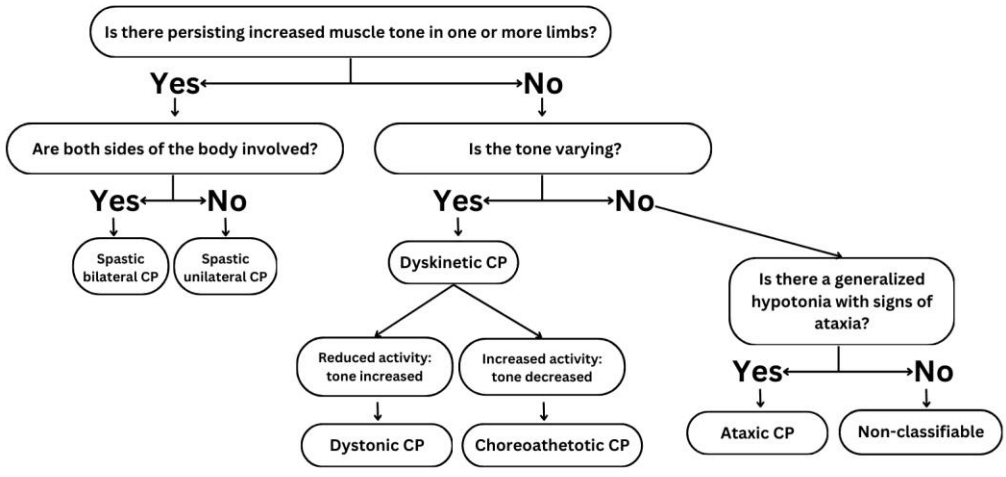

Figure 2.1. Hierarchical decision tree for classifying CP types. Adapted from SCPE [3].

CP classification can also be based on the specific anatomical regions that are affected in the body: monoplegia, hemiplegia, diplegia, triplegia and quadriplegia [5].

Monoplegia means that one limb is impaired, which is commonly a lower limb. Hemiplegia implies that both upper and lower limbs of one side of the body are affected, and in most of the cases, the upper limb is the most affected.

Diplegia involves the lower and upper limbs of both sides, however, the lower limbs are more affected than the upper limbs. Triplegia represents a bilateral impairment of the lower limbs and a unilateral upper limb involvement. The side of the affected upper limb is usually the most affected side in the lower limb. Quadriplegia, or tetraplegia, corresponds to both upper and lower limbs being compromised, with the possibility of complications extending to the trunk, face, and mouth of the patient [4][13]. According to SCPE, the term bilateral includes the topographical types of diplegia, triplegia and quadriplegia, and unilateral incorporates monoplegia and hemiplegia in the context of CP [4]. Figure 2.2 illustrates the mentioned topographic description.

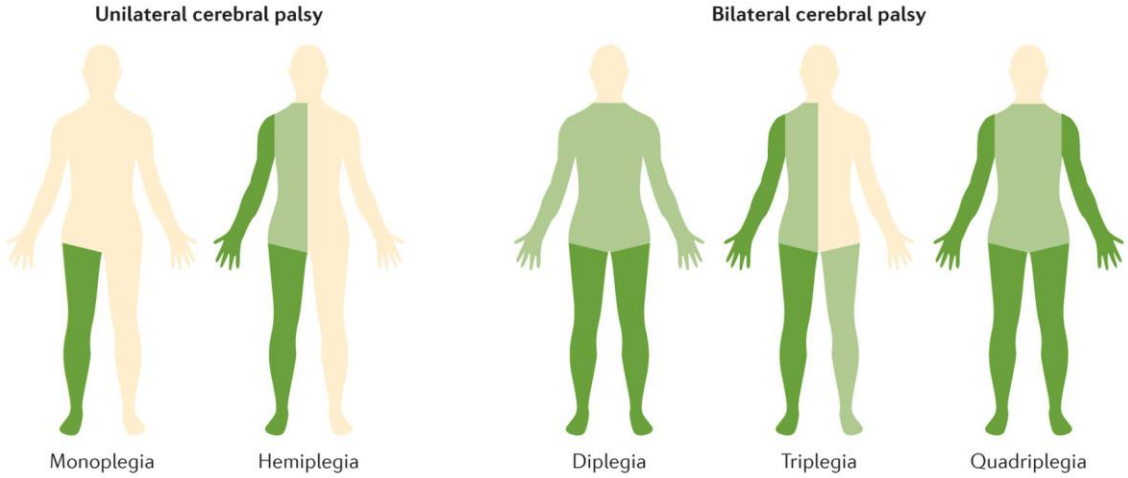

Figure 2.2. Representation of the topographical description in CP [4].

The Gross Motor Function Classification System (GMFCS) for CP is a five-level scale based on self-initiated movement that focuses on the children's mobility and their need for assistance to perform movements such as sitting and walking. Also, the patients are categorized according to their age [17][18]. The lowest level suggests minimal disability, while level 5 implies that the child is limited and constantly requires assistance of a device, such as a wheelchair [17][18]. Compared the previously mentioned classification systems, this focuses on determining the level of activity status at home, school, their participation on society, and not to assess the type and distribution of the impairments or the quality of the movements of CP children [17].

CP Classification approaches enhance communication among health care professionals and optimize treatment planning, allowing personalized interventions to the specific needs of the children.

2.3 Gait Cycle

The gait cycle consists of a sequence of coordinated movements of the lower limbs, that allow an individual to walk or just move forwards, while maintaining stance stability [19]. There is not a specific moment that starts or ends this cycle, which means that any event can be selected as a reference beginning point during gait analysis (GA) [19]. Conventionally, the gait cycle is considered to start when the first contact between the foot and the ground happens, ending in the next same event. In a typical gait, this moment is called heel-strike, which is when the heel lands on the floor. However, individuals with disabilities may not be able to make their first contact with the heel, hence, foot contact or initial contact are the most suitable terms for this event [19][20].

The gait cycle is constituted by the gait phases: a stance and a swing phase. In normal gait, the stance phase constitutes 60% of the cycle, during which the foot is in contact with the ground, serving as a mobile source of support, whereas the swing phase covers the period when the foot is in the air advancing to a new support site [19]. The gait cycle and its subdivisions can be seen in Figure 2.3. The stance phase starts with foot contact and ends with the foot preparing to leave the ground, also referred as toe-off [20]. Three segments subdivide the stance phase: it starts and ends with a double support, meaning that both feet are in contact with the ground. In between, there is a single limb support when only one foot is on the floor [19][20].

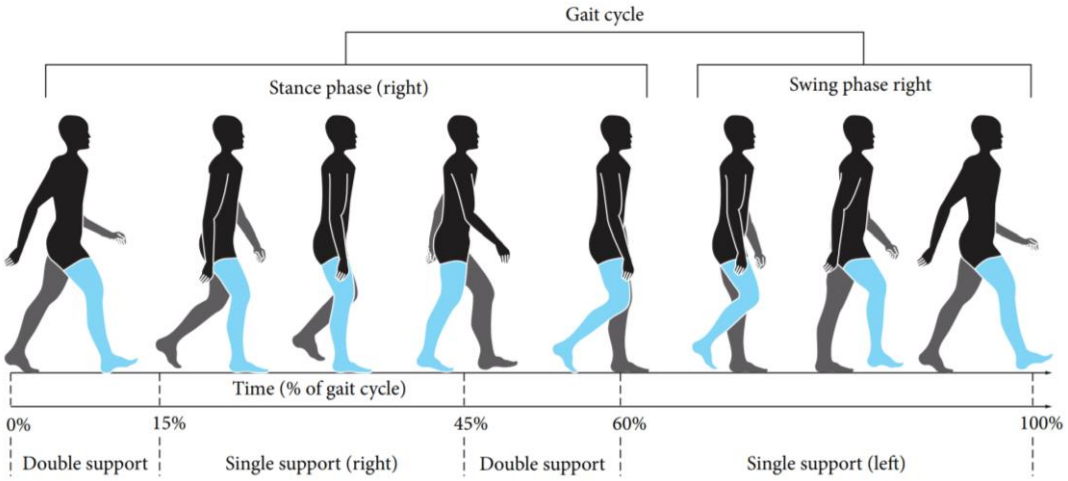

Figure 2.3. Gait cycle and its subdivisions. The reference limb is represented in blue [21].

For a more detailed description of the gait cycle, it can be further subdivided into eight segments. The initial double support comprises the initial foot contact and the loading response, in which the individual's body absorbs the shock of impact and its weight gets distributed between both feet, one being in foot contact while the opposite foot is in toe-off. Following, the single limb support includes the mid-stance phase, which is when the foot on the ground supports the body weight entirely, and the terminal stance occurs as the body continues moving forwards over the stance foot until its heel begins to rise. Finally, the last subdivision of the stance phase is the terminal double support, which starts with the reference foot in toe-off to be lifted in the swing phase and the body weight begins to shift to the opposite leg which is preparing for opposite foot contact. The late stance phase starts at approximately 50% of the cycle and ends with the toe-off [22]. The stance phase is also referred as a step, and a complete gait cycle, which consists of a step following another step of the opposite foot, is also known as a stride [20]. The swing phase can be subdivided into three intervals initial, mid and terminal.

2.4 Gait patterns in Cerebral Palsy

CP children can exhibit a variety of gait deviations, which are not discrete and can fall between the defined categories. Although classification systems are regularly used to group common gait deviations of CP, they fail to include the full spectrum of deviations and their combinations.

Drop foot, or foot drop, can occur unilaterally or bilaterally, and it refers to the lack of capability to dorsiflex the foot and to actively lift it against gravity [23]. The characteristic plantar flexion of the ankle during swing phase results in a failure to make foot contact using the heel, potentially leading to an equinus deformity at foot strike [24]. Patients with this gait deviation have both stance and swing phases affected since there is a compensatory hyperflexion of the knee at foot strike, leading to a hyperflexion of the hip joint, as well as medial rotation of the foot [24][25]. These adjustments aim to lift the forefront of the foot and to avoid it catching on the ground, which results in incorrect loading of the skeletal axis [23].

Equinus gait is associated with the range limitation of ankle dorsiflexion or plantarflexion, and it can be subdivided based on the nature of this restriction. True equinus refers to a full extension of the knee and hips along with ankle plantarflexion (equinus) during the stance phase. In addition, the pelvis can be tilted anteriorly or within its normal range [26]. On the other hand, apparent equinus consists of a normal range of dorsiflexion of the ankle, whereas the knee and hip are excessively flexed during the stance phase, leading to a toe-walking gait and giving impression of equinus [26]. The pelvis can be normal or anteriorly tilted.

Another gait pattern is called the jump gait, and it is described as an excessive flexion of the knee and hip in early stance and an extension in a variable degree towards the end of the stance phase. Also, the ankle is in equinus, and the pelvis can be tilted anteriorly.

Finally, the crouch gait is characterized by an excessive dorsiflexion of the ankle during the stance phase in combination with excessive flexion at the knee and hip [3][26].

CP Children are frequently submitted to clinical procedures that are planned based on their gait patterns, which is why it is essential to accurately assess them. The mentioned gait patterns are represented in Figure 2.4.

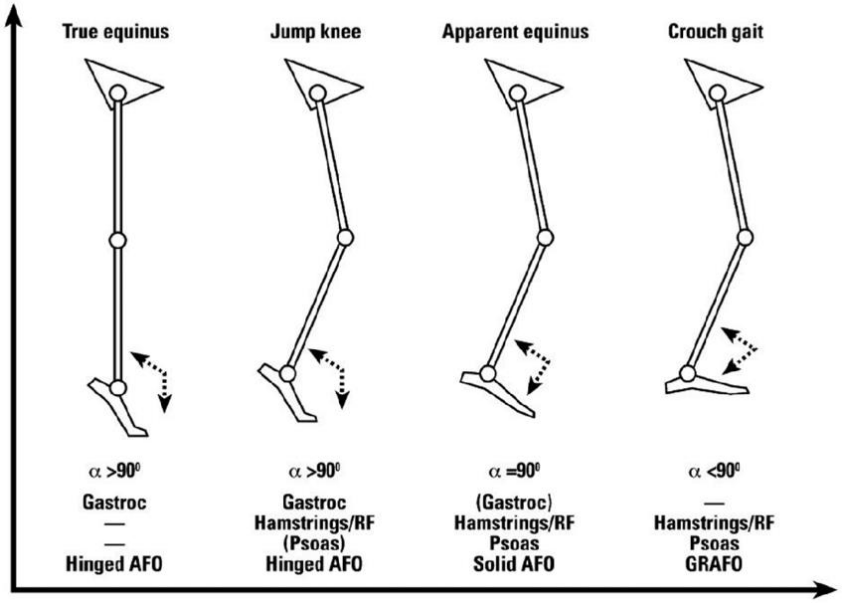

Figure 2.4. Gait patterns in Cerebral Palsy (true equinus, jump knee, apparent equinus and crouch) [27] .

2.5 Instrumented gait analysis

Motion capture (MOCAP) is "the process of recording a live motion event and translating it into usable mathematical terms by tracking a number of keypoints in space over time and combining them to obtain a single three-dimensional (3D) representation of the performance" [28]. It is an important process in biomechanics research studies, having many applications in this field and others, such as entertainment, robotics, and medical simulation.

Instrumented GA uses MOCAP technologies to record and model the movements of a subject, while performing specific tasks according to what needs to be studied. There are four main types of data that can be recorded simultaneously: spatiotemporal, kinematics (represents the motion analysis of a rigid body), kinetics (represents body moments of force and forces) and neuromuscular activity, which is measured by electromyography [8][16].

Kinematics is the study of body motion, providing insight about parameters such as velocities and angles of the joints, while kinetics studies the forces that produce the motion. Joint moments measure the rotation effect of a force that acts on a joint to produce the rotation movement, and joint powers provide information about the power absorption and generation of the muscles at the joint [29][30].

The joint kinematics and kinetics of gait impaired subjects may be different from able-body individuals, which is why it is fundamental to assess them [29]. With the acquired data, researchers and clinicians can analyze gait parameters to quantify and understand what impairments affect it. There are many parameters to study, some examples are the joint angles, the ground force reaction or the duration of the gait phases. Based on the results, it is possible to study the abnormal mechanics of the body associated with musculoskeletal disorders, such as CP, and determine an accurate diagnosis [31][32]. Also, it enables a better treatment planning, the development and evaluation of rehabilitative treatments, and preventive interventions for patients with complex gait disorders [8][33].

This process is widely accepted as a research tool, however, there is a continuum debate about its clinical use, which remains variable yet still important. Factors that affect its clinical practice include the fact that the existent technology may not be adequate to encompass various clinical disorders and the complexity of the performed tests and of the generated reports. In addition, the organizational aspects of the laboratories and the understanding of researchers and clinicians of the obtained results are other examples. The costs and the necessary time for data collection, processing and interpretation are also a significant challenge for its clinical value [34]. There is an increasing need for medical research for healthcare professionals to be able to to rely on to make better and informed decisions, and provide the best care for patients [32][35].

In the past decade, the field of GA has observed increasing research, as well as the development and improvement of new technologies, data collection and analysis methodologies. 3D GA holds a very important role to accurately define gait impairments and their causes, to define diagnostic groups and understanding expected treatment outcomes for different types of patients. Also, it improves agreement between different clinicians, as well as it increases their confidence in their treatment planning, allowing them to prescribe appropriate treatments. There is also strong evidence that it is very efficient in facilitating the change and reinforcement of treatment decision-making in multiple patient populations [32]. Instrumented clinical GA guarantees a more quantitative, repeatability and objective measurements when compared with observational GA [36][35].

There is a very wide range of different 3D MOCAP systems to perform GA, and most common approaches require a laboratory environment, the attachment of markers, fixtures or sensors to the body

segments, such as the marker-based (MB) MOCAP systems [37]. The number of gait laboratories has been increasing but cohesive information about the reliability of the gait measurements from the MOCAP systems and models remain limited [38]. For an appropriate analysis and interpretation, the reliability and validity of these measurements should be known [38][39][40].

2.6 Marker-based motion capture systems

MB MOCAP systems are currently considered the reference method for clinical GA, and they have been used for decades [36][41][41]. This technique requires the use of markers and cameras that capture infra-red light, allowing 3D motion tracking and further analysis using rigid bodies modelling software. Qualisys Track Manager (QTM) and Vicon have been the most common systems used for data acquisition [42].

MB MOCAP systems provide fairly accurate human motion data, which depends on different aspects of the experimental setup, such as the relative distance between each camera and between the cameras and the markers. The amount, type and location of the markers, as well as their motion within the capture volume also affect the accuracy of the measurements [43]. Also, there is a trade-off between the camera resolution and sample frequency [44]. This tool has been very valuable to accurately assess patients with CP and to provide useful information. Most systems model each body segment as a rigid body and use markers to create anatomical axes for each reconstructed segment. Hence, a correct marker placement is essential to accurately define the planes of movement and to estimate the correct movements [45].

The markers define the location of a specific anatomic landmark and allow to create a biomechanical model on a computer, which is the 3D reconstruction of the human movement. With the progress of technology over the years, different marker sets and models have been developed [46][47][48].

2.6.1 Marker sets

The conventional gait model (CGM) includes a group of very similar models, and it has been the most used lower limb model in clinical GA for over 30 years [46]. It divides the body into seven segments (1 pelvis, 2 thighs, 2 shanks and 2 feet), which are linked by joints [20][46]. These joints are considered to have 3 rotational degrees of freedom (DOF) [20]. The segments of this model are hierarchically organized from the pelvis to the feet, which imposes a constraint. This means that in case it is not possible to define a segment, which can happen due to an error, it will not be possible to define its distal segments either. For example, if markers are missing on the thigh, its distal segment (shank) will also not be reconstructed, and so on [20][46]. For this reason, there is the need to use the entire model, even when only one segment needs to be studied [46]. Also, in the case of estimation errors in a joint angle calculation, the error will propagate to its distal joints [48][49]. An important limitation is the fact that the CGM is not suitable for direct use on subjects with anatomical deformities or prostheses [50].

In clinical GA, the CGM has had many variations and can also be referred by many names, such as Plug-in Gait model and Helen Hayes (HH) [46][51]. However, due to limitations of these models, alternatives have been worked on. Models with 6 DOF have the advantage of not being hierarchical like the CGM, defining each segment independently with rotational and translational movement at each joint [20][52]. This group of models are the main replacement of the CGM, considering software like

Visual3D (Has-Motion, Canada) are based on their implementation for GA [20]. Some examples of 6 DOF models are the Calibrated Anatomical Systems Technique (CAST) and the Istituti Ortopedici Rizzoli (IOR) model [20]. These models also often use multiple skin-mounted markers on the thigh and shank [20].

At a joint, the placement of at least three markers allows to define the orientation of the segments in space. The CGM only requires 2 markers on each segment and for that reason, 6 DOF analyses are not possible [50]. The full body IOR marker set is constituted by 36 markers, while the lower limb model requires 26 markers [53]. Having a greater number of markers enables the creation of 6 DOF for each segment.

The CAST marker set also provides the ability for each segment to be modelled with 6 DOF [54]. A marker cluster is the term that describes the combination of three or more markers that are proximate to each other, and within a single segment [45][54]. In this marker set, clusters are placed in both left and right thigh and shank segments, constituted by four markers each. The number of DOF of a cluster is equivalent to the number of its markers multiplied by three, which in the case of the CAST marker set is twelve DOF. The high amount of DOF results in redundant data, with more variables than the necessary to estimate position, however, the model uses this redundancy to optimize pose estimation in each instance of time, improving accuracy and reliability [54]. The use of clusters facilitates the marker placement process, and it minimizes skin movement artifacts [55]. Figure 2.5 illustrates the placement distribution of the markers of the CAST marker set, and it includes the description of each marker.

Qualisys PAF package: CAST lower body marker set[1]

QUALISYS

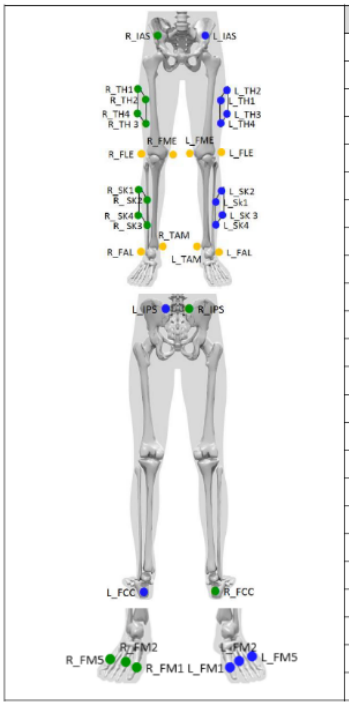

Name	Ref. [2]	Location	Static (36)	Dyn. (28)
L_IAS	IAS	Anterior superior iliac spine	X	X
L_IPS	IPS	Posterior superior iliac spine	X	X
R_IPS	IPS	Posterior superior iliac spine	X	X
R_IAS	IAS	Right anterior superior iliac spine	X	X
L_TH1-4		Cluster	X	X
L_FLE	FLE	Lateral epicondyle	X	
L_FME	FME	Medial epicondyle	X	
L_SK1-4		Cluster	X	X
L_FAL	FAL	Lateral prominence of the lateral malleolus	X	
L_TAM	TAM	Medial prominence of the medial malleolus	X	
L_FCC	FCC	Aspect of the Achilles tendon insertion on the calcaneus	X	X
L_FM1	FM1	Dorsal margin of the first metatarsal head	X	X
L_FM2	FM2	Dorsal aspect of the second metatarsal head	X	X
L_FM5	FM5	Dorsal margin of the fifth metatarsal head	X	X
R_TH1-4		Cluster	X	X
R_FLE	FLE	Lateral epicondyle	X	
R_FME	FME	Medial epicondyle	X	
R_SK1-4		Cluster	X	X
R_FAL	FAL	Lateral prominence of the lateral malleolus	X	
R_TAM	TAM	Medial prominence of the medial malleolus	X	
R_FCC	FCC	Aspect of the Achilles tendon insertion on the calcaneus	X	X
R_FM1	FM1	Dorsal margin of the first metatarsal head	X	X
R_FM2	FM2	Dorsal aspect of the second metatarsal head	X	X
R_FM5	FM5	Dorsal margin of the fifth metatarsal head	X	X

[1] Cappozzo, A., Catani, F., Della Croce, U., Leardini, A. (1995). Position and orientation in space of bones during movement: anatomical frame definition and determination. Clinical Biomechanics, 10, 171-178.
[2] Sint Jan, S. Van (2007). Color Atlas of Skeletal Landmark Definitions. Guidelines for Reproducible Manual and Virtual Palpations. Edinburgh: Churchill Livingstone.

Copyright © Qualisys AB

Figure 2.5. CAST marker set. Markers in green and blue represent the right and left sides of the body, respectively. Yellow markers are required for the static trial but can be removed for the dynamic trials [56].

2.7 Limitations of marker-based motion capture systems

Despite MB MOCAP being the most used method for GA all over the world, there are limitations associated with it [36]. Firstly, it is expensive, since it needs several equipment such as cameras, markers, calibration equipment, mounting hardware, software and others. Also, this method requires a laboratory environment, which means there is reduced accessibility, and its conditions can cause unknown experimental artifacts. In a laboratory, it is not possible to replicate all real life scenarios, affecting the natural pattern of movements [45].

The markers must be placed in specific anatomical references of the body, which requires physical palpation to identify bones and joints, and for this reason, there is the need for a skilled professional with anatomical knowledge to perform this procedure [36]. Furthermore, since CP can affect patients in several different ways and in different limbs, this group of patients can have anatomical differences when compared to healthy individuals. Thus, surface landmark identification can be harder for the researcher, leading to wrong segment definition. Marker misplacement due to lack of experience is one of the greatest sources of error in motion analysis, more than equipment error or skin movement artifact [57]. The process of marker placement as well as the acquisition of data can be time consuming, especially because the markers can move or fall due to a lot of factors, such as sweating, body movement or poor adhesion of the markers to the body [36][34]. Additionally, CP children may use orthotics, which change the geometry around the foot and ankle, as well as walking aids, which can occlude the markers from the camera views [42].

Calibration of the cameras is a crucial step for an accurate capture of data and sometimes it needs to be repeated, prolonging the process. There are many more factors that contribute to the complexity of the MOCAP setup, turning it more time consuming and affecting the naturalness of the patient's motion [36]. Even though this technology is considered accurate, there are some constrains associated that could be removed to achieve optimized results and to provide better treatment for the patients. This group of factors restrict the assessment of subjects in large scale applications, such as clinical and real word environments in case this setup is not accessible, affordable, or practical.

2.8 Markerless motion capture systems

As technology evolves, new systems are developed to minimize errors and erase limitations that can have a negative effect on the outcomes of human GA. Markerless (ML) MOCAP systems are an innovative technology that measures human motion and overcomes practical constrains by eliminating the need for placement of markers [38][42][58].

ML MOCAP systems are divided into two main types of camera hardware, such as depth sensor-based and standard video-based systems. Depth cameras record video and use infra-red light to obtain a depth map, which represents the distance between each pixel and the camera [59]. An example of a commercialized system with an application in entertainment is the Microsoft Azure Kinetic (Microsoft, Washington, USA) [60]. This type of cameras is considered cheap and accessible, but they have limitations associated with the capture rate and capture volume, and the lightning conditions must be controlled. Additionally, there are many studies that compare the depth sensor-based MOCAP to the MB MOCAP, and findings showed large differences between them, which leads to the conclusion that depth sensing cameras have low accuracy for pose estimation in biomechanics research purposes [61][62][63].

On the contrary, video-based ML MOCAP systems are not limited by the sunlight or by the lightning conditions as the systems with infra-red cameras are. Nevertheless, just like any video camera, light can still affect the quality of the video data. The process of data collection and data processing is

similar to the traditional GA, since it can be done with the same software [42]. However, these systems use standard red-green-blue (RGB) video cameras, which offer many advantages [36][42]. As an example, smartphones could be used to record the video data at home or outside, without limiting the environment of acquisition, and it would be a low-cost process. Nonetheless, a precise motion GA requires high accuracy, so systems with synchronized and high quality multi-camera are necessary in the biomechanics laboratories.

ML MOCAP systems are based on computer vision and deep learning algorithms to estimate keypoints such as joint centers and other anatomical landmarks for each pose of the subject. The pose estimation algorithms are trained using Convolutional Neural Networks (CNNs), to perform calculations on the pixels of each image from the training dataset, and to identify the points of interest. The calculations are associated with patterns of color, gradient and texture of the pixels in the training data [59][64]. After training the model with the training dataset, the systems can estimate anatomical landmarks from new images. Thus, the more precise the training data, the better will be the pose estimation algorithm of the system.

Some advantages of the use of algorithms to detect the anatomical points of interest are that it obviates most manual-executed tasks that would be required with the MB methods, such as the marker placement, and it reduces associated error sources [41][65]. It also eliminates variability among different assessors and enhances objectivity of MOCAP [66]. Most approaches do not describe the relationship between the points of interest and the anatomy clearly, and do not describe the chosen model for Inverse Kinematic (IK) approaches [67].

There are open source pose estimation algorithms that have been developed and their use has been growing in biomechanics research, specifically OpenPose [67] and DeepLabCut [58][68]. OpenPose is a technology that can track multiple individuals in one image and biomechanical researchers consider it easy to use [69]. DeepLabCut mainly focuses on pose estimation of animals but also allows human GA. It allows users to re-train a pre-trained pose estimation algorithm by adding a set of manually labeled images that are specific to the task or movement of interest [59]. Also, it uses DeeperCut's [58] feature detectors, which is an accurate software that uses three public datasets, constituted by over 19.000 training data and over 7.000 testing data to train and test its neural network architecture for two-dimensional (2D) estimation poses [70].

By combining synchronized multiple cameras that estimate 2D pose estimation, ML MOCAP can identify 3D human joint center locations. These systems are more expensive than using a single camera but can replicate the same procedure as a traditional MB MOCAP system [69]. The OpenPose algorithm has been compared to the MB MOCAP system, and authors found a 1.0 to 5.0 cm average difference in joint center position estimations [69][71][72]. During the walking movement the average joint differences were from 1.0 to 3.0 cm between the two systems. A study that conducted a comparison between the lower limb MB MOCAP and several pose estimation algorithms, including OpenPose and DeepLabCut, indicated that during gait, the OpenPose and AlphaPose [73] algorithms obtained the smallest joint center differences (1.6-3.4 cm) compared to the MB system [74]. Additionally, the largest systematic differences were observed at the hip joint for all of the ML systems in the study.

Without the need of makers, motion analysis becomes more convenient and time efficient, considering it does not require training for marker placement or an expert to do so (however, the need for an expert to perform the clinical examination is still required). In addition, the setup time is reduced and the patient's movements during the trials do not get affected by the markers, which turns the process of data collection easier, more consistent, and reliable [42].

2.8.1 Theia3D

Theia3D (v2023.1.0.310, Theia ML Inc., Kingston, ON, Canada), is a commercially available pose estimation software that uses ML MOCAP. Recently, its popularity has been growing in the domain of biomechanics [75]. Instead of markers, it uses deep CNNs to recognize human motion through multiple 2D video cameras. Then, it performs a 3D pose estimation using the 3D coordinates obtained by the triangulation of the 2D positions of the points of interest in the video [55][59][75]. Theia3D requires at least six cameras but recommends the use of at least eight, which must be synchronized and calibrated to capture new video data. Multiple subjects can be analyzed at the same time. However, since it is a post-processing ML MOCAP solution, it cannot perform real-time human tracking [76].

Unlike the previously mentioned pose estimation algorithms, Theia3D is a proprietary algorithm, not an open source. It estimates 51 anatomical features and joint locations in new images, however, the exact keypoints used have not been detailed [77]. Open source datasets are not labeled specifically by anatomical experts but by recruited labelers from general population, which can lead to wrong identifications and consequently to major errors in joint center estimations and poor accuracy for biomechanical studies [74]. Additionally, a second verification step is not always implemented on the labeled images, which can lead to inconsistencies in the open source algorithms [78]. On the contrary, Theia3D's CNNs were trained on publicly available digital images of over 500000 humans in different environments, clothing and performing different tasks. These images were manually labeled by experts with anatomical knowledge and went through quality control by at least another expert [77]. This aims to ensure precision in the detection of the keypoints.

This software has attracted interest from clinical gait laboratories due to its many advantages. The duration of data collection depends on the task of interest, but it can take less than five minutes to collect ten walking trials [66]. Also, it does not require a laboratory environment, since markers, infrared light cameras, and controlled lighting conditions are eliminated. This would allow to analyze subjects performing movements in different environments, for example, in sports centers, or while clinical patients are at home walking naturally. Soft tissue artifact and marker placement variability do not influence the results of Theia3D due to the replacement of the markers by the algorithms to estimate the joint keypoints. The system does not require the subject to wear tight-fitting clothes, due to its ability to estimate the joint centers and segments with video data and algorithms, which would improve motion GA in clinical and real world applications [59]. Tight clothes can make the subjects can feel more uncomfortable, interfering with their natural movement pattern, and reducing the accuracy of the data.

This system has shown significant progress in both processing time and accuracy [66]. There have been studies that research repeatability and concurrent validity of Theia3D in healthy adults and have shown that spatiotemporal parameters and joint kinematics in the sagittal plane are similar to MB MOCAP. However, the literature mainly focuses on studying the joint kinematics in the sagittal plane during gait and fails to address the joint kinematics in the other anatomical planes, such as the frontal and transverse planes.

To determine if markerless systems, particularly Theia3D, can accurately assess children with CP, studies comparing the joint kinetics computed with the MB and ML MOCAP systems should also be conducted. Kinetic variables give important insight information about the cause of the movement. Also, there is still the need for testing Theia3D in individuals with disabilities, such as CP, since the participants of most studies are healthy individuals with typical gait patterns, unlike CP children [36][65][66][77].

3 Methods

3.1 Participants

This project took place at the Biomechanics and Functional Morphology Laboratory of the Faculty of Human Kinetics of the University of Lisbon.

A sample of fourteen children, 10 males and 4 females, with an average body mass of 44.95 ± 14.07 kg and an average height of 1.49 ± 0.14 m, were recruited to participate in this study from two Portuguese CP centers. The participants' average age was 16.14 ± 5.79 years old. The characteristics of each participant are summarized in Table 3.1. Inclusion criteria for this project were to be diagnosed with CP and to be aged between 8 and 25 years old. Participants that required assistance of a person or a walking aid to execute the requested task, were excluded from this study. It was recommended for participants to wear comfortable sport shorts and a sports bra for females. They were also asked to be barefoot during the session, since it was necessary to place markers on the foot and ankle. During the sessions, four assessors were present: a biomechanics research expert, a research trainee, and two orthopedic specialists.

The protocol was approved by and executed in accordance with the Faculty of Human Kinetics Ethics Committee (CEFMH-2/2019). An informed consent was previously signed by the parent or the legal guardian of the participant, and the child assent was also obtained after explaining the entire protocol.

*Table 3.1. Characteristics of participants. *Participant 14 was included in the study because of the presence of a gait pattern.*

	Age	***Mass (kg)***	***Height (cm)***	***Affected Side***	***Sagittal gait pattern***
1	13	52.0	157.0	Both	Severe Toe In
2	13	50.0	145.0	Both	Severe Toe Out
3	12	34.0	136.0	Both	Crouch
4	15	62.0	157.0	Both	Crouch
5	16	37.0	153.0	Left	Mild Crouch
6	16	43.0	143.5	Right	Apparent Equinus
7	14	67.3	173.3	Both	True Equinus
8	19	60.0	179.5	Both	True Equinus
9	23	33.0	130.0	Both	Crouch
10	11	30.0	130.0	Left	Apparent Equinus
11	12	25.0	135.0	Both	Jump Gait
12	16	64.0	151.0	Both	Crouch
13	13	34.0	150.0	-	-
14	33*	38.0	149.0	Right	True Equinus

3.2 Experimental setup and procedure

Before starting the data acquisition, the participants were subjected to anthropometric measures, such as height and body mass. Also, a set of physical examination tests were conducted to assess spasticity, muscle strength and other characteristics that are related to movement.

To collect data, the MB MOCAP setup consisted of 10 equally spaced infra-red Ocqus and Arqus cameras (Qualisys AB, Sweden) and a total of 36 retroreflective markers including clusters, placed according to the lower limb CAST marker set [47], shown in Figure 2.5. The markers were placed bilaterally on the anterior and posterior superior iliac spines, lateral and medial epicondyles, lateral and medial prominences of the malleolus, the calcaneus, and the dorsal margin of the first, second, and fifth metatarsal heads. A cluster of four markers was placed laterally on each thigh and each shank. Additionally, four markers were also placed on the upper thoracic region, specifically on the sternum, the seventh cervical vertebrae (C7) and one in each acromion.

For ML MOCAP, 8 red-green-blue (RGB) Miqus video cameras (Qualysis AB, Sweden) were used, and data was collected using Theia3D. Both MB and ML MOCAP systems were connected to QTM (v2021.03.1 Qualisys AB, Gothenburg, Sweden) to allow simultaneous data acquisition. The frame rate of the recording was 85 Hz for both systems, synchronized in time and space with 3 force plates (9283U014, Kistler Instruments Ltd, Winterthur, Switzerland; FP4060-07&FP4060-05-PT, BERTEC, Columbus OH, USA), sampling at 850Hz.

Each subject performed a static trial for the MB capture, which consisted of standing reasonably upright in a standard anatomical pose during a short period of time. This was the trial used to build the 3D model from each subject in Visual 3D software (Visual 3D Professional v2021.03.1, Has-Motion, Canada). After the static trial, some of the markers that were not required for the dynamic trials, such as the ones placed on the lateral and medial epicondyles and malleolus were removed from the subjects to avoid interferences with the participant's natural movements. The dynamic trials consisted of walking in a straight line at a self-selected speed, from a reference point to another, stepping over the force plates. Chairs were placed in those reference points and if necessary, a rest period was allowed after each trial.

For a trial to be included in this study, it was required that at least one foot fully contacted with a force plate, for a correct calculation of joint moments and powers during the gait cycle. Trials where the foot touched outside the force places or between them, were excluded. The data acquisition would finish when at least 10 successful trials were acquired for each foot, the session took approximately 1 hour for each participant.

3.3 Data processing

To make sure the lower body segments were correctly tracked by the MB MOCAP, the 36 markers were manually labeled for each trial using QTM. The PAF (Project Automation Framework) Clinical Gait Module from Qualisys (PAF version 2.0.2.516 Qualisys AB, Sweden) was used in a post-processing way to export the data to C3D files and process the data in Visual 3D software directly. An immediate report was generated containing the spatiotemporal metrics, 3D kinematics and kinetics for each subject. When using PAF, the following configurations were chosen: 1) The gait events were automatically defined using the force plates (heel strike, toe off and heel strike) for both left and right sides); 2) the CAST marker set was applied allowing the computation of the 3D model that consisted in 1 pelvis, 2 thighs, 2 shanks and 2 feet. Lower limb joint angles were calculated using an XYZ Cardan sequence, and ZYX for the pelvis angle relative to the Lab [79]. Joint moments were calculated using Newton-Euler Inverse Dynamics (ID), normalized to subjects' body mass. Marker trajectories were low pass filtered using a Butterworth filter (6Hz), as well as analog signals (25Hz).

For the ML data, the same PAF Clinical Gait Module from Qualisys (PAF version 2.0.2.516 Qualisys AB, Sweden) was used. In this case, video data were processed with Theia3D (version 2023.1.0.310, Theia ML Inc., Kingston, ON, Canada), using the default IK 3D pose-estimation, with 6 DOF at the pelvis and 3 DOF at the hip, knee, and ankle joints. To smooth the pose from the IK results, a GCVSPL lowpass filter (8 Hz) was used. The resulting 4x4 pose matrices, for each frame, were exported to C3D format and the report was also generated. From the reports, it was possible to export the data to an ASCII file format.

The exported data was normalized to 101 points of the gait cycle (0-100%), and it consisted of the values of the variables in the successful trials, as well as the mean values and standard deviation of all the trials. Each file contained the data obtained for both sides. The extracted kinematic variables consisted of angles of the pelvis, hip, knee, and ankle joints. The moments and powers of the hip, knee and ankle were the extracted kinetic data.

3.4 Data analysis

An average of 7.1 $\pm$1.7 trials per participant were considered for the study, and the data of these trials were averaged for the data analysis, which was performed using MATLAB (version R2023b, MathWorks, USA).

To compare the mean difference between MB and ML MOCAP systems during the gait cycle, the average joint kinematics and kinetics were calculated. For this study, all anatomical planes were considered for the joint kinematics. For the kinetic measurements, sagittal and frontal planes were considered for joint moments, and only the sagittal plane for joint powers. To ease interpretation, the variables' outcomes for each point of the gait cycle were plotted in graphs. Most joint angle graphs were scaled from -30º to +30º, except from hip flexion (-20º to 70º) and knee flexion (-15º to 75º). Ankle dorsiflexion, knee and hip flexion, adduction and internal rotation angles were considered positive. The hip and knee extensor moments, ankle plantar-flexion moments and abductor moments were also recorded as positive. Power generation, which means concentric contractions, was also recorded as positive for all lower limb joints.

Because CP is a condition that affects the participants' body in several different ways such as mobility, coordination and muscle control, instead of choosing a representative side of the body to study, both the left and right legs were considered. The results for each side are represented in separated graphs.

3.5 Statistical Analysis

Before applying any statistical tests, a Shapiro-Wilk test was taken to evaluate the normality of the data. This normality test was chosen for being the most powerful and adequate for small samples and it was performed using the software SPSS Statistics (version 29.0.2.0 IBM SPSS Statistics, Armonk, NY). The angles of the ankle, knee, hip and pelvis joints acquired with the MB and ML MOCAP systems were compared using a two-tailed paired sample t-test with a level of significance of 5%. On the other hand, for the joint moments and powers, a non-parametric two-tailed paired t-test ($\alpha = 0.05$) was conducted with 10000 iterations.

To perform the comparison between the MB and the ML MOCAPs, an open-source package for one dimensional statistical parametric mapping (SPM1D) was used with the 0.4.11 version on MATLAB. SPM calculates the t-statistic of the kinematic and kinetic parameters at each point of the gait curve and represents it graphically. The critical t-value is represented as a red dashed line in the graph, defining the upper and lower thresholds for a significant difference. A label indicating the value of the critical t-value and the significance level are also displayed, and when the critical threshold was exceeded, the assigned p-value was represented in the graph.

The null hypothesis states that the gait parameters from the ML MOCAP do not differ significantly from the parameters obtained with the MB MOCAP. The alternative hypothesis states that the gait parameters from MB MOCAP are significantly different from the ones acquired by the ML MOCAP.

The t-test is meant to compare the means of the results obtained with MB and ML MOCAP from the same sample of subjects. This statistical metric allows an inter-technology comparison of the averages of the population of this study with each method, however, considering the CP condition and its heterogeneity, the individual values can also be very different. So, to compare the difference between both systems for each participant, the root mean square difference (RMSD) of the pelvic, hip, knee and ankle joint angles, and the RMSD of the moment and power of the lower limb joints of each participant was calculated. The individual RMSD results were averaged for each variable.

4 Results

4.1 Static trials

A static trial is required to obtain a biomechanical model with the MB method. Considering the MB and ML MOCAP systems are synchronized, the static pose was measured with both systems. To determine whether there are differences in the results estimated with these methods during the static trial, the angle biases between the MB and ML systems were calculated for each participant. The angle biases of the left pelvic and left lower limb joints are detailed in Tables 4.1, 4.3 and 4.5, for the sagittal, frontal and transverse planes, respectively, while Tables 4.2, 4.4, 4.6 show the angle biases of the same joints in the right side and in the same planes. The bias resulted from the subtraction of the ML angle value from the MB angle value (angle bias = MB – ML).

Table 4.1. Angle bias between the marker-based (MB) and markerless (ML) systems of the ankle, knee, hip and pelvic joints in the sagittal plane for the left side.

Joint Angle Bias

P	**Ankle (º)**			**Knee (º)**			**Hip (º)**			**Pelvis (º)**		
	MB	**ML**	**Bias**	**MB**	**ML**	**Bias**	**MB**	**ML**	**Bias**	**MB**	**ML**	**Bias**
1	7.52	2.28	**5.24**	6.05	1.61	**4.44**	14.41	1.65	**12.76**	20.39	5.79	**14.60**
2	1.89	-0.88	**2.77**	1.84	-3.93	**5.77**	26.56	-0.32	**26.88**	25.15	5.13	**20.02**
3	18.54	11.39	**7.15**	24.52	19.12	**5.40**	26.60	17.63	**8.97**	19.97	11.67	**8.30**
4	23.11	12.58	**10.53**	39.61	32.26	**7.35**	37.48	22.78	**14.70**	21.21	7.59	**13.62**
5	17.05	11.21	**5.84**	10.90	8.48	**2.42**	20.54	15.59	**4.94**	10.57	7.01	**3.55**
6	3.07	-6.87	**9.94**	4.31	0.64	**3.67**	37.78	23.74	**14.04**	34.83	18.70	**16.13**
7	-27.08	-18.45	**-8.63**	16.47	6.81	**9.67**	24.15	8.99	**15.16**	21.90	9.87	**12.02**
8	-1.78	1.58	**-3.37**	-10.11	-5.05	**-5.05**	9.89	4.80	**5.10**	21.09	12.69	**8.40**
9	14.67	11.28	**3.39**	24.88	28.73	**-3.86**	7.07	10.53	**-3.46**	-2.33	1.03	**-3.36**
10	14.42	12.30	**2.12**	24.22	23.04	**1.18**	25.58	16.01	**9.57**	20.25	9.23	**11.02**
11	7.40	3.46	**3.94**	10.65	11.32	**-0.67**	24.37	9.74	**14.63**	21.79	4.94	**16.85**
12	41.21	17.23	**23.98**	71.74	76.12	**-4.29**	33.14	30.61	**2.53**	3.51	-3.38	**6.89**
13	11.58	6.27	**5.31**	7.37	6.62	**0.76**	4.91	0.66	**4.24**	12.52	4.92	**7.60**
14	9.86	4.53	**5.32**	6.08	5.16	**0.91**	11.79	4.55	**7.24**	18.54	8.07	**10.47**
Mean	10.10	4.85	**5.25**	17.04	15.07	**1.98**	21.73	11.93	**9.81**	17.81	7.38	**10.44**

Table 4.1 shows that while the knee presents the lowest average difference between the MB and ML systems, with an average of 1.98º, the pelvis and hip exhibit the highest biases, of 10.44º and 9.81º, respectively. In between, there is a 5.25º average bias of the ankle flexion angle during the static trial.

Looking at individual angle values, at the ankle joint, participant 12 appears to have a much more increased dorsiflexion with the MB method, more specifically 41.21º, and a 23.98º average difference between the methods. This leads to the increase of the overall average bias of this joint. Also, P12 appears to have an excessive knee flexion and an increased hip flexion, both measured similarly between the systems, and showing good agreement with angle biases of -4.29º and 2.53º for the knee and hip joints, respectively.

The highest average difference between systems happens at the hip joint for participant 2 (26.88º), with the MB and ML MOCAP systems marking 26.56º and -0.32º, respectively.

Table 4.2. Angle bias between the marker-based (MB) and markerless (ML) systems of the ankle, knee, hip and pelvic joints in the sagittal plane for the right side.

Joint Angle Bias

P	Ankle (º)			Knee (º)			Hip (º)			Pelvis (º)		
	MB	**ML**	**Bias**	**MB**	**ML**	**Bias**	**MB**	**ML**	**Bias**	**MB**	**ML**	**Bias**
1	2.88	-1.35	**4.24**	3.63	-3.52	**7.15**	12.85	1.17	**11.68**	20.39	5.79	**14.60**
2	-0.52	-1.70	**1.18**	-3.81	-1.51	**-2.30**	26.43	1.83	**24.61**	25.15	5.13	**20.02**
3	21.71	14.13	**7.59**	34.08	28.80	**5.28**	29.13	22.48	**6.65**	19.97	11.68	**8.30**
4	20.24	16.51	**3.73**	44.21	39.51	**4.71**	34.06	21.30	**12.76**	21.21	7.59	**13.62**
5	-5.10	-6.41	**1.32**	21.88	25.25	**-3.37**	14.80	16.54	**-1.74**	10.57	7.01	**3.55**
6	22.92	5.30	**17.62**	22.89	11.22	**11.67**	34.86	16.09	**18.76**	34.83	18.70	**16.13**
7	-27.30	-23.58	**-3.72**	20.70	7.44	**13.26**	32.50	17.24	**15.26**	21.90	9.87	**12.02**
8	-0.05	-1.08	**1.02**	-4.87	-5.01	**0.15**	13.90	7.44	**6.46**	21.09	12.69	**8.40**
9	19.56	16.58	**2.98**	32.00	36.55	**-4.55**	7.27	12.41	**-5.14**	-2.33	1.56	**-3.89**
10	10.03	7.36	**2.67**	18.06	21.02	**-2.94**	27.11	19.74	**7.38**	18.06	9.23	**8.83**
11	9.42	3.29	**6.13**	14.58	11.57	**3.01**	24.97	8.35	**16.62**	21.79	4.94	**16.85**
12	38.26	32.38	**5.88**	80.85	77.85	**3.00**	41.52	33.48	**8.04**	3.51	-3.38	**6.89**
13	-5.62	-4.62	**-1.00**	-2.16	-3.51	**1.35**	14.84	7.88	**6.96**	12.52	4.92	**7.60**
14	4.29	-4.70	**9.00**	5.36	3.31	**2.05**	18.28	8.53	**9.75**	18.54	8.07	**10.47**
Mean	7.91	3.72	**4.19**	20.53	17.78	**2.75**	23.75	13.89	**9.86**	17.66	7.41	**10.24**

According to Table 4.2, the joint average differences of the right side of the body were similar to the left side, presented in Table 4.1.

The average bias of the right hip and pelvic joints were also the ones that show less agreement between systems, obtaining values of 9.86º and 10.24º, respectively. These results differ less than 0.50º when compared to the opposite side. Again, the knee is the joint with the lowest average difference, with a value of 2.75º, which is a greater difference than the in left side. Participant 6 shows large biases for all joints, which are greater than 10.0º, demonstrating bad agreement between the methods for this subject.

The estimations of the joint angles in the frontal plane were very similar between the MB and ML systems for the left and right sides, which are described in Tables 4.3 and 4.4, respectively.

Table 4.3. Angle bias between the marker-based (MB) and markerless (ML) systems of the ankle, knee, hip and pelvic joints in the frontal plane for the left side.

Joint Angle Bias

P	Ankle (º)			Knee (º)			Hip (º)			Pelvis (º)		
	MB	**ML**	**Bias**	**MB**	**ML**	**Bias**	**MB**	**ML**	**Bias**	**MB**	**ML**	**Bias**
1	7.29	8.09	**-0.81**	-11.72	-3.52	**-8.20**	-3.68	-0.69	**-2.99**	-0.63	0.35	**-0.98**
2	10.27	8.36	**1.91**	-6.07	-6.71	**0.65**	0.97	-0.84	**1.81**	-1.38	0.35	**-1.73**
3	8.66	-3.71	**12.38**	0.83	-0.64	**1.48**	9.94	7.74	**2.21**	4.93	4.56	**0.38**
4	16.53	10.04	**6.49**	-1.10	-9.51	**8.41**	2.74	-2.35	**5.10**	2.70	1.59	**1.10**
5	-6.64	4.45	**-11.10**	-2.98	-3.50	**0.52**	10.43	0.97	**9.46**	9.31	3.40	**5.90**
6	8.87	6.66	**2.21**	-2.40	-2.18	**-0.22**	-1.07	-6.60	**5.53**	6.05	0.46	**5.59**
7	-9.04	2.57	**-11.61**	2.14	-1.19	**3.34**	-7.99	-0.12	**-7.87**	-3.41	0.30	**-3.72**
8	-5.00	8.57	**-13.56**	-5.27	-5.65	**0.38**	-3.20	-1.96	**-1.24**	-1.28	-0.09	**-1.19**
9	6.24	0.72	**5.52**	-6.05	-4.64	**-1.41**	2.38	0.75	**1.63**	0.24	0.40	**-0.16**
10	9.62	4.77	**4.85**	-0.89	-4.59	**3.70**	-2.94	-1.38	**-1.56**	-1.76	-0.91	**-0.86**
11	6.58	4.61	**1.97**	-2.91	-3.83	**0.93**	-3.44	-1.25	**-2.19**	-1.22	1.14	**-2.36**
12	24.68	16.26	**8.42**	20.09	-7.23	**27.32**	4.63	-2.74	**7.38**	7.00	5.29	**1.71**
13	12.01	8.50	**3.51**	-4.56	-5.20	**0.64**	-4.48	-4.50	**0.02**	-1.94	-0.99	**-0.95**
14	11.20	7.25	**3.96**	-6.48	-6.97	**0.49**	-2.07	-2.42	**0.35**	-1.46	-0.91	**-0.55**
Mean	7.23	6.22	**1.01**	-1.95	-4.67	**2.71**	0.16	-1.10	**1.26**	1.22	1.07	**0.16**

Regarding the average left joint angles, both systems estimate a similar ankle joint angle, with a difference of approximately 1.0º. The pelvic joint angle is slightly tilted upwards, and the systems measure this obliquity angle similarly (approximately 1.0º). At the hip, small difference was noticed between the system, as the MB system estimated a null angle, and the ML estimated slight abduction. The left knee showed the highest angle bias (2.71º), and the left side of the pelvis joint presented an angle bias of 0.16º, being the joint with the smallest difference between systems in the left side of the body.

Even though these average differences of the joint angles in the frontal plane are minimal, the individual values show some discrepancies between the systems for some participants. The greatest difference between the systems is at the knee joint of participant 12 (27.32º), in which the MB system demonstrates an increased knee adduction (20.09°) while the ML shows an abduction of 7.23° at that joint. At the left ankle joint, participants 3, 5, 7 and 8 obtained angle biases greater than 10.0º between the systems.

Table 4.4. Angle bias between the marker-based (MB) and markerless (ML) systems of the ankle, knee, hip and pelvic joints in the frontal plane for the right side.

Joint Angle Bias

P	Ankle (º)			Knee (º)			Hip (º)			Pelvis (º)		
	MB	**ML**	**Bias**	**MB**	**ML**	**Bias**	**MB**	**ML**	**Bias**	**MB**	**ML**	**Bias**
1	6.74	5.49	**1.25**	-8.83	-2.03	**-6.80**	-1.71	-0.72	**-0.99**	0.63	-0.35	**0.98**
2	10.24	11.86	**-1.62**	-6.56	-7.47	**0.91**	-0.48	-3.84	**3.36**	1.38	-0.35	**1.73**
3	10.09	9.08	**1.01**	-3.88	-7.04	**3.16**	-5.35	-8.78	**3.43**	-4.93	-4.56	**-0.38**
4	22.27	12.34	**9.94**	1.83	-10.34	**12.17**	-0.86	-1.43	**0.57**	-2.70	-1.59	**-1.10**
5	11.79	7.15	**4.63**	-1.99	-6.62	**4.63**	-9.87	-4.14	**-5.73**	-9.31	-3.40	**-5.90**
6	2.76	5.38	**-2.62**	-0.63	-2.20	**1.57**	-7.02	-3.92	**-3.11**	-6.05	-0.46	**-5.59**
7	14.54	2.76	**11.78**	-5.63	-3.71	**-1.92**	-1.44	-3.60	**2.16**	3.41	-0.30	**3.72**
8	4.86	3.60	**1.25**	-1.99	0.38	**-2.37**	-3.11	-5.57	**2.46**	1.28	0.09	**1.19**
9	10.47	5.67	**4.80**	-0.65	-0.42	**-0.23**	-4.74	-1.87	**-2.88**	-0.24	1.21	**-1.45**
10	12.96	7.82	**5.14**	-3.30	-4.17	**0.87**	-0.12	-0.25	**0.13**	-3.30	0.91	**-4.20**
11	11.21	9.99	**1.22**	-5.24	-4.99	**-0.25**	-3.74	-6.48	**2.74**	1.22	-1.14	**2.36**
12	22.77	22.28	**0.50**	-23.46	-13.14	**-10.33**	-2.92	7.36	**-10.29**	-7.00	-5.29	**-1.71**
13	9.57	14.21	**-4.64**	-1.28	-3.67	**2.39**	-6.60	-6.96	**0.37**	1.94	0.99	**0.95**
14	7.33	6.29	**1.03**	-4.83	-4.74	**-0.08**	0.05	-0.98	**1.03**	1.46	0.91	**0.55**
Mean	11.26	8.85	**2.41**	-4.75	-5.01	**0.27**	-3.42	-2.94	**-0.48**	-1.59	-0.95	**-0.63**

In the right side, the magnitude of the differences between the angle estimations varied between 0.27º and 2.41º, which were the average differences for the knee and ankle joints, respectively.

The average joint angles showed a more adducted ankle in the MB system (11.26º) than in the ML system (8.85º). There is an abduction of the knee, which is accurately measured between the MB and the ML, since the difference between them was minimal (0.27º). The hip also shows similar angles between the systems, both showing a slight abduction. Both systems estimated the pelvic joint slightly tilted downwards with an average angle bias of 0.63º between them.

The systems obtained the worst agreement at the knee for participant 4 with an angle bias of 12.17º. Within each participant, the pelvic joint is the only that obtained a lower average angle bias than 6.0º for the left and right sides of the body in the frontal plane.

Table 4.5. Angle bias between the marker-based (MB) and markerless (ML) systems of the ankle, knee, hip and pelvic joints in the transversal plane for the left side.

Joint Angle Bias

P	Ankle (º)			Knee (º)			Hip (º)			Pelvis (º)		
	MB	**ML**	**Bias**	**MB**	**ML**	**Bias**	**MB**	**ML**	**Bias**	**MB**	**ML**	**Bias**
1	5.93	7.89	**-1.96**	-18.83	9.20	**-28.03**	-19.99	-3.18	**-16.82**	4.18	6.50	**-2.32**
2	10.27	4.69	**5.58**	-12.73	-13.21	**0.48**	-10.08	-5.73	**-4.36**	-1.71	-0.25	**-1.47**
3	3.74	-10.09	**13.83**	-31.60	-9.98	**-21.61**	6.82	-5.64	**12.46**	17.79	22.76	**-4.97**
4	-7.19	-1.25	**-5.94**	-16.65	-9.62	**-7.03**	21.96	1.32	**20.64**	-18.87	-13.67	**-5.20**
5	7.46	-17.05	**24.51**	5.58	5.69	**-0.10**	27.42	0.62	**26.80**	1.64	-24.74	**26.38**
6	-5.95	2.42	**-8.38**	13.28	-3.64	**16.92**	-3.46	-0.57	**-2.89**	11.35	10.34	**1.01**
7	12.25	6.43	**5.82**	-29.81	-6.57	**-23.24**	-4.05	-5.16	**1.11**	9.79	7.28	**2.51**
8	2.36	2.10	**0.26**	-23.88	-25.22	**1.34**	3.33	8.05	**-4.72**	3.20	4.19	**-0.99**
9	2.93	-2.33	**5.26**	-10.17	-15.84	**5.67**	-0.80	-0.25	**-0.55**	-9.81	-2.86	**-6.96**
10	2.20	6.31	**-4.11**	-10.94	-15.16	**4.23**	4.20	-2.11	**6.31**	3.79	5.96	**-2.18**
11	1.32	14.10	**-12.78**	-9.01	-8.51	**-0.50**	5.82	-0.03	**5.85**	-10.36	-9.64	**-0.73**
12	-9.05	-2.25	**-6.80**	-24.97	-14.84	**-10.13**	39.65	0.04	**39.60**	-21.75	-10.14	**-11.61**
13	2.93	-6.44	**9.37**	-10.84	-12.42	**1.57**	-22.35	-10.34	**-12.01**	5.75	-0.08	**5.82**
14	2.83	3.04	**-0.21**	-18.25	-7.83	**-10.42**	-5.64	-5.99	**0.35**	8.45	2.57	**5.89**
Mean	2.29	0.54	**1.75**	-14.20	-9.14	**-5.06**	3.06	-2.07	**5.13**	0.24	-0.13	**0.37**

Concerning the average joint angles of the left side of the body computed with each system, the pelvic joint showed the best agreement between them, with an average difference of 0.37º. Following, the ankle joint obtained an average angle bias of 1.75º, and the knee and hip joint angles showed larger differences, of approximately 5.0º.

The ankle joint showed a slight internal rotation, which was minimal in the ML method (0.54º). The average knee joint angles show an external rotation, which is approximately 5.0º more pronounced in the MB system than in the ML. The joint with the largest difference between the rotation angle estimations is the hip joint (5.13º), since the MB estimates an internal rotation of approximately 3.0º while the ML indicates an external rotation of approximately 2.0º. Finally, the systems barely assign a rotation in the left side of pelvis.

These joints obtained 17 results in which the systems obtained an increased angle bias (>10.0º), including 8 inaccurate estimations of the joint angles (>20.0º). There is a 39.6º difference between the measurements of the MB and ML systems at the hip joint of participant 12, in which the ML system measured approximately a null rotation of the hip, and the MB indicated an increased internal rotation. This participant also shows over 10º angle biases at the knee and pelvic joints. The knee joint of participant 1 showed a 28.0º angle bias between the systems. Participant 5 appears to be the subject with the most inaccuracies, which happen at the ankle (24.5º), the hip (26.8º), and at the pelvic joint (26.38º). This pelvic angle bias is the only major discrepancy between the systems in this joint compared to the other participants. However, this participant obtained the best agreement at the knee joint (-0.1º)

Table 4.6. Angle bias between the marker-based (MB) and markerless (ML) systems of the ankle, knee, hip and pelvic joints in the transverse plane for the right side.

Joint Angle Bias

P	Ankle (º)			Knee (º)			Hip (º)			Pelvis (º)		
	MB	**ML**	**Bias**	**MB**	**ML**	**Bias**	**MB**	**ML**	**Bias**	**MB**	**ML**	**Bias**
1	6.37	2.04	**4.32**	-12.76	0.67	**-13.43**	-19.85	-1.36	**-18.48**	-4.18	-6.50	**2.32**
2	14.07	3.04	**11.04**	-10.22	-11.92	**1.69**	-21.28	-2.42	**-18.86**	1.71	0.25	**1.47**
3	0.29	-6.50	**6.79**	-29.98	-14.51	**-15.47**	5.87	-2.56	**8.43**	-17.79	-22.76	**4.97**
4	-9.75	-2.32	**-7.43**	-29.14	-14.39	**-14.76**	15.61	-1.52	**17.13**	18.87	13.67	**5.20**
5	2.51	22.03	**-19.52**	-48.45	-18.59	**-29.86**	-13.82	-6.46	**-7.36**	-1.64	24.74	**-26.38**
6	-8.81	3.23	**-12.04**	-3.13	-10.07	**6.94**	9.12	-6.43	**15.55**	-11.35	-10.34	**-1.01**
7	25.49	5.46	**20.03**	-21.51	-13.40	**-8.11**	-18.75	-2.45	**-16.31**	-9.79	-7.28	**-2.51**
8	1.54	2.15	**-0.61**	-26.83	-19.51	**-7.33**	7.59	-1.68	**9.27**	-3.20	-4.19	**0.99**
9	7.19	-13.38	**20.57**	-19.53	-17.02	**-2.51**	-8.91	-0.55	**-8.35**	9.81	5.62	**4.19**
10	-4.64	-0.80	**-3.84**	-8.10	-10.45	**2.35**	-0.11	-1.16	**1.05**	-8.10	-5.96	**-2.14**
11	-1.90	3.03	**-4.93**	-8.49	-10.92	**2.43**	-6.68	-6.55	**-0.12**	10.36	9.64	**0.73**
12	-13.80	-15.41	**1.61**	-27.72	-29.96	**2.24**	-13.04	6.28	**-19.33**	21.75	10.14	**11.61**
13	16.58	15.49	**1.10**	4.43	-1.78	**6.21**	-12.49	0.59	**-13.07**	-5.75	0.08	**-5.82**
14	5.66	6.90	**-1.24**	-13.18	-9.06	**-4.12**	7.97	-2.16	**10.13**	-8.45	-2.57	**-5.89**
Mean	2.92	1.78	**1.13**	-18.19	-12.92	**-5.27**	-4.91	-2.03	**-2.88**	-0.55	0.32	**-0.88**

In the right side, the ankle (1.13º) and the pelvic (0.88º) joint angles were similarly measured between the systems in the transverse plane, with biases lower than 1.14°. The knee and the hip joints obtained an average angle bias lower than 5.30º.

The average of the participant's results shows a slight internal rotation at the ankle, which is more pronounced in the MB system. A greater difference is observed at the knee joint, which is externally rotated during the static pose. At this joint, the MB assigns a rotation of approximately 18.20º while the ML approximately estimates it as a 12.90º rotation. An external rotation of 4.9º in the hip was estimated by the MB system, which is approximately 2.9º more increased than in the ML. Finally, the pelvis joint shows a minimal rotation of 0.55º externally in the MB and 0.32 internally in the ML system.

The previously mentioned results come from the average estimations of all participants, however, when looking to the individual angle biases, there are inconsistencies that need to be addressed.

For all participants, the joints in the right side of the body acquired 16 values of considerably large angle biases (10.0º), however, only 4 were major discrepancies (>20.0º). Participant 5 remains the individual with the most joints with large divergences between the systems: at the ankle (-19.52º), the knee (-29.86º) and the pelvic (-26.88º) joints. The ML system estimated greater joint rotations than the MB for this participant. The knee joint angle of this participant obtained the greatest difference between the systems out of all the results from Table 4.6.

Most participants obtained an increased angle bias (>10.0º) between the methods at the hip joint, and on the contrary, it is observed that the pelvic joint shows the least differences between the systems in the transverse plane.

4.2 Dynamic trials

The study of the dynamic trials consisted of the kinematic (joint angles) and kinetic (joint moments and powers) analysis of the 14 participants during gait, considering the pelvic and lower limb joints.

4.2.1 Kinematics (angle comparison)

The pelvic and lower limb joint angles of each participant were measured with both systems during the gait cycle. As an example, the joint angles that were computed with the MB MOCAP system are shown in Figure 4.1, representing the left and right sides of the body in the left and right columns, respectively. This figure only considers the sagittal plane. The individual joint angle estimations of the ML system can be found in Figure A.1 of Appendix A.

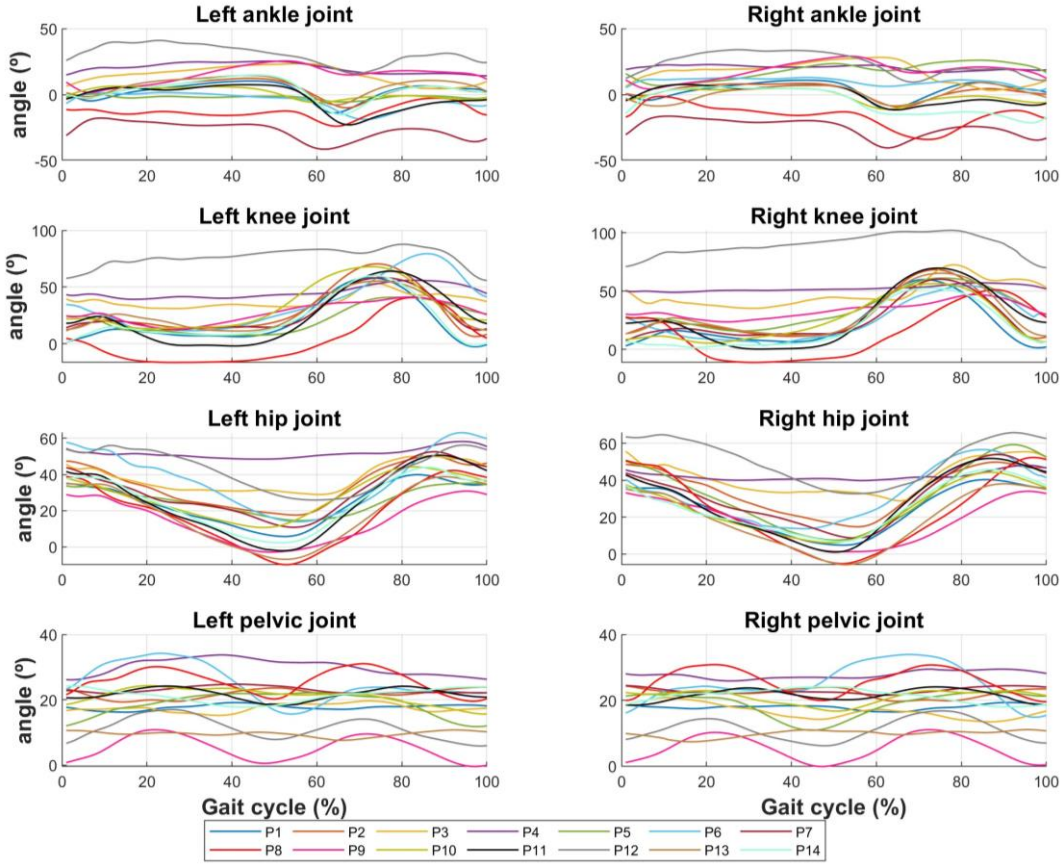

Figure 4.1. Mean angles of the ankle, knee, hip and pelvic joints for each participant, computed with the marker-based system.

According to Figure 4.1, participants 3, 4 and 12 appear to have an excessive knee and hip flexion for both left and right sides of the body during the entire gait cycle, especially during the stance phase. Also, participant 4 shows reduced plantarflexion during toe-off, and exhibits an elevated and consistent flexion of the pelvis during the entire stride cycle when compared to the rest of the participants. Participant 12 shows the most pronounced flexion of the right hip when compared to the rest of the participants. Also, participant 8, shows a hyperextension of the knee during the stance phase for both sides of the body. The sample of participants of this study has in fact different gait patterns and variable joint angles during the gait cycle, which can differ between both sides.

To compare the joint kinematics of the MB and the ML systems during the gait cycle, Figures 4.2-4.5, illustrate the average of the estimated angles of the ankle, knee, hip and pelvic joints, respectively, acquired with both MOCAP systems. Each figure contains 12 subplots, with the first two rows corresponding to the left side of the body, and the two bottom rows corresponding to the right side. For each side, the first row illustrates the waveform of the average joint angles across the 14 participants over a gait cycle, normalized to 100%. Left and right ML MOCAP lines are black, while the colored curves (red for the left side and blue for the right side) are correspondent to the angles acquired with MB MOCAP. Also, the gray shaded area in each plot represents the standard deviation of a population with a typical gait pattern, for comparison. The second and fourth rows correspond to the result of the SPM function, which graphically illustrates the two-tailed paired t-test for each point of the gait cycle. The t-value and the threshold for statistical significance are also displayed in the SPM graphs. The three columns define the sagittal, frontal and transverse planes, respectively.

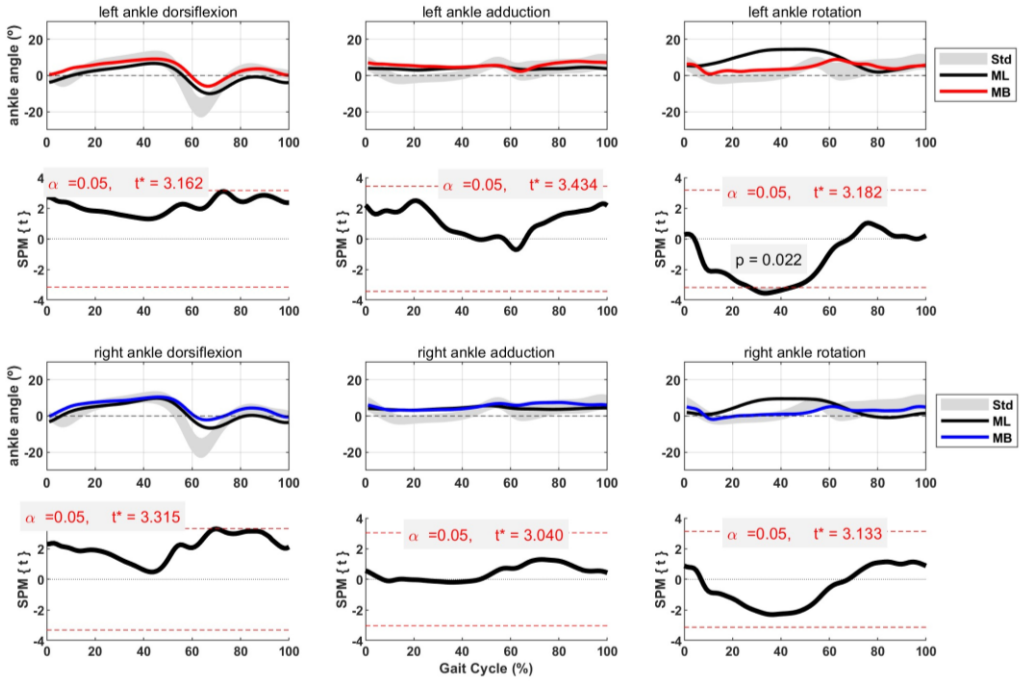

Figure 4.2. Ankle joint angles comparison between the marker-based (MB) and markerless (ML) systems. First and third rows: average joint angles for the left and right sides, respectively. Second and fourth rows: results of the correspondent paired t-test. From left to right columns: sagittal, frontal and transverse planes.

For left and right ankle dorsiflexion angle, the MB system obtained greater values than the ML system. Nevertheless, both curves seem very proximate to each other and with a very similar pattern that mostly fits within the standard range represented by the gray shadow, except for the loading response and the early swing phase. There is a greater difference between the MB and the ML methods for the left ankle angle in the sagittal plane during initial contact, between 0 to 5%, and during the swing phase, however those are not assigned to a statistical difference. For the right side, it is observable an interval from 67% to 95% (swing phase) with the greatest offset. According to SPM1D, the t-values correspondent to the greatest differences are borderline with the threshold but do not surpass it, therefore, there is not a significant statistical difference between the MB and ML MOCAP systems in the sagittal plane. No statistical differences were found between the techniques in the other planes, except for the left ankle rotation, which happens at mid-stance between 27% and 47% of the gait cycle (p=0.022). In

the frontal plane, the systems obtained slight differences at initial contact and in the swing phase, and in the transverse plane, the ankle angles were very inconsistent during the entire cycle.

To evaluate differences between the methods for each participant, the intra-participant variability of the ankle, knee, hip and pelvic joint angles were assessed with the RMSD, shown in Tables 4.7-4.10.

Table 4.7. Root mean square differences of the ankle angles in the sagittal, frontal and transverse planes. Individual results are shown, as well as the average.

	Angle RMSD (º)					
Participant	**Left Ankle**			**Right Ankle**		
	Sagittal	**Frontal**	**Transverse**	**Sagittal**	**Frontal**	**Transverse**
1	3.12	3.20	8.63	2.93	4.69	6.82
2	4.34	4.55	9.68	3.15	4.10	9.72
3	8.21	5.74	5.08	6.84	5.97	3.80
4	8.28	3.55	7.71	4.69	13.92	10.81
5	5.60	3.58	30.09	4.04	3.91	20.92
6	7.35	4.02	24.14	14.45	3.04	19.12
7	4.75	5.68	8.16	3.81	5.75	7.51
8	6.14	10.86	13.42	3.48	3.53	14.42
9	4.17	3.85	7.69	4.35	7.76	18.87
10	2.00	1.56	6.05	1.98	7.80	11.66
11	1.80	6.93	5.70	3.22	6.39	12.54
12	21.32	11.47	4.60	5.93	10.25	3.90
13	2.09	5.13	7.44	5.38	34.85	27.72
14	2.02	3.09	10.80	5.80	3.97	7.51
Average	5.80	5.23	10.66	5.00	8.28	12.52
Std dev	5.02	2.85	7.44	3.03	8.21	6.98

The left ankle angle in the sagittal component has an average RMSD of approximately 5.80º, which could be lower if not for participant 12, who has a much larger RMSD than the rest of the subjects (21.32º). Similarly to the static trial, the right side of this participant does not obtain such a larger joint angle difference as the left side does. For that reason, the average RMSD of the right side in the sagittal is smaller than for the left side (5.00º).

The frontal plane obtained an average RMSD of 5.23º and 8.28º for left and right ankles, respectively, and the average RMSD was larger for the ankle rotation angle, especially for the right side (12.52º) where most participants had a RMSD higher than 10.0º.

Looking at each participant's results, the sagittal (left and right sides) and the left frontal planes show very good agreement between systems, considering most participant's RMSD are lower than 5.0º. Participants that exhibit a RMSD lower or approximately equal to 2º for the left side are P10 (x and y components), P11, P13 and P14 (x-component), which shows very good agreement between the systems.

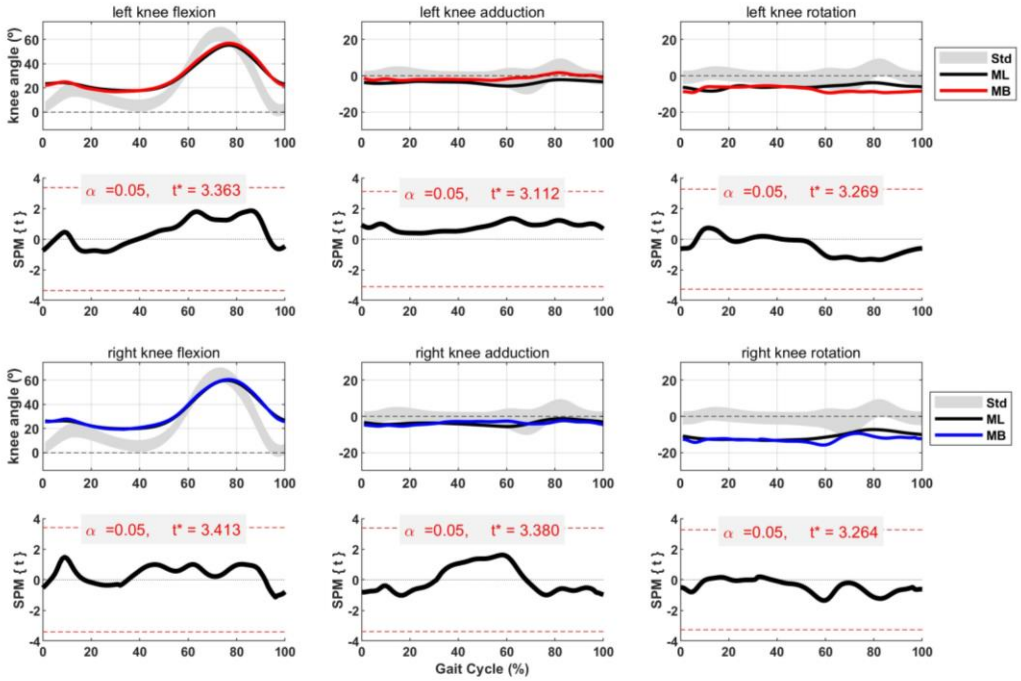

Figure 4.3. Knee joints angle comparison between the marker-based (MB) and markerless (ML) systems. First and third rows: average joint angles for the left and right sides, respectively. Second and fourth rows: results of the correspondent paired t-test. From left to right columns: sagittal, frontal and transverse planes.

The mean results for the knee show that both systems obtained very similar results for both left and right knee angle measurements, especially in the sagittal plane, where the curves are practically coincident during the whole gait cycle. This result is consistent with the findings from the Tables 4.1 and 4.2, which show a very good agreement between the MB and ML systems for the knee flexion during the static trial.

SPM does not indicate any significant differences between the MB and the ML systems in any anatomical planes. However, the curves in the frontal and transverse plane are not so coincident, especially during the swing phase. The estimation of the knee rotation angles seems very inconsistent between the systems during initial stance, and from terminal stance to terminal swing. The transverse plane is the most inconsistent for knee joint angle estimation.

Table 4.8. Root mean square differences of the knee angles in the sagittal, frontal and transverse planes. Individual results are shown, as well as the average.

Participant	***Angle RMSD (º)***					
	Left Knee			**Right Knee**		
	Sagittal	**Frontal**	**Transverse**	**Sagittal**	**Frontal**	**Transverse**
1	3.37	4.36	20.72	1.85	4.18	19.37
2	8.85	5.49	10.78	4.84	6.51	9.18
3	4.58	9.82	9.11	4.02	3.95	4.14
4	5.45	8.63	6.72	9.12	6.76	16.16
5	3.13	6.39	2.90	2.11	4.15	19.94
6	3.65	6.30	29.09	5.85	7.01	17.53
7	6.63	1.45	20.49	4.80	6.34	9.83
8	6.44	8.98	22.10	3.23	5.86	12.77
9	5.02	2.94	8.90	5.46	2.56	3.79
10	3.79	5.68	3.75	5.50	9.91	3.72
11	3.62	2.46	8.68	2.65	2.14	5.21
12	11.01	34.31	13.63	3.40	11.31	3.35
13	2.57	7.80	9.84	2.81	1.78	14.93
14	2.78	3.05	6.26	2.47	3.61	10.79
Average	5.06	7.69	12.36	4.15	5.43	10.77
Standard deviation	2.36	7.79	7.51	1.89	2.70	5.89

Apart from the transverse plane in both sides of the body and the frontal plane in the left side, the average knee angle RMSDs were lower than 5.50º. Participant 12 shows a RMSD of 34.3° in the left knee angle in the frontal plane, which increases the overall average of the RMSD of the left knee in that anatomical plane. Otherwise, the value would be much smaller.

In the transverse plane, 4 participants obtained RMSDs greater than 20.00º (subjects 1, 6, 7 and 8) in the left knee and 4 obtained higher RMSDs than 15.0º in the right knee (subjects 1, 4, 5 and 6), demonstrating very bad agreement between the systems during the estimation of the angles during the gait cycle.

The average knee joint angle in the frontal plane shows better RMSD in the right side (5.43°) than in the left side (7.69°), which is accordance with the graphs in Figure 4.3 that show more consistent angle estimations in the right side between the systems.

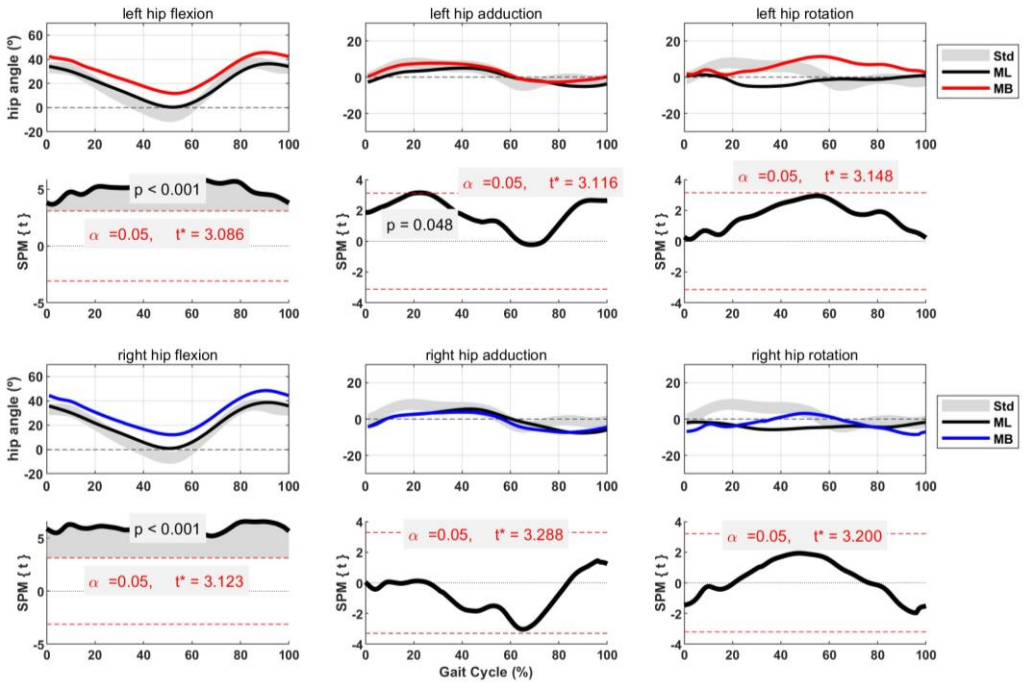

Figure 4.4. Hip joint angles comparison between the marker-based (MB) and markerless (ML) systems. First and third rows: average joint angles for the left and right sides, respectively. Second and fourth rows: results of the correspondent paired t-test. From left to right columns: sagittal, frontal and transverse plane.

Table 4.9. Root mean square differences of the hip angles in the sagittal, frontal and transverse planes. Individual results are shown, as well as the average.

	Angle RMSD (º)					
Participant	**Left Hip**			**Right Hip**		
	Sagittal	**Frontal**	**Transverse**	**Sagittal**	**Frontal**	**Transverse**
1	*9.65*	2.77	12.19	10.19	3.18	18.88
2	*24.15*	2.63	*11.20*	20.28	2.67	17.83
3	*8.70*	4.16	*9.37*	6.32	2.98	7.21
4	*16.12*	8.82	*21.26*	15.74	1.81	19.65
5	*6.23*	10.62	*31.06*	6.53	7.05	6.28
6	*13.18*	6.39	*9.65*	12.39	3.38	17.48
7	*15.42*	4.32	*7.78*	13.84	5.79	11.43
8	*12.68*	3.08	*30.64*	12.38	1.59	20.66
9	*2.17*	2.15	*8.30*	2.72	3.85	8.47
10	*12.25*	2.01	*10.81*	8.55	2.53	14.10
11	*12.26*	4.91	*4.85*	14.20	6.36	8.49
12	*4.62*	11.15	*39.68*	5.86	6.94	12.95
13	*4.13*	1.34	*14.10*	3.46	1.39	5.44
14	*11.76*	1.71	*9.28*	10.92	2.83	11.00
Average	*10.95*	4.72	*15.73*	10.24	3.74	12.85
Standard deviation	5.51	3.18	10.27	4.80	1.90	5.11

The comparison between the acquisition of the hip angles with both methods, illustrated in Figure 4.4, shows that the MB registered greater values than the ML for hip flexion. This also occurs in most of the gait cycle for the other anatomical planes. The entire gait cycle is assigned to a statistically significant difference ($p<0.001$) for both left and right hip flexion angles. The minimum difference between the methods' measurements is approximately 8.00º for both sides and its peak difference is 11.47º at 48% of the gait cycle for the right side and 11.77º at 46% for the left side.

Regarding other anatomical planes, there is a statistically significant difference in the left hip adduction at around 20% to 26% (mid-stance), with a p-value of 0.048. The curves are more coincident for the right hip adduction and no supra-threshold clusters were assigned for this side. No other supra-threshold clusters were assigned for the hip, however, the systems in the transverse plane did not measure the angles accordingly at all, and there is not any waveform agreement, especially in the left hip, which obtained a RMSD of 15.7º.

Unlike the ankle and knee joints, the hip exhibits a significant average RMSD in the sagittal plane, and similarly, the transverse plane obtained an increased RMSD with a difference greater than 10.0º in both sides. Nevertheless, the frontal plane obtained a mean RMSD of 4.7º and 3.7º for the left and right sides, respectively, showing good agreement between the systems.

The transverse plane remains the plane with the weakest concordance between the MOCAP methods. The increased average RMSD for the hip joint in sagittal plane is due to 8 participants that obtained a higher RMSD than 10.0º in the left side and 9 in the right side.

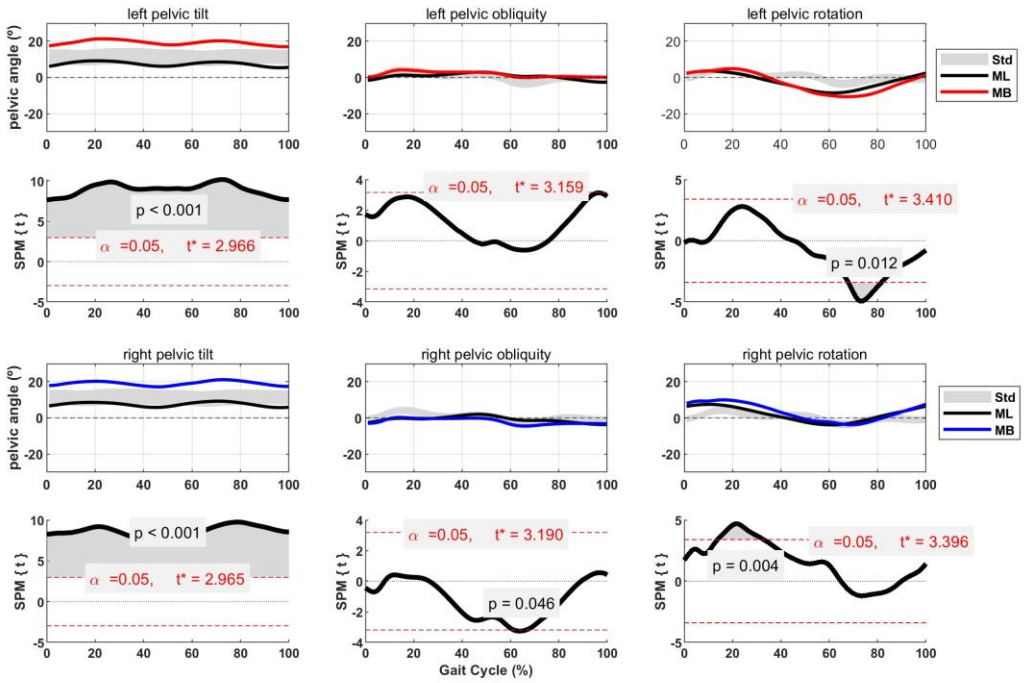

Figure 4.5. Pelvic joint angle comparison between the marker-based (MB) and markerless (ML) systems. First and third rows: average joint angles for the left and right sides, respectively. Second and fourth rows: results of the correspondent paired t-test. From left to right columns: sagittal, frontal and transverse planes.

Table 4.10. Root mean square differences of the pelvic joint angles in the sagittal, frontal and transverse planes. Individual results are shown, as well as the average.

Participant	***Angle RMSD (º)***					
	Left side of the pelvis			**Right side of the pelvis**		
	Sagittal	**Frontal**	**Transverse**	**Sagittal**	**Frontal**	**Transverse**
1	*12.52*	2.61	2.44	13.04	2.42	2.78
2	*18.45*	3.04	1.53	18.76	3.33	1.65
3	*10.15*	5.21	7.34	6.26	3.18	2.82
4	*15.76*	3.27	2.09	15.65	3.62	7.19
5	*7.32*	7.09	1.93	7.66	7.37	3.89
6	*13.89*	3.42	1.82	13.97	3.40	1.47
7	*14.13*	4.47	3.40	13.73	4.62	3.46
8	*15.14*	2.47	3.80	15.58	2.75	4.06
9	*4.29*	3.09	5.56	4.30	3.04	5.25
10	*13.60*	1.59	3.56	13.94	1.47	2.60
11	*16.59*	4.19	2.83	16.24	4.28	3.72
12	*5.94*	6.52	8.70	6.10	6.41	8.93
13	*3.62*	0.80	3.24	4.04	0.74	2.62
14	*14.20*	1.05	3.12	14.04	0.95	3.17
Average	*11.83*	3.49	3.67	11.66	3.40	3.83
Standard deviation	4.58	1.80	2.05	4.73	1.80	1.99

Figure 4.5 shows that the pelvic joint angles from both systems follow a very similar pattern in the sagittal plane, however, there is an underestimation of the ML method in comparison to the MB. The difference between the average MB and ML angles range between 8.06º and 11.77º in this plane. This leads to a statistical difference between the methods during the entire gait cycle (p-value < 0.001) for both left and right sides.

In the other planes, the results of both methods are nearby each other during most of the gait cycle, except for three intervals with statistical differences assigned, the first being between 60% and 67% of the cycle (early swing) for right pelvic obliquity (p-value = 0.046) in the frontal plane. From 14% to 33% (early to mid stance) of the gait cycle, a significant difference is observed for right pelvic rotation with p-value = 0.004, and for the left pelvic rotation, it happens from 68% to 82% of the gait cycle (swing phase) with p-value = 0.012.

The average RMSD of the frontal and transverse planes are lower than 3.9º, which means that within participant, the pelvic joint angle estimations from the MB system matched closely to the ML, while the sagittal plane had an average RMSD of over 11.5º in both sides, showing low agreement between the methods in this anatomical plane. Also, the results of the pelvic joint in the sagittal plane are concordant with the observed angle biases in Tables 4.1-4.6, that show larger differences between the methods during the static pose in the sagittal plane but small differences in the other planes.

4.2.2 Kinetics (moment and power comparison)

For this study, the considered kinetic gait variables were the joint moments and powers during the gait cycle. The moments of the lower limb joints in the sagittal and frontal planes are represented in Figures 4.6-4.8. The average RMSD of the joint moments are presented in Tables 4.11-4.13, which also show the results for each participant in the anatomical planes. The individual lower limb joint moments are presented in Figure A.2 and Figure A.3 of the Appendix A, representing respectively, the estimations of the MB system and the ML system.

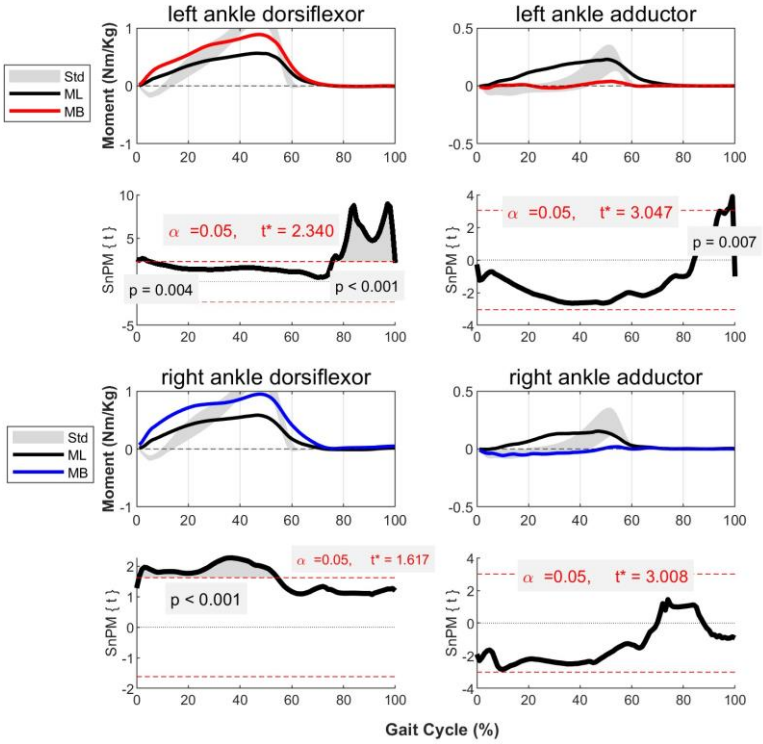

Figure 4.6. Ankle joint moments comparison between the marker-based (MB) and markerless (ML) systems. First and third rows: average joint moments for the left and right sides, respectively. Second and fourth rows: results of the correspondent paired t-test. Left and right columns represent the sagittal and the frontal planes, respectively.

For the plantarflexor moment in the right side, there is a supra-threshold cluster from the beginning until 55% of the gait cycle ($p<0.001$), which comprises the rapid increase of the moment estimations during the stance phase.

For the left ankle, the MB system estimated a rapidly increase of the plantarflexor moment at initial contact when compared to the ML, corresponding to a significant difference ($p=0.004$) at 0-4%, and thereafter, the stance phase did not obtain any other significant differences. However, another significant difference ($p<0.001$) occurred between the systems from mid to terminal swing (76-100%) in the same anatomical plane.

In the frontal plane, there is a divergence between the MB and ML curves during the stance phase of the left and right ankle abduction moments, in which the ML overestimates the MB moments. However, no significant differences were assigned for these joint moment estimations during the stance phase, but there were during terminal swing ($p=0.007$) at 98-100% for the left ankle.

Table 4.11. Root mean square differences of the ankle moments for the sagittal, frontal and transverse plane for the left and right sides. Individual results are shown as well as the average.

Participant	***Moment RMSD (Nm/kg)***			
	Left Ankle		**Right Ankle**	
	Sagittal	**Frontal**	**Sagittal**	**Frontal**
1	0.0239	0.1318	0.0716	0.0899
2	0.0616	0.0388	0.0832	0.0960
3	0.0711	0.0877	0.0681	0.0438
4	1.6984	0.4501	1.8337	0.3390
5	0.1502	0.2943	0.0340	0.0675
6	0.2015	0.4217	0.1038	0.3564
7	0.2630	0.1831	0.2747	0.0982
8	0.1408	0.2709	0.0708	0.3331
9	0.0481	0.0982	0.0298	0.0761
10	0.0601	0.0544	0.0548	0.0711
11	0.0555	0.0145	0.0403	0.0772
12	0.0480	0.0102	0.0803	0.0197
13	0.1746	0.0205	0.4688	0.1838
14	0.0588	0.0431	0.1708	0.0447
Average	0.2182	0.1514	0.2418	0.1355
Standard deviation	0.4318	0.1506	0.4735	0.1184

As observed in Figure 4.6, an increased divergence between the systems was seen in the sagittal plane, and the RMSD was larger than 0.20 Nm/kg. It is important to mention that the standard deviation of the RMSDs in this plane is double the average value, which shows an increased variability within participants. Participant 4 has the highest RMSD, of over than 1.6 Nm/kg for both sides, which does not happen for any other participant. This value constitutes an outlier, and it increases the degree of variability of the average results.

In the frontal plane, since there is a difference between the systems during the entire stance phase, the RMSD is also increased. Participants 11 and 12 show very good RMSD results (<0.015 Nm/kg), which shows that for these participants, the systems estimate similar joint moments at the left ankle.

In Figure A.2 from Appendix A, it is possible to observe the discrepancies between the ankle angles of participant 4 compared to the rest of the participants, which was obtained from the estimation of the MB technology. The average MB curve and RMSD is noticeably much more increased due to the enhanced joint moments of participant 4.

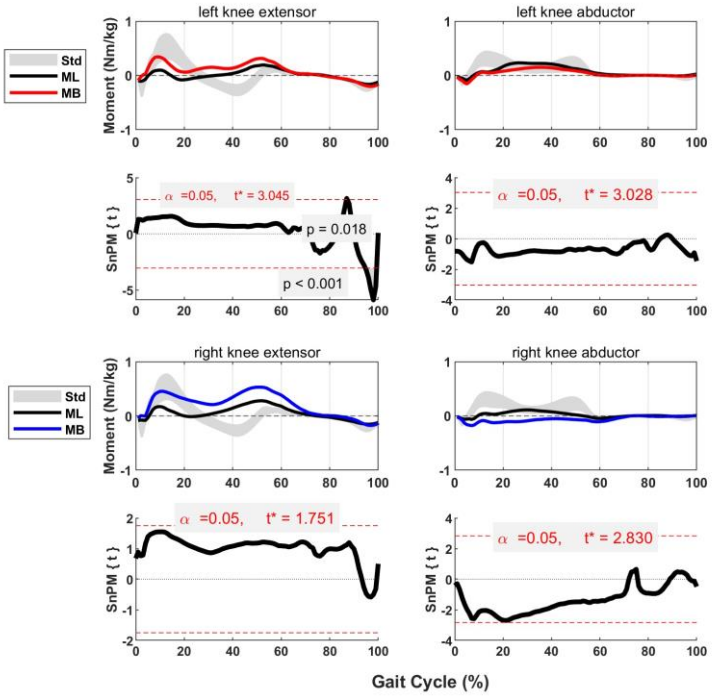

Figure 4.7. Knee joint moment comparison between the marker-based (MB) and markerless (ML) systems. First and third rows: average joint moments for the left and right sides, respectively. Second and fourth rows: results of the correspondent paired t-test. Left and right columns represent the sagittal and the frontal planes, respectively.

The MB system estimated greater knee extensor moments during the stance phase than the ML system, which was much more pronounced in the right side, since the right knee showed a greater difference between the measured moment magnitudes. Despite the divergences, there is no significant differences in this phase of the gait cycle.

Regarding the frontal plane, during the mid to terminal stance phase, the MB method estimates a left knee abductor moment but a right knee adductor moment, while the ML estimates an abductor moment for both sides during the same phase.

No significant outcome differences were assigned to the right knee joint moments during the entire gait cycle, however, for the left side in the sagittal plane, there are significant differences in the swing phase. The significance threshold was exceeded during the terminal swing phase at 86.9-87.1% ($p=0.018$), and at 94.7-99.3% ($p<0.001$) where MB estimates a slightly larger flexor moment.

Table 4.12. Root mean square differences of the knee moments for the sagittal, frontal and transverse plane for the left and right sides. Individual results are shown as well as the average.

Participant	***Moment RMSD (Nm/kg)***			
	Left Knee		**Right Knee**	
	Sagittal	**Frontal**	**Sagittal**	**Frontal**
1	0.0339	0.0764	0.0812	0.0558
2	0.0798	0.0357	0.0593	0.0383
3	0.1938	0.0908	0.3564	0.1780
4	1.5822	0.2158	2.2542	0.6128
5	0.1437	0.1752	0.0538	0.0227
6	0.0888	0.1118	0.1318	0.1220
7	0.1480	0.1619	0.1282	0.0958
8	0.3084	0.6404	0.1449	0.3693
9	0.0542	0.0557	0.0392	0.0737
10	0.0479	0.0249	0.0687	0.0426
11	0.0313	0.0140	0.0290	0.0348
12	0.0504	0.2338	0.1296	0.2192
13	0.0831	0.0490	0.1526	0.0634
14	0.0255	0.0344	0.0503	0.0311
Average	0.2051	0.1371	0.2628	0.1400
Standard deviation	0.4040	0.1618	0.5791	0.1664

For both sides, the sagittal plane obtained an increased average RMSD, and the right knee joint obtained an even larger RMSD than the left side. The standard deviation is much larger than the average RMSD. Again, participant 4 shows the largest RMSD (>1.50 Nm/kg) for the knee moment in the sagittal plane, and an even more significant and increased RMSD in the right knee (2.25 Nm/kg).

In the frontal plane, the left and right sides obtained similar RMSD results, however, the difference between the systems in the right side was slightly greater, which is also observed in Figure 4.7.

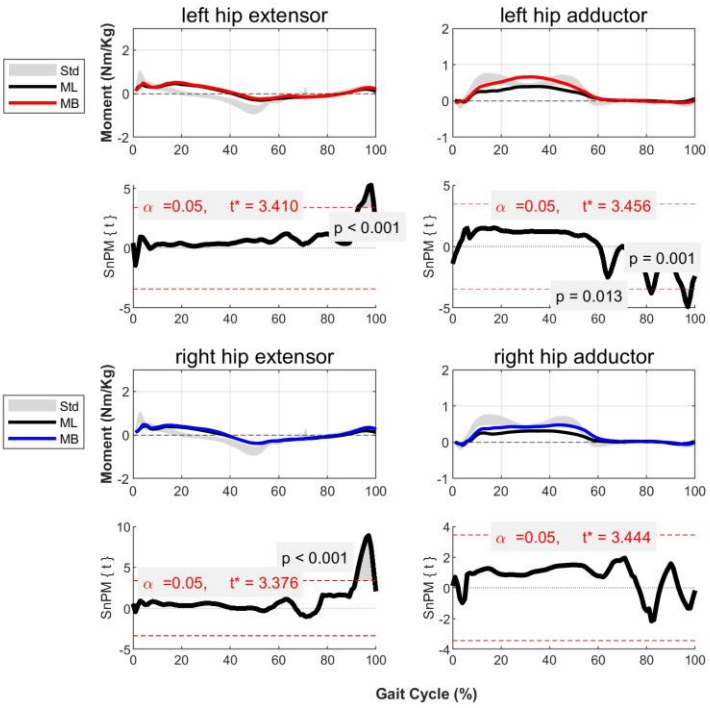

Figure 4.8. Hip joint moments comparison between the marker-based (MB) and markerless (ML). First and third rows: average joint moments for the left and right sides, respectively. Second and fourth rows: results of the correspondent paired t-test. Left and right columns represent the sagittal and the frontal planes, respectively.

The estimated hip joint moments obtained similar patterns in both anatomical planes, with slight differences observed in hip abduction moments, where the MB system showed increased moments compared to the ML system during mid to terminal stance phase. The difference is more enhanced in the left hip abductor moment than in the right hip. Nevertheless, no statistical difference was assigned during this period of the gait cycle.

For both sides in the sagittal plane, statistically inconsistent regions ($p<0.001$) between the systems happened around the same interval of the swing phase, more specifically at 92.74-99.24% for the left side and 91.65-99.5% for the right side.

The left hip abductor moment shows significant differences at 81.18-82.72% ($p=0.013$) and at 95%-98.57 ($p=0.001$) in the swing phase, and the right hip joint abductor moment did not obtain any statistical differences.

Table 4.13. Root mean square differences of the hip moments for the sagittal, frontal and transverse plane for the left and right sides. Individual results are shown as well as the average.

Participant	***Moment RMSD (Nm/kg)***			
	Left Hip		**Right Hip**	
	Sagittal	**Frontal**	**Sagittal**	**Frontal**
1	0.1209	0.0982	0.1161	0.0395
2	0.0682	0.0643	0.0908	0.0590
3	0.1227	0.2436	0.1947	0.1842
4	1.2145	1.5916	0.9039	1.2810
5	0.0822	0.1557	0.0543	0.0787
6	0.1463	0.0586	0.0850	0.0904
7	0.1049	0.2552	0.0764	0.3054
8	0.2449	0.1594	0.2781	0.0839
9	0.1570	0.0712	0.1805	0.0997
10	0.0755	0.0292	0.0690	0.0437
11	0.0609	0.0316	0.0647	0.0263
12	0.1078	0.0559	0.1550	0.0756
13	0.0581	0.1153	0.2622	0.1701
14	0.0451	0.0274	0.0884	0.0901
Average	0.1864	0.2112	0.1871	0.1877
Standard deviation	0.3004	0.4042	0.2188	0.3231

Participant 4 shows an increased RMSD for the hip moments in both anatomical planes, which are over 1.0 Nm/kg, and in particular, the left hip moment in frontal plane obtained a greater value than 1.5 Nm/kg. These results are much higher than for the other participants.

The overall left and right hip joint moment average RMSD outcomes are similar in the sagittal plane, of approximately 0.19 Nm/kg, and for the other plane, the left side exhibits higher average RMSD than the right side.

Finally, the power of the lower limb joints in the sagittal plane is represented in Figure 4.9. The average RMSD of the joint powers are presented in Tables 4.14, which also shows the results for each participant.

The individual lower limb joint powers are presented in Figure A.4 and Figure A.5 of the Appendix A, representing respectively, the estimations of the of the MB system and the ML system.

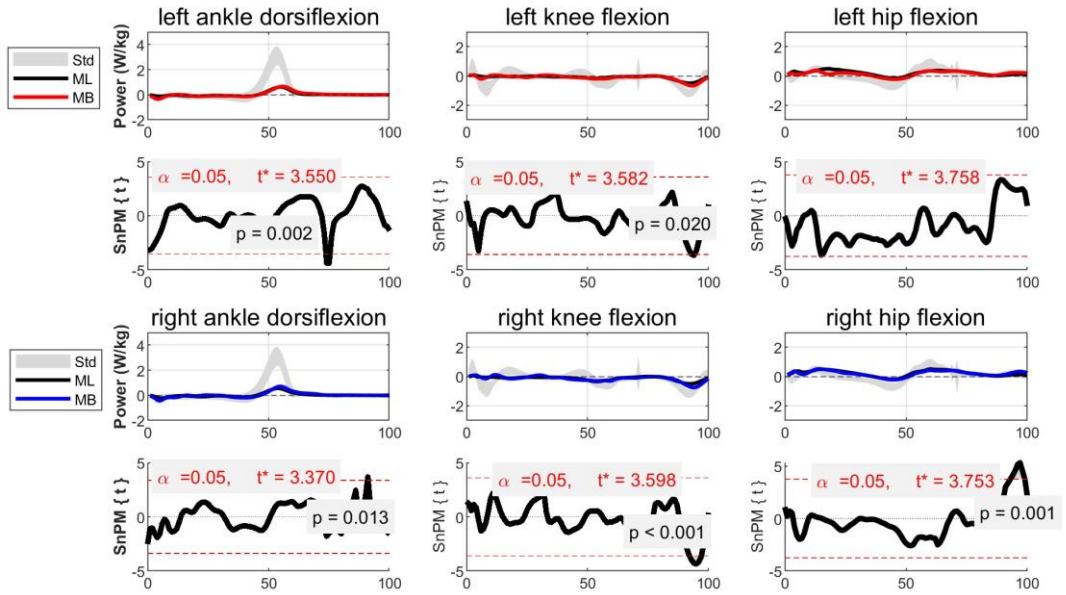

Figure 4.9. Lower limb joint powers comparison between the MB and ML systems. First and third rows: average joint powers for the left and right sides, respectively. Second and fourth rows: results of the correspondent paired t-test. Left and right columns represent the sagittal and the frontal planes, respectively.

At the ankle joint, little power absorption is observable at initial contact, and power generation occurs during the terminal stance. During these phases, the curves of MB and ML techniques show very little differences, being practically coincident during the rest of the stride cycle. No statistical differences were assigned during the stance phase. In the swing phase, there is a significant difference in the left ankle joint indicated at mid swing (p=0.002), around 73.7-75.3%, while for the right ankle power it happens at terminal swing (p=0.013), approximately around 90.8-91.1%.

There are some divergences between the knee joint power estimations of the systems, especially at terminal swing. Additionally, during the stance phase, variation between the systems is also observed for both sides. Apart from a significant difference at terminal swing around 93-94.26% for the left knee (p=0.020) and around 92-97% for the right knee (p<0.001), no other significant clusters for the knee joint power difference between the MB and ML MOCAP systems were found. The divergences observed at the right knee joint power are more pronounced than in the left knee joint.

Initially at initial stance, both systems accordingly registered power generation in the right hip joint. In this interval, a little difference in the left hip joint power estimations was observed. Thereafter, around 20%, the ML system overestimated the power of the left hip joint from the MB, but the difference was not significant. At terminal stance, around 93.0-98.9%, the MB overestimates the hip power generation, which is more evident in the right hip joint and obtained a significant difference (p=0.001).

Table 4.14. Root mean square differences of the lower limb joint powers in the sagittal plane for the left and right sides. Individual results are shown as well as the average.

Participant	Power RMSD (W/kg)					
	Left joint			Right joint		
	Ankle	Knee	Hip	Ankle	Knee	Hip
1	0.1349	0.1165	0.1501	0.1508	0.1545	0.1827
2	0.1546	0.1054	0.0679	0.1285	0.1167	0.1057
3	0.0636	0.1240	0.1201	0.1401	0.2629	0.1406
4	0.3941	0.5821	0.2131	0.4275	0.4867	0.2381
5	0.1000	0.1379	0.1978	0.1769	0.0821	0.1781
6	0.1346	0.2933	0.3336	0.1570	0.0875	0.1499
7	0.3315	0.1597	0.1864	0.3205	0.1918	0.1816
8	0.2593	0.1362	0.5361	0.2567	0.2517	0.3772
9	0.0816	0.1477	0.2674	0.0413	0.1496	0.2589
10	0.0977	0.1718	0.1512	0.1077	0.2582	0.1499
11	0.0771	0.1367	0.1805	0.0688	0.0730	0.1317
12	0.0715	0.1513	0.1463	0.0929	0.2545	0.1523
13	0.2190	0.2163	0.1591	0.5678	0.3488	0.4435
14	0.0572	0.1376	0.1191	0.1392	0.0957	0.1364
Average	0.1555	0.1869	0.2020	0.1983	0.2010	0.2019
Standard deviation	0.1063	0.1233	0.1163	0.1479	0.1185	0.0981

Regarding the RMSDs of the lower limb joint powers in the sagittal plane, it is observed that the average RMSD between the MB and ML technologies of all joints is lower than 0.21 W/kg. The ankle joint power obtained the smallest average RMSD for the left and right sides, and the hip joint obtained the highest RMSD.

Based on the RMSD, the power of the joints in left side of the body was estimated more accordingly than for the right side joints. That is because the RMSD of the left side joints were lower than for the right side, expect for the hip joint power, that obtained very similar RMSDs between both sides.

Participant 4 shows the highest RMSD compared to the other participants at the ankle and knee joints. At the hip joint, participants 8 and 13 show the least agreement between the systems, since they obtained a difference of 0.54 W/kg in the left hip and a difference of 0.44 W/kg in the right hip joint power, respectively.

5 Discussion

This research study aimed to understand whether the MB and the ML MOCAP methods estimate gait parameters similarly when assessing children with CP, who typically display mobility conditions. To achieve this, this project had two main goals. The first goal was to compare the joint kinematics of the pelvic girdle and the lower limb joints, obtained with the MB and the ML systems. The second one was to compare the joint kinetics with both systems. For that purpose, the angles of the pelvis, hip, knee, and ankle joints were measured during the static and dynamic trials. The moments and powers of the lower extremity joints were measured during the dynamic trials.

This chapter was designed to interpret the findings of this study, to compare them with outcomes from the current literature, and then determine research concerns and limitations.

5.1 Kinematics assessment

5.1.1 Static trials

The joint angles were simultaneously monitored with the MB and ML systems during the static trials in the sagittal, frontal and transverse plane.

Postural abnormalities are an important complication in children with CP, and to maintain the standing position, it is necessary for the center of gravity of the trunk to be vertical to the ground. To achieve that, subjects with CP may need to change the position of a joint, which then results in compensatory changes in the other joints [80]. Considering this information, it was not expected for the participants to stand straight like a standard healthy person but for the angles of their pelvic and lower limb joints to be different than the typical anatomical pose.

The comparison between the measurements of the two technologies was performed by subtracting the average ML angles to the average MB angles. Tables 4.1-4.6 show that when measuring the pelvic and lower limb joints, for both left and right sides of the body, there is already a bias between the angles of the MB and the ML systems in the static pose, and in general, the MB captured greater values than the ML system.

In the sagittal plane, the ankle and knee joint angles showed a slight difference between the two systems, which was lower than 6.0º. On the other hand, the hip and pelvic joint angles showed larger differences between the systems with values of approximately 10.0º. The average difference was minimal at the knee joint with results of 1.98º for the left side and 2.75º for the right side, which shows very good agreement between both systems in the static pose. The left and right ankle joints obtained variations of 5.25º and 4.19º respectively, which are more significant than the knee joint biases, but still an acceptable result for an angle bias between the methods. The MB and ML systems seem to estimate the angles of the hip and pelvis much differently. The MB showed a more pronounced anteriorly pelvic tilt and an increased hip flexion than the ML technique during the static trial.

In fact, the marker placement in the pelvic joint can be a complicated task due to the complexity of this joint. Since it contains soft tissue, such as muscle and fat, finding the bony landmarks to place the markers can be more complicated. Clothing can also interfere with the markers by covering or moving them, which can lead to wrong estimations. Nevertheless, the ML system also has limitations, and clothing can also complicate the detection of the joint landmarks, since it is easier for the system to detect when the landmarks are visible.

The MB and ML systems seem to estimate the average joint angles in the frontal plane accordingly, since the average angles showed differences < 2.8º for all joints in the static trials. The right knee, right hip, and the right and left sides of the pelvic joint indicate minimal differences between the systems (<0.64º), and left knee and right ankle joints showed differences of over 2.0º, which are still acceptable differences. Regarding the individual values, there is a very good agreement between the systems in the frontal plane, most individual results obtained little angle biases, except for the left ankle joint, which exceeded 10.0º angles biases for 4 participants. An outlier is the 27.32º adduction angle difference between the systems that computed the left knee joint angle of participant 12. None of the joints in the right side of body obtained an angle bias greater than 12.5º.

The average joint angles in the transverse plane showed good agreement between the systems, especially at the ankles and pelvic joints (<1.80º), and approximately a 5.0º average difference at both knees and at the left hip joint.

In this anatomical plane, more discrepancies were observed in the individual results, especially for participant 12 who obtained an angle bias of 39.6º at the left hip joint, and participant 5 who obtained an angle bias of -29.86º and -26.38º, at the right knee joint and at the right side of the pelvic joints, respectively. Regarding the left joint angles of participant 5, the angle biases did not show good agreement at the ankle (-24.51º), the hip (26.80º) and the pelvis (26.38º). The MB method seems to have estimated both knee joints with an increased 5º internal rotation than the ML system.

The difference between the joint angles measured with the MB and the ML MOCAP systems during the static trial indicates either a variation between the data capturing, or the data modelling and processing. This discrepancy can be due to many factors, being one of them the modelling definitions and their joint constraints, since each system use different models.

The MB MOCAP was performed with the CAST marker set to create the biomechanical model, and for the ML, the Theia3D's default model was used. The Theia3D lower limb model has 24 DOF: 6 at the pelvis and 9 for each leg. This means that the pelvis is allowed three translational movements (in the x, y, and z coordinates) and three rotational movements (tilt, obliquity and rotation). The lower limb joints (hip, knee and ankle) have 3 DOF each, allowing rotation movements such as flexion/extension, abduction/adduction and internal/external rotation [66]. Theia3D allows to define the ankle with 6 DOF, however, for this study, the default model was used, only allowing 3 DOF at the ankle joint. In the CAST model, each joint is defined with 6 DOF, which allows three rotation movements and three translation movements. This model is known by its feasibility, and it is widely used in clinical settings to assess subjects with abnormal gait patterns, since it assumes that the segments are rigid bodies that can move freely with no joint constrains, with 6 DOF [81].

Also, both systems are prone to other sources of errors. In the case of the MB MOCAP system, inconsistency in marker placement is a factor that usually leads to errors. As a result of different operators who may follow different protocols, errors in the measurements of lower limb joint angles can go up to 5.0º [63][82]. Nevertheless, the markers of the 14 participants were placed by the same assessor to minimize variability within-assessor. Up to 3.0º of errors can also occur in lower limb joint angles due to joint center position estimation errors [83].

Environmental factors, such as the lighting conditions, affect both systems. The video cameras of the ML technology record frame-by-frame and can introduce noise to the kinematic measurements. Additionally, the camera quality and resolution are also factors that can affect the accuracy of estimation of the joint kinematics. Regarding the algorithm, the training dataset was not trained using images of

subjects with markers placed on their body, so that can affect the estimation of the ML biomechanic parameters [77].

5.1.2 Dynamic trials

During the dynamic trials, which consisted of walking at a self-selected speed, the MB and the ML systems were simultaneously estimating joint kinematics and kinetics. To compare the systems, a SPM statistical analysis was conducted to perform a paired t-test study, and the RMSD of the pelvic and lower limb joints was also estimated. Studies in literature state that motion in planes other than the sagittal are highly susceptible to skin artifacts and errors, and most choose to focus on only studying the sagittal plane [84]. Nevertheless, this study focuses on all anatomical planes for the joint kinematics during the dynamic trials.

Before comparing the joint kinematics between the MB and ML systems, a graphic comparison of the subjects' gait cycle with the MB system was plotted to illustrate the variation of the angles of the pelvic and lower limb joints of all participants during the gait cycle. Analyzing Figure 4.1, it is observed that participants 3, 4 and 12 have an excessive knee and hip flexion, which is characteristic of a common gait pattern in CP named crouch gait. The estimated joint angles seem to be similar between the left and right sides. These results are in accordance with the assigned gait patterns of these participants in Table 3.1. The graph shows how heterogeneous the sample of the participants is.

As mentioned previously, there are already angle biases between the curves of the MB and the ML during the static trial. For that reason, to eliminate the initial angle offsets between the systems, it was considered to adjust the estimated curves of the dynamic trials by adding the average angles biases of the static trials (Tables 4.1-4.6) to the average curve of the ML dynamic trials. However, this adjustment was not performed, since D. Gordon E. Robertson and colleagues [85] define a joint angle as the relative orientation between two local coordinate systems and not a vector, which means that addition and subtraction of the angles cannot be performed between the two MOCAP techniques. Despite that, it is important to highlight that the shape of the angle curves of the pelvis and lower limb joints would remain unchanged and there would only be a vertical translation of the ML curve, which would be approximating it to the MB method's curve. In this case, the ML system would estimate the joint angles similarly to the standard MOCAP system. This curve translation would potentially lower the error of measurement and increase the accuracy of the ML method during the dynamic trials when compared to the MB system.

Comparing the ankle angles from the MB and the ML MOCAP, no statistical differences were identified, except for the left ankle rotation during mid-stance. In the sagittal plane, there is an observable offset between the curves of the left flexion angle, which is smaller during the stance phase but greater in the swing phase, however the differences seem constant in each phase of the cycle. For the right ankle flexion, the difference between the curves is smaller during the stance phase, and they are coincident from 40-50% of the cycle.

The estimation from the MB and the ML MOCAP systems match very closely when assessing the knee joint flexion angle. When compared to the other joints, the knee is the joint that presents more exposed skin, facilitating the algorithms from the ML technology to detect and estimate the joint center consistently. The result is in accordance with the findings from the static trials, being the joint with the smallest average bias for both sides. No statistical differences were identified at the knee joint in any anatomical plane.

In the sagittal plane, the knee and ankle joints obtained a RMSD <5.9º for the left and right sides. Additionally, the right side of the joints obtained better results, this is, lower RMSDs than the left side for this anatomical plane. The largest RMSD for these joints were observed for the left and right ankle and knee rotations and ankle adduction/abduction for the right side. These results are partially consistent with Kanko's study [77].

For the hip and pelvic joints in the sagittal plane, the ML curve seems to follow the same pattern as the MB, however, there is a systematic offset in the angles measured during the gait cycle, demonstrating that the ML method underestimates the values of the MB method. The bias between the systems for the hip and pelvic joints during the gait cycle is approximately between 8.0º and 11.0º. By removing the offset, the hip and pelvic joint angles of the ML would obtain much smaller RMSDs.

There is a significant difference of the pelvic obliquity in the right side during the early swing phase (60-67% of the cycle). The MB system captured a pelvic drop, which means the right side of the pelvis tilted downward, while the ML system considered it approximately neutral. Pelvic obliquity can occur due to muscle weaknesses, imbalances, skeletal deformities, abnormal muscle activation patterns, or compensatory mechanisms, which are highly common in CP [86]. It is likely that the ML may not be able to capture it. This pelvic movement may lead to other compensatory movements, such as a more pronounced pelvic rotation on the opposite side. It is observable that the left pelvis shows a retraction of approximately 10° during the swing phase. The ML did not capture this increasing of the pelvic rotation as the MB system did, leading to a significant difference from 68% to 82% of the gait cycle. Excessive pelvic retraction is also common in children with CP and can be due to a secondary biomechanical condition such as muscle tightness, or it can even be a voluntary response to internal rotation of the lower limb [87]. Finally, there is a significant difference from 12% to 33%, when there is a pelvic protraction on the right side during the stance phase. As mentioned, the pelvic landmarks may be the most complex for the algorithm of the ML system to identify, which results in a more increased difficulty to track the pelvic segment and its orientation during gait.

Wren's study [42], which compares Theia3D and Vicon kinematics, obtained a RMSD of 4.9º, 4.8º, 11.9º, 11.0º for the ankle, knee and hip flexion/extension movements and pelvic tilt, respectively. This study also showed good agreement for the ankle and knee, and worse results for the hip and pelvis in the sagittal plane. The transverse plane obtained the worst results of RMSD for the lower limb joints, ranging from 9.0º to 19.3º, but a good agreement for the pelvic rotation, which obtained a RMSD of 5.2º. Our study and Wren's compare the MB and ML in clinical patients and the results match closely. This current study shows better RMSD at the ankle in the frontal plane (< 8.2º) than Wren's study (11.2º). On the other hand, this study obtained worse RMSD at the knee (>5.4º) while Wren obtained a value of 4.7º.

There are other studies that estimate the RMSD between the joint kinematics of the MB and the ML methods. For example, Song's article [65] compares them across eight movements of healthy subjects. Regarding the walking movement in the sagittal plane, our results were consistent with the findings of this study. At the ankle and knee joints, both studies obtained RMSD < 5.9º and a hip RMSD > 10.0º. The pelvic joint is not assessed in Song's study, nevertheless the assessed RMSDs are consistent with the current study.

Since there are already differences between the MB and ML angles in the static trials, the differences between the curves in the dynamic trials seem to arise from the modelling definitions and not from the tracking. The offsets in pelvic tilt and hip flexion may be due to the definition of the pelvis neutral position, which has to do with the joint center estimations of the systems. The MB defines the pelvis tilted more anteriorly and a more flexed hip than Theia3D during the static trial and during gait.

In general, the kinematic estimations of the ankle and knee joints from the ML MOCAP aligned closely to the MB in the sagittal plane, while the hip and pelvic joint angles showed large systematic offsets between the methods. These results support the investigations of Kanko *et al*. [77], that indicates that lower limb kinematics are highly comparable between MB and ML MOCAP systems during gait and are also consistent with other studies in the literature [65][42][88].

5.2 Kinetics assessment

The study of joint kinetics contributes to the understanding of the forces acting on a joint, including the forces of muscles, tendons and ligaments [89]. CP children are likely to present abnormal patterns of joint kinetics during gait, which explains why measuring joint moments and powers is an essential part of clinical analysis to understand pathological gait [30][90].

5.2.1 Joint moments

In clinical GA, joint moments consist of the total moment exerted by all internal structures that act across a joint, and factors such as height and weight have an influence on its value [91]. To reduce the effect of variability of the data acquired from these factors, there are a few normalization techniques for joint moments. For this study, the extracted joint moment data from Visual3D were, by default, normalized by body mass (Nm/kg). However, according to Kirsten C. Moisio et al [91], a normalization of joint moments by body weight (W) times height (H) (unitless or % W x H), could be more effective than by body mass, on some occasions. This technique seems to reduce variability due to gender more successfully, and height may have a greater influence than weight in the joint moments in the sagittal plane. However, in the frontal plane, for example in the estimation of the hip adduction moment, height may not be such a useful parameter as weight is. Considering the participants are children and that the height distribution is relatively uniform, the chosen joint moment normalization method may be sufficiently good for this research study.

Figure 4.6 shows that during the stance phase, the ankle joint moments in the sagittal plane are much greater in the MB curve than in the ML curve on both sides. Between initial contact and loading response, as heel contact may be challenging or impossible for children with CP due to spasticity of the ankle plantar-flexors or weakness and poor selective control of dorsiflexors [92], a dorsiflexion moment is not observed in any MOCAP system's curve. There is a statistically significant difference assigned for both ankles during this phase, since the MB estimates a larger plantar-flexor moments than the ML method. Following, the plantar-flexor moment continuously increases, as ankle plantar-flexors contract eccentrically until mid-stance and then concentrically while the shank progresses forwards over the foot until the toe-off phase is reached [93]. This increasing of the ankle joint moment is much more pronounced in the MB curve than in the ML for both sides. It is observed that during this period, there is a statistically significant difference in the right ankle joint but not in the left ankle joint.

Clinical GA does not commonly report ankle moments in the coronal or transverse planes because the nature of the ankle joint movement is very complex, and there is high variability between individuals. The coronal plane was considered in the current study, and the MB system seems to estimate the ankle joint moment practically null during the stance phase, while the ML shows more variability, however, no statistically significant differences were assigned in this phase.

The MB system seems to overestimate the knee joint moments in the sagittal plane and underestimate in the frontal plane, when compared to the ML system during the stance phase, however,

no statistical significant differences were attributed. The hip joint extensor moment shows good waveform agreement and accurate estimation between the systems during the stance phase. This joint's adduction moment appears to be accordingly measured between both systems during early stance, and thereafter until terminal stance, the MB estimates higher hip adduction moments than the ML does. The knee and hip joint moments don't show any statistical differences during the stance phase in any component.

Overall, the lower limb joint moments showed RMSD ≤ 0.27 Nm/kg in the sagittal plane and RMSD ≤ 0.22 Nm/kg in the frontal plane. In the sagittal plane, the hip joint obtained the lowest RMSD, of approximately 0.19 Nm/kg for both sides, and larger RMSDs were observed at the right ankle and knee joints, obtaining 0.24 Nm/kg and 0.26 Nm/kg respectively. In the frontal plane, the hip joint obtained the worst RMSD, of approximately 0.21 Nm/kg and 0.19 Nm/kg at the left and right joints respectively, and the other lower limb joints obtained lower than 0.16 Nm/kg.

Most significant differences between the systems occurred during the swing phase, especially at the knee and hip joints. At this phase, since the foot of reference is not in contact with the ground, the ground force reaction is non-existent. Hence, it is expected that both systems estimate near zero for the ankle joint moment, however, a statistically significant difference was assigned for the left ankle joint.

On the other hand, movement at the knee and hip joints is fundamental to allow the leg to swing during the swing phase, so variability is expected. Also, the hip joint moments are known as the most variable out of the lower limb joints during the entire gait cycle. It is responsible for controlling the lower limb joints and for balancing the torso, which is a very important task since the torso holds at least two thirds of the body weight of an average subject [85]. Also, the hip joint moment calculation takes into account the knee and ankle joint moments, so errors in those joint moments propagate to the hip joint moment.

The differences between the MB and ML systems are in accordance with the investigation of Hui Tang *et al*. [94], obtaining lower limb joint moment differences at around the same phases of the stride cycle, especially at the hip and knee at terminal stance. During peak joint moments such as at around 10% of the cycle, for the knee joint, and around 20% for the ankle joint, differences were observed in both studies.

Kanko *et al.* [95] concluded that during the running movement of healthy subjects, the joint moments of the MB and ML systems differed by 0.3 Nm/kg or less. The results of the current study are in agreement with Kanko's investigation findings, since all lower limb joints showed RMSDs of 0.26 Nm/kg or lower.

The article written by Song *et al*. [65] also assesses the lower limb joint moments of healthy subjects captured with the MB and ML systems. This study normalized the moment by body weight times height, so, because the normalization methods differ, direct comparisons are not possible. Nevertheless, the results indicate that the moments at ankle plantar-dorsiflexion (RMSD ≤ 1.44% W×H), knee extension (RMSD ≤ 2.66% W×H), hip extension (RMSD ≤ 1.35% W×H) and hip adduction (RMSD ≤ 1.42% W×H) showed a low RMSD between the MB and the ML measurements. They also conclude that the joint moment estimation results exhibit strong waveform agreement and a good agreement between the average curves of the MB and ML systems. Those results are similar to ours regarding the fact that the left and right hip joint extension moment obtained the lowest RMSD, and the knee joint extension moment obtained the highest RMSD in both studies.

T. Huang *et al.* [96] also compared lower limb joint moments estimated with the MB and ML systems during gait by assessing healthy subjects in the sagittal plane and obtained RMSDs lower than

18 Nm for all joints, which were smaller at the ankle joint (4 Nm) and larger at the hip joint (17.1 Nm). In contrast to this current study, Huang showed that the ankle joint obtained much better agreement between the systems than the hip joint. The participants of that study are able bodied, so the ankle movements may be clearer and easier to detect for the ML system, unlike CP patients.

Figure A.2 in Appendix A demonstrates how much larger the MB system estimated the joint moments of participant 4 compared to the other participants. On the other hand, this discrepancy does not occur in the ML system, shown in Figure A.3. This results in a significantly increased RMSD, which was much greater than the in rest of the participants. The average RMSD would show much better results if it were not for the error in the MB estimation joint moments.

5.2.2 Joint powers

For this study, only the sagittal plane was considered to assess the lower extremity joint powers. The individual joint powers estimated with MB and ML are depicted in Figures A.4 and A.5.

Joint power is defined as the rate of work at which the muscles around a joint generate or absorb energy from the system [85]. Children with CP present much smaller magnitudes of joint powers than healthy subjects, which was noticeable in all lower limb joints. A factor that influences the magnitude of the joint powers (and joint moments) is the gait speed, and it is a fact that CP patients walk at a reduced speed as shown in Table B.1 of Appendix B. The participants walked at an average speed of 0.8 ± 0.3 m/s.

Despite the power magnitude being smaller, both systems estimated it similarly. The lower limb joint powers showed good waveform agreement between the MB and ML technologies in both left and right sides of the body, and the curves appeared coincident during most of the entire gait cycle.

All statistical differences occurred during the swing phase and the left hip was the only joint that did not obtain any significant differences. Most statistical differences took place at terminal swing, particularly, at the right ankle, both hip and both knee joints, while the left ankle joint power obtained a statistical difference at mid swing.

Even though the statistical differences occur in the swing phase at the ankle joint, visually, the average joint powers seem equal between the systems during that phase. The ankle joint power should be minimal during the entire swing phase, as the foot prepares for the next foot contact and does not need to generate energy. The average curves seemed minimal and coincident, however, Figures A.4 and A.5 show little but some variation between the systems estimations of the power joints.

At the knee joint, the statistical differences happen at around the same time of the gait cycle for both left and right joints, when there is absorption of energy as the quadricep muscles eccentrically contract to control the knee extension and prepare for foot contact. The ML system estimated greater absorption than the MB system, especially in the right side.

The right hip joint showed statistical significance as both systems estimate power generation at terminal swing. At this time of the gait cycle, the hip muscles contract eccentrically, and the MB measured increased power values when compared to the ML system.

The left ankle (<0.16 W/kg), left knee (<0.19 W/kg) and left hip (<0.21 W/kg) joints, obtained better results than the right ankle (<0.20 W/kg), right knee (<0.21 W/kg) and right hip (<0.21 W/kg) joints, respectively. The ankle joint obtained the best agreement between the lower extremity joints. The hip joint power RMSDs showed the worst results of agreement. As mentioned, the hip joint is accounted

for important tasks during gait, and for that reason, its moment may be very variable, implying power variability, since joint power is calculated from the joint moment.

The calculation of the joint kinetics is hierarchical, which means the joint estimations happen orderly from the distal joints to the proximal joints, so errors also propagate in the same order. This can explain why the ankle power showed the lowest RMSD, and the hip joint showed the largest differences.

Song *et al*. article [65] demonstrates that the hip is also the lower limb joint with fewer agreement and with more noticeable differences between the systems, acquiring a RMSD of up to 7.15% W×H.

Additionally, the results are partially in agreement with the findings from Hui Tang *et al.* [94]. At the hip and knee joints, both studies obtained a statistical difference at terminal swing. On the other hand, at the ankle joint, that article found differences (not significant) between the systems during the stance phase but none during the rest of the cycle, whereas the current study identified a statistical difference in terminal stance.

5.3 Concerns and limitations

The interpretations of the results of the current study should be done with limitations, the first limitation is the fact that different biomechanical models were used in the MB and ML MOCAP systems. The second limitation of this study is that the sample of participants involves different gait patterns which enhances variability in the joint estimations, observable in the Figures A.1-A.5 of Appendix A.

As noticed, the joint angle differences could be due to different modelling definitions, since the used models were distinct and had a different number of DOF, which could then lead to different joint estimations between the systems. Also, even though the pelvis has 6 DOF in both MOCAP systems, they seem to define the neutral segment position differently, since the CAST model defined it more anteriorly tilted. It is likely that the systems estimate the pelvic joint centers differently, due to the difficulty in determining the anatomical landmarks of both systems. Also, the anatomical keypoints that Theia3D uses for posing estimation is unknown, which means that it can be different to the MB method.

Additionally, the segment coordinate reference axes are identified by video image and machine learning algorithms in the ML system, while the MB system estimates it by the relative position between the markers. Different technology may be associated with different estimation methods, and the differences between the systems seem to be sensitive to the definitions of the segment coordinate systems [95].

Despite being mathematically wrong to subtract or add joint angles, visually, the systematic offsets in the pelvic and hip joints during the gait cycle could be much smaller or even inexistent if the angle bias adjustment had been done. To provide the best care for CP children, the errors must be minimal, and a 10º difference can lead to wrong diagnosis and treatment planning.

In instrumented GA, MOCAP systems use ID to estimate joint kinetics by combining kinematic data, segmental inertial characteristics, and external forces [85][97]. ID is a widely used tool, however, it has limitations. Its inaccuracies due to kinematic and anthropometric data is well known [98]. There are different methods to perform an ID analysis, which means the MB and ML systems may execute them differently. For the MB analysis, the Newton-Euler method was used, however, Theia3D does not specify which method it uses to obtain the kinetic data. Nevertheless, even if these systems use the same ID method, the estimated input data from the systems can differ, leading to discrepancies between them.

The observed moment and power estimation differences in the current study could be due to inconsistency of the segment center of mass (COM) and joint center position estimations. These parameters have been assessed by some studies that compare the MB and ML systems [94][95][69].

Pose estimation is one of the kinematic inputs necessary to perform the ID analysis. Errors in pose estimation lead to inconsistencies in the joint angle estimation, which can propagate to the joint kinetics estimation. Also, the joint center position can also be differently computed between the MB and ML systems, which can also explain the variation of the joint angles estimation between them. The segment joint center determines the axis of rotation of the joint, hence, a wrong estimation can lead to errors in the joint kinematics and consequently in the joint kinetics.

Tang and colleagues [94] studied the differences in the lower limb joint center positions and COM between Theia3D and the MB system and came across a 2 cm difference in the hip joint centers, in which the ML technology defined it posteriorly than the MB did. This difference can explain the joint angle differences that occur between the systems during the static and the dynamic trials, and consequently, differences in the hip joint moments and powers. This difference can affect the knee joint moment in the same phase. Moreover, Tang showed that in the sagittal plane, the joint center difference

between the MB and ML at the ankle and knee joints was variable during the stride cycle, however, the ML estimated those joint centers posteriorly than the MB at initial contact.

Kanko [95] also concluded that the joint center positions estimated from the MB and ML systems differed up to 3 cm. The previously mentioned studies compare both systems during running conditions.

This current study assesses CP children during gait at a reduced speed, and slow walking should exhibit smaller joint center position errors [69]. Nevertheless, these children can present anatomical deformities and gait patterns that may restrict the ability of the Theia3D algorithm to estimate the segment joint centers and limit the marker placement for the MB system.

Regarding the difference between the ML and MB COMs, H. Tang *et al.*, revealed that the COM of the foot, shank and thigh segments was 1.0 cm more laterally in the ML than in the MB. In the sagittal plane, the ML estimation of the foot segment COM is 1.0 to 4.0 cm anteriorly, while the shank and thigh are mostly 2.0 cm or less posteriorly than in the MB system during the gait cycle [94].

The MOCAP systems can employ different methods to estimate the segment COM, and an important parameter in its determination is the segment length, which is computed by the systems and depends on their algorithm. Ito [88] compared the length of the lower limb segments using MB and ML systems across different trials. The MB segment length estimations were consistent between trials, while the ML method showed variability in the length of the segments. Also, a static trial was measured with and then without the markers to study their effect in the ML estimations. The results showed that after the markers were placed on the participants, the ML model presented longer segment length in the thigh. This means that the markers may affect the ML estimation results.

Apart from different estimation methods between the systems, there are other factors that can affect the results within each system and that should be checked before the MOCAP. That is the number of cameras used and if they are all on and focusing. The quality of the markers should be checked, and their placement should be done properly and carefully, since if not done consistently, differences can arise.

Since the participants have CP and most present an abnormal gait, the 5.4 contractures on joints can provide misleading information about the moment and consequently about joint power values [30]. Also, clusters were mounted on both thighs and shanks of the subjects, which can move relative to the underlying bone during gait. Translation movements can go up to 1.5 cm at the shank and 2.5 cm at the thigh, and rotation movements can occur until 8º [99].

Just like in any statistical test, a small sample size provides statistical limitations in the SPM1D package, and it can be associated with a higher degree of random errors [100]. This technique uses permutations, which influence the minimum p-value that the SPM can detect in the statistical analysis. The recruitment of children with CP is challenging because of the small population available for participation. In this study, there were fourteen participants which means the total number of permutations was 16384 and the minimum possible p-value was 0.000062. This allows very small p-values, and it did not limit the statistical analysis of the study. However, studies with smaller sample sizes could limit the minimum p-value possible to detect, as it happens in another study [22].

It is said that algorithms can correctly detect the segments regardless of the subject's clothing, however, it is still important to control the clothing conditions to assess joint kinetics and kinematics in clinical settings. Another study from Kanko et al. [95] state that most joint kinematic and kinetic results are consistent between the MB and ML systems with different clothing. That study even compared the

ML estimations in different clothing conditions and came to the same conclusion, indicating variations in Theia3D's detection of the anatomical features but with small magnitude [95]. However, others indicate that different clothing was responsible for 4.0 cm differences in segment lengths [88]. Nevertheless, differences due to loosen clothing in segment length and spatiotemporal parameters are smaller than the differences that arise due to marker placement errors, or than minimal movement changes due to pathologies that affect movement, such as Multiple Sclerosis and CP [101][102].

6 Conclusion

The lower limb joint kinematics are highly comparable between MB and ML MOCAP systems in the sagittal plane. The knee flexion angle showed very good alignment and agreement between the systems in the static and in the dynamic trials, hence it was the most comparable joint. On the other hand, the other studied joints were also comparable in the sagittal plane, however, the systematic offsets at the hip and pelvic joint angles were much larger (~10º). Modeling definitions differed between the systems mostly in the pelvic joint and the differences propagated to the hip joint, which led to large systematic offsets in these joint angles during the gait cycle in the sagittal plane.

The low magnitude of the kinetic gait parameters made its interpretation more difficult. There were divergences between the average joint kinetics between the systems, which could be due to their methods of estimation of the joint centers and segment center of mass. The assigned significant differences in the joint kinetics occurred mostly during the swing phase.

In general, the Theia3D kinematics followed similar patterns compared to the MB MOCAP system, and the ML MOCAP system seems to be a great tool for assessing the sagittal plane kinematics of children with CP during gait. The joint kinematics in the frontal plane showed acceptable results, but the transverse plane showed much more variability and the worst results between the systems, so the utility of ML in that anatomical plane is questionable. The results were consistent with the findings observed in other studies that assess healthy subjects and subjects with abnormal gait. Mostly, the ML system seems to underestimate the measurements of the MB system.

Both systems inherently have errors, however, the progress of the software would enhance the accuracy and precision of the markerless system, allowing its application in clinical settings and providing a promising future in research biomechanics. It is important to note that it is not possible to determine which system estimates more accurately, since there has not been a comparison with a gold standard method MOCAP system such as imaging. With markerless technology, data collection would be much faster and more convenient, eliminating time-consuming tasks. Additionally, participants would be able to wear comfortable clothes and markers would not need to be placed on their body, so the natural movement would not be affected.

This research study is a crucial step to the validation of the ML motion system for quantifying lower limb joint kinematics and kinetics of children with CP. This technology is not perfect yet, and improvement of the algorithm is essential to acquire the best results possible to provide better diagnosis, treatment plans, monitoring, and surgery plans.

6.1 Future Work

Theia3D holds exciting potential, however, more improvement in the accuracy of the algorithms is necessary for its use in clinical settings.

Most studies focus on joint kinematics, and few include the assessment of joint kinetics. Hence, more studies comparing lower limb joint kinetics between the MB and ML should be conducted, especially including joint powers.

Gait is a movement that mainly takes place in the sagittal plane, however, in the case of impaired gait, the other anatomical planes may also be important to include in the analysis. When comparing joint kinematics of both systems, studies should also include the frontal and transverse planes. Also, despite gait being the standard movement to assess CP children, other movements should be tested with this ML technology, such as seating to stand and stand to seating transitions.

Diversification of the datasets, including musculoskeletal disorders and pathologies that affect movement would be fundamental for the increasing of the accuracy of Theia3D in clinical settings. Also, more studies comparing the MB and ML systems with CP children are recommended, its progress would make the ML applications in clinical settings very promising. Further analysis with larger samples is necessary to perform more accurate and strong statistical analyses. Studies should also include clinical patients that use walking aids.

Since joint kinetics are so important to assess in CP children and other impaired gait conditions, adequate and reliable ID parameters are fundamental, so bettering the algorithm to accurately estimate parameters such as the COM and segment joint centers would be a great step towards the use of ML MOCAP systems in research and clinical applications.

The utility of the ML MOCAP system in assessing children with CP depends on the accuracy of its estimations, so it is recommended for the biomechanics community research to continue the verification and validation of Theia3D to assess the lower limb joint gait parameters in clinical settings. Theia3D's outstanding performance would bring many benefits to the patients, clinicians and researchers.

7 References

[1] K. Himmelmann, G. Hagberg, and P. Uvebrant, "The changing panorama of cerebral palsy in Sweden. X. Prevalence and origin in the birth-year period 1999-2002," *Acta Paediatrica, International Journal of Paediatrics*, vol. 99, no. 9, pp. 1337–1343, Sep. 2010, doi: 10.1111/j.1651-2227.2010.01819.x.

[2] A. Johnson, "Prevalence and characteristics of children with cerebral palsy in Europe.," *Dev Med Child Neurol*, vol. 44, no. 9, pp. 633–40, Sep. 2002, Accessed: May 15, 2024. [Online]. Available: https://www.cambridge.org/core/journals/developmental-medicine-and-child-neurology/article/abs/prevalence-and-characteristics-of-children-with-cerebral-palsy-in-europe/9F0B521B05BB3C3CA7A4C7487360FAEA

[3] C. Cans, "Surveillance of cerebral palsy in Europe: a collaboration of cerebral palsy surveys and registers," *Dev Med Child Neurol*, vol. 42, no. 12, pp. 816–824, Dec. 2000, doi: 10.1111/j.1469-8749.2000.tb00695.x.

[4] H. K. Graham *et al.*, "Cerebral palsy," Jan. 07, 2016, *Nature Publishing Group*. doi: 10.1038/nrdp.2015.82.

[5] P. Rosenbaum, N. Paneth, A. Leviton, M. Goldstein, and M. Bax, "A report: The definition and classification of cerebral palsy April 2006," 2007, *Blackwell Publishing Ltd*. doi: 10.1111/j.1469-8749.2007.tb12610.x.

[6] National Guideline Alliance (Great Britain), National Institute for Health and Care Excellence (Great Britain), and Royal College of Obstetricians and Gynaecologists (Great Britain), "Cerebral palsy in under 25s: assessment and management." Accessed: Apr. 17, 2024. [Online]. Available: https://pubmed.ncbi.nlm.nih.gov/28151611/

[7] M. C. O. Bax, "Terminology and classification of cerebral palsy," *Dev Med Child Neurol*, vol. 6, no. 3, pp. 295–297, Jun. 1964, doi: 10.1111/j.1469-8749.1964.tb10791.x.

[8] S. Armand, G. Decoulon, and A. Bonnefoy-Mazure, "Gait analysis in children with cerebral palsy," *EFORT Open Rev*, vol. 1, no. 12, pp. 448–460, Dec. 2016, doi: 10.1302/2058-5241.1.000052.

[9] D. R. Patel, M. Neelakantan, K. Pandher, and J. Merrick, "Cerebral palsy in children: A clinical overview," 2020, *AME Publishing Company*. doi: 10.21037/tp.2020.01.01.

[10] D. R. Patel, D. E. Greydanus, J. L. Calles, and H. D. Pratt, "Developmental disabilities across the lifespan," Jun. 2010. doi: 10.1016/j.disamonth.2010.02.001.

[11] M. Shevell, "Cerebral palsy to cerebral palsy spectrum disorder," Jan. 29, 2019, *Lippincott Williams and Wilkins*. doi: 10.1212/WNL.0000000000006747.

[12] K. W. Krigger, "Cerebral Palsy: An Overview," Jan. 2006. Accessed: Apr. 08, 2024. [Online]. Available: https://pubmed.ncbi.nlm.nih.gov/16417071/

[13] A. M. Al-Sowi, N. AlMasri, B. Hammo, and F. A. Z. a. Al-Qwaqzeh, "Cerebral Palsy classification based on multi-feature analysis using machine learning," *Inform Med Unlocked*, vol. 37, Jan. 2023, doi: 10.1016/j.imu.2023.101197.

[14] S. Gulati and V. Sondhi, "Cerebral Palsy: An Overview," *Indian J Pediatr*, vol. 85, no. 11, pp. 1006–1016, Nov. 2018, doi: 10.1007/s12098-017-2475-1.

[15] "Cerebral palsy: hope through research." Accessed: Apr. 23, 2024. [Online]. Available: https://www.nichd.nih.gov/health/topics/factsheets/cerebral-palsy

[16] R. D. Tugui and D. Antonescu, "Cerebral Palsy Gait, Clinical Importance," *Maedica A Journal of Clinical Medicine*, vol. 8, no. 4, pp. 388–393, Sep. 2013, Accessed: Apr. 15, 2024. [Online]. Available: https://pmc.ncbi.nlm.nih.gov/articles/PMC3968479/

[17] R. Palisano, P. L. Rosenbaum, D. Russell, and B. E. Galuppi, "Development and reliability of a system to classify gross motor function in children with Cerebral Palsy," *Article in Developmental Medicine & Child Neurology*, 1997, doi: 10.1111/dmcn.1997.39.issue-4.

[18] J. W. Gorter *et al.*, "Limb distribution, motor impairment, and functional classification of cerebral palsy," *Dev Med Child Neurol*, vol. 46, no. 7, pp. 461–467, Jul. 2004, doi: 10.1017/S0012162204000763.

[19] J. Perry and J. Burnfield, *Gait analysis: normal and pathological function*, 2nd ed. SLACK Incorporated, 1992.

[20] R. Baker, *Measuring Walking: A Handbook of Clinical Gait Analysis*. Hampshire: Mac Keith Press, 2013.

[21] M. Abid, N. Mezghani, and A. Mitiche, "Knee joint biomechanical gait data classification for knee pathology assessment: A literature review," 2019, *Hindawi Limited*. doi: 10.1155/2019/7472039.

[22] A. Mustafaoglu, "Feasibility of markerless motion capture in clinical gait analysis in children with cerebral palsy," MSc. Dissertation, Faculty of Sports and Health Sciences of University of Jyväskylä, 2021. Accessed: May 05, 2024. [Online]. Available: http://urn.fi/URN:NBN:fi:jyu-202312088223

[23] A. E. Carolus, M. Becker, J. Cuny, R. Smektala, K. Schmieder, and C. Brenke, "The interdisciplinary management of foot drop," *Dtsch Arztebl Int*, vol. 116, no. 20, pp. 347–354, May 2019, doi: 10.3238/arztebl.2019.0347.

[24] T. F. Winters, J. R. Gage, and R. Hicks, "Gait Patterns in Spastic Hemiplegia in Children and Young Adults," *J Bone Joint Surg*, no. 69, pp. 437–441, 1987.

[25] T. C. Vlahovic *et al.*, "A case of peroneal neuropathy-induced footdrop. Correlated and compensatory lower-extremity function.," *J Am Podiatr Med Assoc*, vol. 90, no. 8, pp. 414–419, Sep. 2000, doi: 10.7547/87507315-90-8-411.

[26] J. M. Rodda, H. K. Graham, L. Carson, M. P. Galea, and R. Wolfe, "Sagittal gait patterns in spastic diplegia," *Research Physiotherapist J Bone Joint Surg [Br]*, vol. 86, no. 2, pp. 251–259, Mar. 2004, doi: 10.1302/0301-620X.86B2.

[27] J. Rodda and H. K. Graham, "Classification of gait patterns in spastic hemiplegia and spastic diplegia: a basis for a management algorithm," *Eur J Neurol*, no. 8, pp. 98–108, 2011.

[28] R. Parent *et al.*, *Computer Animation Complete*. Morgan Kaufmann Publishers, 2010. Accessed: Apr. 05, 2024. [Online]. Available: https://books.google.pt/books?hl=pt-PT&lr=&id=1gbh2wgK564C&oi=fnd&pg=PP1&dq=R.+Parent,+D.+Ebert,+and+M.+Pauly,+Computer+Animation+Complete.+Morgan+Kaufmann+Publishers,+2010&ots=c

3pXl-1dVa&sig=iLP_kKI0b3ibhYjMZ0znZ8SmKrY&redir_esc=y#v=onepage&q=isb&f=false

[29] J. R. Gage, “The clinical use of kinetics for evaluation of pathologic gait in cerebral palsy.,” *Instr Course Lect*, vol. 76, no. 4, pp. 622–631, 1994, doi: 10.2106/00004623-199404000-00020.

[30] C. J. Lin, L. Y. Guo, F. C. Su, Y. L. Chou, and R. J. Cherng, “Common abnormal kinetic patterns of the knee in gait in spastic diplegia of cerebral palsy,” *Gait Posture*, vol. 11, no. 3, pp. 224–232, Jun. 2000, doi: 10.1016/S0966-6362(00)00049-7.

[31] T. P. Andriacchi and E. J. Alexander, “Studies of human locomotion: past, present and future,” *J Biomech*, vol. 33, pp. 1217–1224, 2000, doi: 10.1016/s0021-9290(00)00061-0.

[32] T. A. L. Wren, G. E. Gorton, S. Õunpuu, and C. A. Tucker, “Efficacy of clinical gait analysis: A systematic review,” Jun. 2011. doi: 10.1016/j.gaitpost.2011.03.027.

[33] A. Mündermann, C. O. Dyrby, D. E. Hurwitz, L. Sharma, and T. P. Andriacchi, “Potential Strategies to Reduce Medial Compartment Loading in Patients With Knee Osteoarthritis of Varying Severity: Reduced Walking Speed,” *Arthritis Rheum*, vol. 50, no. 4, pp. 1172–1178, Apr. 2004, doi: 10.1002/art.20132.

[34] S. R. Simon, “Quantification of human motion: Gait analysis - Benefits and limitations to its application to clinical problems,” *J Biomech*, vol. 37, no. 12, pp. 1869–1880, Dec. 2004, doi: 10.1016/j.jbiomech.2004.02.047.

[35] T. A. L. Wren, C. A. Tucker, S. A. Rethlefsen, G. E. Gorton, and S. Õunpuu, “Clinical efficacy of instrumented gait analysis: Systematic review 2020 update,” *Gait Posture*, vol. 80, pp. 274–279, Jul. 2020, doi: 10.1016/j.gaitpost.2020.05.031.

[36] R. M. Kanko *et al.*, “Assessment of spatiotemporal gait parameters using a deep learning algorithm-based markerless motion capture system,” *J Biomech*, vol. 122, Jun. 2021, doi: 10.1016/j.jbiomech.2021.110414.

[37] Corazza S, Mündermann L, and Andriacchi T, “Markerless Motion Capture Methods for the Estimation of Human Body Kinematics,” Stanford, 2006. Accessed: May 06, 2024. [Online]. Available: https://citeseerx.ist.psu.edu/document?repid=rep1&type=pdf&doi=5e2080eca90de9fdb969088a40b49c4524d5b230

[38] J. L. McGinley, R. Baker, R. Wolfe, and M. E. Morris, “The reliability of three-dimensional kinematic gait measurements: A systematic review,” *Gait Posture*, vol. 29, no. 3, pp. 360–369, Apr. 2009, doi: 10.1016/J.GAITPOST.2008.09.003.

[39] S. Riazati, T. E. McGuirk, E. S. Perry, W. B. Sihanath, and C. Patten, “Absolute Reliability of Gait Parameters Acquired With Markerless Motion Capture in Living Domains,” *Front Hum Neurosci*, vol. 16, Jun. 2022, doi: 10.3389/fnhum.2022.867474.

[40] J. M. Rothstein, J. L. Echternach, and American Physical Therapy Association, *Primer on measurement : an introductory guide to measurement issues*. Alexandria, VA: American Physical Therapy Association, 1993. Accessed: Sep. 22, 2024. [Online]. Available: https://search.worldcat.org/pt/title/474683858

[41] S. L. Colyer, M. Evans, D. P. Cosker, and A. I. T. Salo, “A Review of the Evolution of Vision-Based Motion Analysis and the Integration of Advanced Computer Vision Methods Towards Developing a Markerless System,” Dec. 01, 2018, *Springer*. doi: 10.1186/s40798-018-0139-y.

[42] T. A. L. Wren, P. Isakov, and S. A. Rethlefsen, “Comparison of kinematics between Theia markerless and conventional marker-based gait analysis in clinical patients,” *Gait Posture*, vol. 104, pp. 9–14, Jul. 2023, doi: 10.1016/j.gaitpost.2023.05.029.

[43] L. P. Maletsky, J. Sun, and N. A. Morton, “Accuracy of an optical active-marker system to track the relative motion of rigid bodies,” *J Biomech*, vol. 40, no. 3, pp. 682–685, 2007, doi: 10.1016/j.jbiomech.2006.01.017.

[44] E. van der Kruk and M. M. Reijne, “Accuracy of human motion capture systems for sport applications; state-of-the-art review,” Jul. 03, 2018, *Taylor and Francis Ltd.* doi: 10.1080/17461391.2018.1463397.

[45] L. Mündermann, S. Corazza, and T. P. Andriacchi, “The evolution of methods for the capture of human movement leading to markerless motion capture for biomechanical applications,” Mar. 15, 2006. doi: 10.1186/1743-0003-3-6.

[46] R. Baker, F. Leboeuf, J. Reay, and M. Sangeux, “The Conventional Gait Model-Success and limitations,” Springer, Ed., 2020, p. 1. Accessed: Jun. 04, 2024. [Online]. Available: https://salford-repository.worktribe.com/output/1383183

[47] A. Cappozzo, F. Catani, U. Della Croce, and A. Leardini, “Position and orientation in space of bones during movement: anatomical frame definition and determination,” *Clinical Biomechanics*, vol. 10, no. 4, pp. 171–178, 1995.

[48] C. Menez and J. Coquart, “Orthotic Insoles Improve Gait Symmetry and Reduce Immediate Pain in Subjects With Mild Leg Length Discrepancy,” *Front Sports Act Living*, vol. 2, Dec. 2020, doi: 10.3389/fspor.2020.579152.

[49] A. Cereatti, V. Camomilla, G. Vannozzi, and A. Cappozzo, “Propagation of the hip joint centre location error to the estimate of femur vs pelvis orientation using a constrained or an unconstrained approach,” *J Biomech*, vol. 40, no. 6, pp. 1228–1234, 2007, doi: 10.1016/j.jbiomech.2006.05.029.

[50] “Tutorial: Building a Conventional Gait Model - Visual3D Wiki Documentation.” Accessed: Apr. 22, 2024. [Online]. Available: https://www.c-motion.com/v3dwiki/index.php/Tutorial:_Building_a_Conventional_Gait_Model

[51] F. Leboeuf, R. Baker, A. Barré, J. Reay, R. Jones, and M. Sangeux, “The conventional gait model, an open-source implementation that reproduces the past but prepares for the future,” *Gait Posture*, vol. 69, pp. 235–241, Mar. 2019, doi: 10.1016/j.gaitpost.2019.04.015.

[52] T. D. Collins, S. N. Ghoussayni, D. J. Ewins, and J. A. Kent, “A six degrees-of-freedom marker set for gait analysis: Repeatability and comparison with a modified Helen Hayes set,” *Gait Posture*, vol. 30, no. 2, pp. 173–180, Aug. 2009, doi: 10.1016/j.gaitpost.2009.04.004.

[53] HAS-Motion, “IOR Marker Sets,” c-motion. Accessed: Feb. 03, 2024. [Online]. Available: https://wiki.has-motion.com/doku.php?id=other:ior_gait:ior_gait_overview

[54] A. Cappozzo, A. Cappello, U. D. Croce, and F. Pensalfini, “Surface-marker cluster design criteria for 3-d bone movement reconstruction,” *IEEE Trans Biomed Eng*, vol. 44, no. 12, pp. 1165–1174, 1997, doi: 10.1109/10.649988.

[55] A. Cappello, A. Cappozzo, P. Francesco, L. Palombara, L. Lucchetti, and A. Leardini, “Multiple anatomical landmark calibration for optimal bone pose estimation,” *Hum Mov Sci*, vol. 16, pp. 259–274, 1997.

[56] QUALISYS, “Marker sets.” Accessed: May 08, 2024. [Online]. Available: https://docs.qualisys.com/getting-started/content/10_how_to_prepare_your_subject/marker_sets.htm

[57] U. Della Croce, A. Leardini, L. Chiari, and A. Cappozzo, “Human movement analysis using stereophotogrammetry Part 4: Assessment of anatomical landmark misplacement and its effects on joint kinematics,” 2005, *Elsevier Ireland Ltd*. doi: 10.1016/j.gaitpost.2004.05.003.

[58] A. Mathis *et al.*, “DeepLabCut: markerless pose estimation of user-defined body parts with deep learning,” *Nat Neurosci*, vol. 21, no. 9, pp. 1281–1289, Sep. 2018, doi: 10.1038/s41593-018-0209-y.

[59] L. Wade, L. Needham, P. McGuigan, and J. Bilzon, “Applications and limitations of current markerless motion capture methods for clinical gait biomechanics,” *PeerJ*, vol. 10, Feb. 2022, doi: 10.7717/peerj.12995.

[60] R. A. Clark, B. F. Mentiplay, E. Hough, and Y. H. Pua, “Three-dimensional cameras and skeleton pose tracking for physical function assessment: A review of uses, validity, current developments and Kinect alternatives,” *Gait Posture*, vol. 68, pp. 193–200, Feb. 2019, doi: 10.1016/J.GAITPOST.2018.11.029.

[61] R. Tanaka, H. Takimoto, T. Yamasaki, and A. Higashi, “Validity of time series kinematical data as measured by a markerless motion capture system on a flatland for gait assessment,” *J Biomech*, vol. 71, pp. 281–285, Apr. 2018, doi: 10.1016/J.JBIOMECH.2018.01.035.

[62] T. B. Rodrigues, C. Catháin, D. Devine, K. Moran, N. E. O’Connor, and N. Murray, “An evaluation of a 3D multimodal marker-less motion analysis system,” *Proceedings of the 10th ACM Multimedia Systems Conference, MMSys 2019*, pp. 213–221, Jun. 2019, doi: 10.1145/3304109.3306236.

[63] E. Pantzar-Castilla *et al.*, “Knee joint sagittal plane movement in cerebral palsy: a comparative study of 2-dimensional markerless video and 3-dimensional gait analysis,” *Acta Orthop*, vol. 89, no. 6, pp. 656–661, 2018, doi: 10.1080/17453674.2018.1525195.

[64] A. Mathis, S. Schneider, J. Lauer, and M. W. Mathis, “A Primer on Motion Capture with Deep Learning: Principles, Pitfalls, and Perspectives,” *Neuron*, vol. 108, no. 1, pp. 44–65, Oct. 2020, doi: 10.1016/J.NEURON.2020.09.017.

[65] K. Song, T. J. Hullfish, R. Scattone Silva, K. G. Silbernagel, and J. R. Baxter, “Markerless motion capture estimates of lower extremity kinematics and kinetics are comparable to

marker-based across 8 movements," *J Biomech*, vol. 157, Aug. 2023, doi: 10.1016/j.jbiomech.2023.111751.

[66] R. M. Kanko, E. Laende, W. S. Selbie, and K. J. Deluzio, "Inter-session repeatability of markerless motion capture gait kinematics," *J Biomech*, vol. 121, May 2021, doi: 10.1016/j.jbiomech.2021.110422.

[67] Z. Cao, G. Hidalgo, T. Simon, S.-E. Wei, and Y. Sheikh, "OpenPose: Realtime Multi-Person 2D Pose Estimation using Part Affinity Fields," Dec. 2018, [Online]. Available: http://arxiv.org/abs/1812.08008

[68] T. Nath, A. Mathis, A. C. Chen, A. Patel, M. Bethge, and M. W. Mathis, "Using DeepLabCut for 3D markerless pose estimation across species and behaviors," *Nature Protocols 2019 14:7*, vol. 14, no. 7, pp. 2152–2176, Jun. 2019, doi: 10.1038/s41596-019-0176-0.

[69] N. Nakano *et al.*, "Evaluation of 3D Markerless Motion Capture Accuracy Using OpenPose With Multiple Video Cameras," *Front Sports Act Living*, vol. 2, p. 538330, May 2020, doi: 10.3389/FSPOR.2020.00050.

[70] E. Insafutdinov, L. Pishchulin, B. Andres, M. Andriluka, and B. Schiele, "Deepercut: A deeper, stronger, and faster multi-person pose estimation model," *Lecture Notes in Computer Science (including subseries Lecture Notes in Artificial Intelligence and Lecture Notes in Bioinformatics)*, vol. 9910 LNCS, pp. 34–50, 2016, doi: 10.1007/978-3-319-46466-4_3/TABLES/9.

[71] M. Zago, M. Luzzago, T. Marangoni, M. De Cecco, M. Tarabini, and M. Galli, "3D Tracking of Human Motion Using Visual Skeletonization and Stereoscopic Vision," *Front Bioeng Biotechnol*, vol. 8, p. 508997, Mar. 2020, doi: 10.3389/FBIOE.2020.00181/BIBTEX.

[72] M. Slembrouck *et al.*, "Multiview 3D Markerless Human Pose Estimation from OpenPose Skeletons," *Lecture Notes in Computer Science (including subseries Lecture Notes in Artificial Intelligence and Lecture Notes in Bioinformatics)*, vol. 12002 LNCS, pp. 166–178, 2020, doi: 10.1007/978-3-030-40605-9_15.

[73] H. S. Fang, S. Xie, Y. W. Tai, and C. Lu, "RMPE: Regional Multi-person Pose Estimation," *Proceedings of the IEEE International Conference on Computer Vision*, vol. 2017-October, pp. 2353–2362, Dec. 2017, doi: 10.1109/ICCV.2017.256.

[74] L. Needham *et al.*, "The accuracy of several pose estimation methods for 3D joint centre localisation," *Scientific Reports 2021 11:1*, vol. 11, no. 1, pp. 1–11, Oct. 2021, doi: 10.1038/s41598-021-00212-x.

[75] B. Kumar Lahkar, A. Chaumeil, R. Dumas, A. Muller, and T. Robert, "Description, Development and Dissemination of Two Consistent Marker-based and Markerless Multibody Models," 2022, doi: 10.1101/2022.11.08.515577.

[76] "Theia3D Troubleshooting & FAQs — Theia3D Troubleshooting 2023.1 documentation." Accessed: Apr. 23, 2024. [Online]. Available: https://www.theiamarkerless.ca/faqs/

[77] R. M. Kanko, E. K. Laende, E. M. Davis, W. S. Selbie, and K. J. Deluzio, “Concurrent assessment of gait kinematics using marker-based and markerless motion capture,” *J Biomech*, vol. 127, Oct. 2021, doi: 10.1016/j.jbiomech.2021.110665.

[78] N. J. Cronin, “Using deep neural networks for kinematic analysis: Challenges and opportunities,” *J Biomech*, vol. 123, p. 110460, Jun. 2021, doi: 10.1016/J.JBIOMECH.2021.110460.

[79] R. Baker, “Pelvic angles: a mathematically rigorous definition which is consistent with a conventional clinical understanding of the terms,” *Gait Posture*, vol. 13, no. 1, pp. 1–6, 2001, doi: 10.1016/S0966-6362(00)00083-7.

[80] J. Reimers, “Static and dynamic problems in spastic cerebral palsy,” *Journal of Bone and Joint Surgery - Series B*, vol. 55, no. 4, pp. 822–827, Nov. 1973, doi: 10.1302/0301-620X.55B4.822/LETTERTOEDITOR.

[81] D. Ricardo, J. Teles, M. R. Raposo, A. P. Veloso, and F. João, “Test-Retest Reliability of a 6DoF Marker Set for Gait Analysis in Cerebral Palsy Children,” *Applied Sciences 2021, Vol. 11, Page 6515*, vol. 11, no. 14, p. 6515, Jul. 2021, doi: 10.3390/APP11146515.

[82] M. H. Schwartz, J. P. Trost, and R. A. Wervey, “Measurement and management of errors in quantitative gait data,” *Gait Posture*, vol. 20, no. 2, pp. 196–203, Oct. 2004, doi: 10.1016/J.GAITPOST.2003.09.011.

[83] F. Leboeuf, J. Reay, R. Jones, and M. Sangeux, “The effect on conventional gait model kinematics and kinetics of hip joint centre equations in adult healthy gait,” *J Biomech*, vol. 87, pp. 167–171, Apr. 2019, doi: 10.1016/J.JBIOMECH.2019.02.010.

[84] M. Akbarshahi, A. G. Schache, J. W. Fernandez, R. Baker, S. Banks, and M. G. Pandy, “Non-invasive assessment of soft-tissue artifact and its effect on knee joint kinematics during functional activity,” *J Biomech*, vol. 43, no. 7, pp. 1292–1301, May 2010, doi: 10.1016/J.JBIOMECH.2010.01.002.

[85] D. G. E. Robertson, G. E. Caldwell, J. Hamill, G. Kamen, and S. N. Whittlesey, *Research methods in biomechanics*. Human Kinetics, 2014.

[86] J. J. Salazar-Torres, B. C. McDowell, C. Kerr, and A. P. Cosgrove, “Pelvic kinematics and their relationship to gait type in hemiplegic cerebral palsy,” *Gait Posture*, vol. 33, no. 4, pp. 620–624, Apr. 2011, doi: 10.1016/J.GAITPOST.2011.02.004.

[87] R. O’Sullivan, M. Walsh, A. Jenkinson, and T. O’Brien, “Factors associated with pelvic retraction during gait in cerebral palsy,” *Gait Posture*, vol. 25, no. 3, pp. 425–431, Mar. 2007, doi: 10.1016/J.GAITPOST.2006.05.004.

[88] N. Ito *et al.*, “Markerless motion capture: What clinician-scientists need to know right now,” *JSAMS Plus*, vol. 1, p. 100001, Oct. 2022, doi: 10.1016/J.JSAMPL.2022.100001.

[89] G. S. Keenan, J. R. Franz, J. Dicharry, U. Della Croce, and D. C. Kerrigan, “Lower limb joint kinetics in walking: the role of industry recommended footwear,” *Gait Posture*, vol. 33, no. 3, pp. 350–355, Mar. 2011, doi: 10.1016/J.GAITPOST.2010.09.019.

[90] M. M. van der Krogt, L. H. Sloot, A. I. Buizer, and J. Harlaar, “Kinetic comparison of walking on a treadmill versus over ground in children with cerebral palsy,” *J Biomech*, vol. 48, no. 13, pp. 3577–3583, Oct. 2015, doi: 10.1016/J.JBIOMECH.2015.07.046.

[91] K. C. Moisio, D. R. Sumner, S. Shott, and D. E. Hurwitz, “Normalization of joint moments during gait: a comparison of two techniques,” *J Biomech*, vol. 36, no. 4, pp. 599–603, Apr. 2003, doi: 10.1016/S0021-9290(02)00433-5.

[92] I. Moll *et al.*, “Functional electrical stimulation of the ankle dorsiflexors during walking in spastic cerebral palsy: a systematic review,” *Dev Med Child Neurol*, vol. 59, no. 12, pp. 1230–1236, Dec. 2017, doi: 10.1111/DMCN.13501/ABSTRACT.

[93] C. L. Brockett and G. J. Chapman, “Biomechanics of the ankle,” *Orthop Trauma*, vol. 30, no. 3, p. 232, Jun. 2016, doi: 10.1016/J.MPORTH.2016.04.015.

[94] H. Tang, J. Pan, B. Munkasy, K. Duffy, and L. Li, “Comparison of Lower Extremity Joint Moment and Power Estimated by Markerless and Marker-Based Systems during Treadmill Running,” *Bioengineering*, vol. 9, no. 10, Oct. 2022, doi: 10.3390/bioengineering9100574.

[95] R. M. Kanko, J. B. Outerleys, E. K. Laende, S. Selbie, and K. J. Deluzio, “Comparison of Concurrent and Asynchronous Running Kinematics and Kinetics From Marker-Based and Markerless Motion Capture Under Varying Clothing Conditions,” *J Appl Biomech*, vol. 40, no. 2, pp. 129–137, 2024, doi: 10.1123/JAB.2023-0069.

[96] T. Huang, M. Ruan, S. Huang, L. Fan, and X. Wu, “Comparison of kinematics and joint moments calculations for lower limbs during gait using markerless and marker-based motion capture,” *Front Bioeng Biotechnol*, vol. 12, p. 1280363, Mar. 2024, doi: 10.3389/FBIOE.2024.1280363/BIBTEX.

[97] S. J. Thomas, J. A. Zeni, and D. A. Winter, *Winter’s biomechanics and motor control of human movement*, 5th ed. John Wiley & Sons, Inc., 2022. Accessed: Sep. 15, 2024. [Online]. Available: https://www.wiley.com/en-ie/Winter’s+Biomechanics+and+Motor+Control+of+Human+Movement%2C+5th+Edition-p-9781119827047

[98] R. Riemer, E. T. Hsiao-Wecksler, and X. Zhang, “Uncertainties in inverse dynamics solutions: a comprehensive analysis and an application to gait,” *Gait Posture*, vol. 27, no. 4, pp. 578–588, May 2008, doi: 10.1016/J.GAITPOST.2007.07.012.

[99] D. L. Benoit, M. Damsgaard, and M. S. Andersen, “Surface marker cluster translation, rotation, scaling and deformation: Their contribution to soft tissue artefact and impact on knee joint kinematics,” *J Biomech*, vol. 48, no. 10, pp. 2124–2129, Jul. 2015, doi: 10.1016/j.jbiomech.2015.02.050.

[100] A. K. Akobeng, “Understanding type I and type II errors, statistical power and sample size,” Jun. 01, 2016, *Blackwell Publishing Ltd*. doi: 10.1111/apa.13384.

[101] V. T. Keller, J. B. Outerleys, R. M. Kanko, E. K. Laende, and K. J. Deluzio, “Clothing condition does not affect meaningful clinical interpretation in markerless motion capture,” *J Biomech*, vol. 141, Aug. 2022, doi: 10.1016/J.JBIOMECH.2022.111182.

[102] U. Della Croce, A. Leardini, L. Chiari, and A. Cappozzo, “Human movement analysis using stereophotogrammetry Part 4: Assessment of anatomical landmark misplacement and its effects on joint kinematics,” *Gait Posture*, vol. 21, no. 2, pp. 226–237, 2005, doi: 10.1016/J.GAITPOST.2004.05.003.

Appendix A – Individual joint kinematics and kinetics

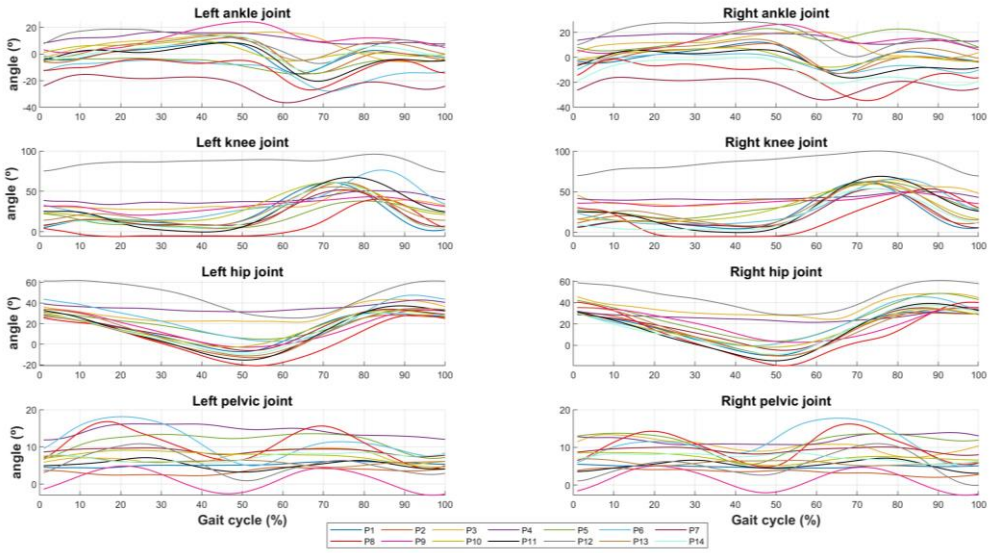

Figure A. 1. Pelvic and lower limb joint angles computed with the ML MOCAP system.

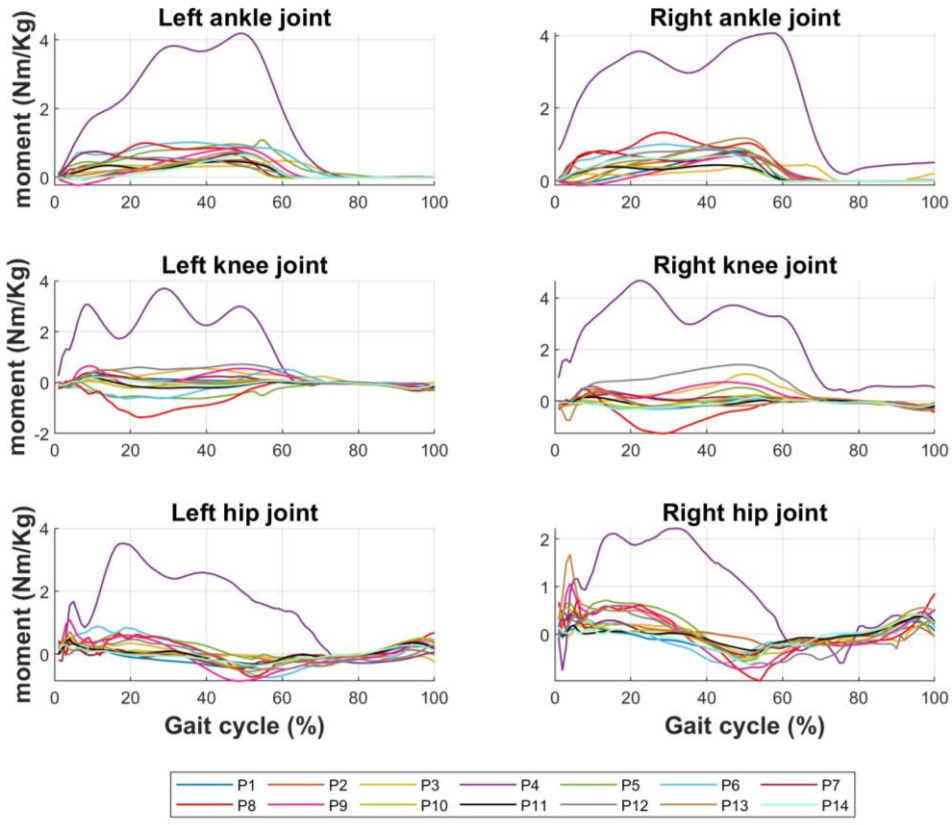

Figure A. 2. Lower limb joint moments computed with the MB MOCAP system.

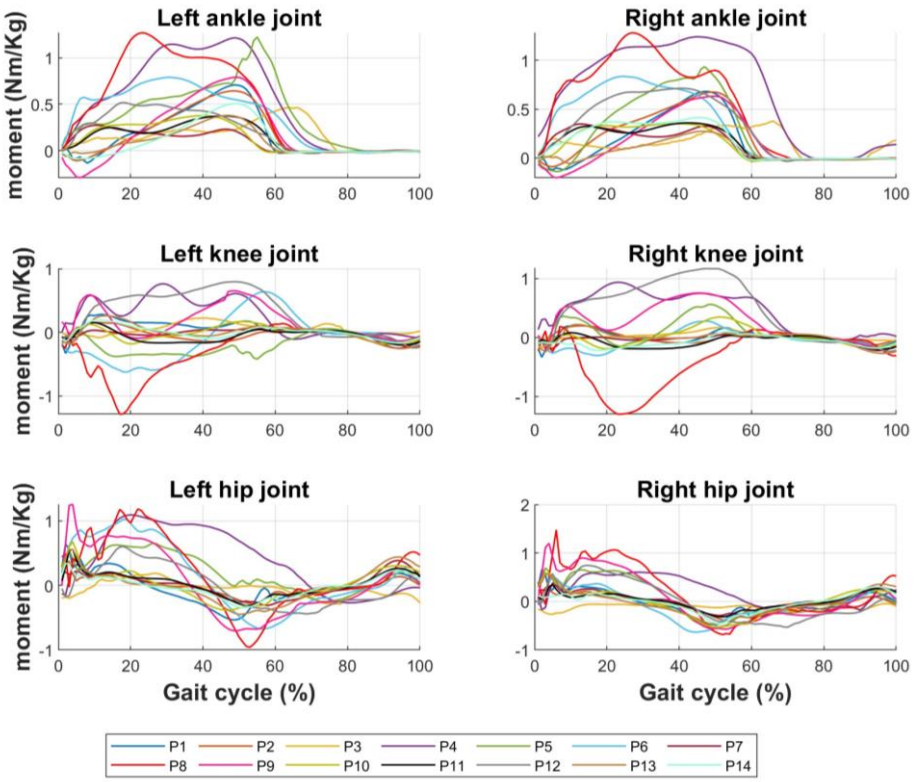

Figure A. 3. Lower limb joint moments computed with the ML MOCAP system.

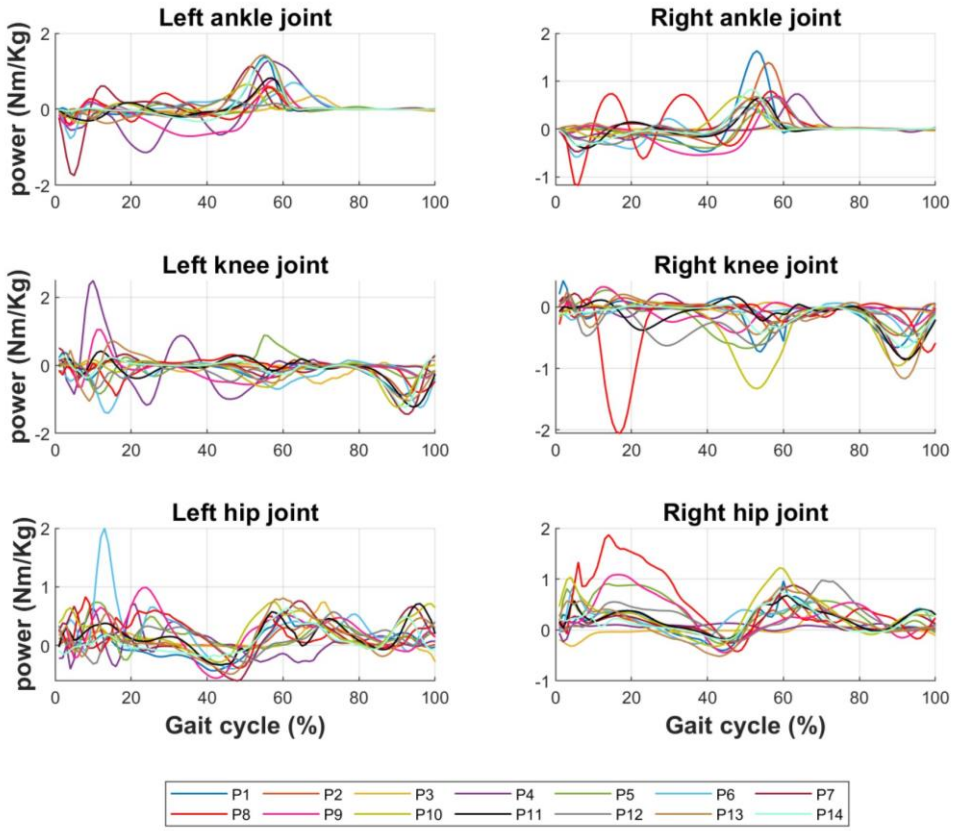

Figure A. 4. Lower limb joint powers computed with the MB MOCAP system.

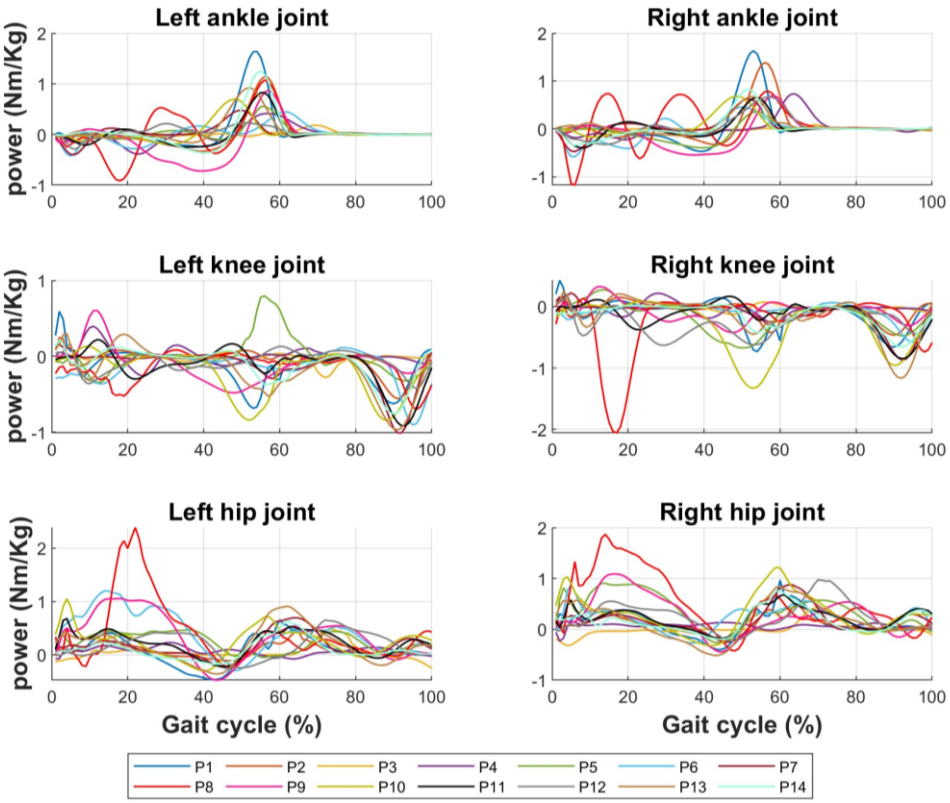

Figure A. 5. Lower limb joint powers computed with the ML MOCAP system.

Appendix B – Spatio-temporal parameters

Table B. 1. Individual gait speed computed with MB and ML systems.

Participant	***Gait speed (m/s)***		
	MB	**ML**	**Difference**
1	1.05	1.06	-0.01
2	0.86	0.85	0.01
3	0.13	0.13	0.00
4	0.20	0.20	0.00
5	0.76	0.76	0.01
6	0.69	0.63	0.06
7	1.13	1.08	0.04
8	0.84	0.83	0.01
9	0.69	0.68	0.01
10	1.06	0.99	0.08
11	0.99	0.99	-0.01
12	0.72	0.70	0.02
13	1.38	1.39	-0.02
14	1.00	0.99	0.01
Average	0.82	0.81	0.02
Std dev	0.34	0.35	0.03